University of Alberta

# Pharmacokinetics, biodistribution, toxicity and therapeutic efficacy of liposomal doxorubicin formulations in mice

By

**Gregory John Robert Charrois**

A thesis submitted to the Faculty of Graduate Studies and Research in partial fulfillment of the requirements for the degree of Doctor of Philosophy

Department of Pharmacology

Edmonton, Alberta

Fall 2003

National Library
of Canada

Acquisitions and
Bibliographic Services

395 Wellington Street
Ottawa ON K1A 0N4
Canada

Bibliothèque nationale
du Canada

Acquisisitons et
services bibliographiques

395, rue Wellington
Ottawa ON K1A 0N4
Canada

*Your file Votre référence*
*ISBN: 0-612-87949-6*
*Our file Notre référence*
*ISBN: 0-612-87949-6*

The author has granted a non-exclusive licence allowing the National Library of Canada to reproduce, loan, distribute or sell copies of this thesis in microform, paper or electronic formats.

The author retains ownership of the copyright in this thesis. Neither the thesis nor substantial extracts from it may be printed or otherwise reproduced without the author's permission.

L'auteur a accordé une licence non exclusive permettant à la Bibliothèque nationale du Canada de reproduire, prêter, distribuer ou vendre des copies de cette thèse sous la forme de microfiche/film, de reproduction sur papier ou sur format électronique.

L'auteur conserve la propriété du droit d'auteur qui protège cette thèse. Ni la thèse ni des extraits substantiels de celle-ci ne doivent être imprimés ou aturement reproduits sans son autorisation.

Canada

**University of Alberta**

**Library Release Form**

| | |
|---|---|
| **Name of Author:** | Gregory John Robert Charrois |
| **Title of Thesis:** | Pharmacokinetics, biodistribution, toxicity and therapeutic efficacy of liposomal doxorubicin formulations in mice |
| **Degree:** | Doctor of Philosophy |
| **Year this Degree Granted:** | 2003 |

Permission is hereby granted to the University of Alberta Library to reproduce single copies of this thesis and to lend or sell such copies for private, scholarly or scientific research purposes only.

The author reserves all other publication and other rights in association with the copyright in the thesis, and except as herein provided, neither the thesis nor any substantial portion thereof may be printed, or otherwise reproduced an any material form whatever without the author's prior written permission.

Date: July 28, 2003

**University of Alberta**

**Faculty of Graduate Studies and Research**

The undersigned certify that they have read, and recommend to the Faculty of Graduate Studies and Research for acceptance, a thesis entitled **Pharmacokinetics, biodistribution, toxicity and therapeutic efficacy of liposomal doxorubicin formulations in mice**, submitted by **Gregory John Robert Charrois** in partial fulfillment of the requirements for the degree of **Doctor of Philosophy**.

Dr. T. M. Allen (Supervisor)

Dr. W.P. Gati (Committee member)

Dr. D. Murray (Committee member)

Dr. D. R. Brocks (Examiner)

Dr. F. C. Szoka Jr. (External Examiner)

Date: 22 JULY 2003

*To my family, the ones that make it all worthwhile:*
*Micheline, Ray, Joan, Jeff, Teri*
*and the Goudreau Family*

**Abstract**

Mice bearing the orthotopically implanted 4T1 murine mammary carcinoma were used as a model system to explore the therapeutic and toxicological implications of different dosing schedules and dose intensities of STEALTH® liposomal doxorubicin (SL-DXR). The pharmacokinetics, biodistribution, and therapeutic efficacy of SL-DXR were studied as a function of liposome size, drug release rate, dose, and dose intensity. In humans the dose-limiting toxicities of Caelyx® (the clinical formulation of SL-DXR) are mucocutaneous, resulting, e.g., in palmar-plantar erythrodysesthesia (PPE). Therefore, the tissue distribution of STEALTH® liposomes and total doxorubicin (DXR) into cutaneous tissues (skin and paws) and tumors was determined for naïve or orthotopically implanted mice after single or multiple injections of SL-DXR.

Liposomes larger than approximately 150 nm in diameter showed reduced tissue uptake in all tissues and reduced therapeutic activity against the 4T1 murine mammary carcinoma in mice. Compared to liposomes with faster drug release rates, liposomes with slower release rates resulted in higher concentrations of DXR in tissues and had greater therapeutic efficacy against the 4T1 murine mammary carcinoma. In mice receiving four doses of Caelyx® (9 mg/kg) in short intervals (q1wk), drug concentrations in cutaneous tissues were sustained at high levels, or increased during the course of the experiment, even though plasma levels returned close to baseline between subsequent doses. Drug accumulation in cutaneous tissues was correlated with the development of PPE-like lesions. Lengthening the dose

interval to q2wk resulted in lower concentrations of DXR in cutaneous tissues and fewer PPE-like lesions. When the dose interval was extended to q4wk, drug was cleared from all tissues between doses, but therapeutic activity was reduced compared to q1wk or q2wk dose schedules. For identical dose intensities of Caelyx® (9 mg/kg/week), infrequent larger doses appeared to have superior therapeutic activity compared to frequent smaller doses. Overall, the results show that the mouse is a valuable animal model for the development of optimal liposomal drug delivery systems.

**Acknowledgement**

First I would like to thank my supervisor Dr. Terry Allen allowing me work in her laboratory and for her guidance and support during my time in her laboratory, especially in the preparation of manuscripts, presentations and this thesis.

Financial support from the Alberta Heritage Foundation for Medical Research, the Faculty of Medicine and Dentistry at the University of Alberta, the Canadian Institutes for Health Research and ALZA Corporation is gratefully acknowledged.

I would also like to thank my supervisory committee, Dr. Wendy Gati and Dr. David Murray for their help and guidance with this project, as well as the Department of Pharmacology for its support during the time of this work. I would also like to thank Dr. Dion Brocks, Faculty of Pharmacy and Pharmaceutical Sciences at the University of Alberta for helpful discussions with my pharmacokinetic experiments.

I have been associated with Dr. Allen's laboratory for many years and there is a wonderful group of people, known as the "Lipozoids", who made coming to work a treat and daily adventure. I would particularly like to thank Chris Hansen, Elaine Moase, Susan Cubitt and Heather Vandertol-Vanier for making the lab run smoothly and for being good friends. To my fellow graduate and summer students over the years, especially Darrin Stuart, Daniel Lopes de Menezes, Joao Moreira, Puja Sapra, Debbie Iden, Wilson Cheng, Kim Laginha, George Wardle, Zsolt Gabos, and Sylvia Verwoert I have greatly enjoyed working with you and you have all taught me a great deal. I would also like to acknowledge the other members of the Allen lab over the years: Jihan Marjan, Marc Kirchmeier, Tatsuhiro Ishida, Jennifer Szydlowski, Rene

LeClerc, Cheryl Santos, Grace Kao, Weimin Qi, Hamid Mohgini, Janny Zhang, Fabio Pastorino, Manuella Colla, Davis Mumbengegwi, Dipankar Das, Sarah Halleran, Felicity Wang, Jessie Dhillon and Amanda Reichart for their friendship and support. The technical assistance of the Health Sciences Laboratory Animal Services was greatly appreciated in tumor implantations and pathological examinations (Drs. Nick Nation and Richard Uwiera).

Most importantly, I would like to thank my wife Micheline, whose constant love and support made this adventure worthwhile. To my parents, who instilled the importance of learning and who provided endless support and encouragement, I thank you. And to my brother, who has always been there for me as an example of the rewards of hard work and dedication. I thank you and love you all.

Lastly, to Professor Reuben Kaufman, Department of Biological Sciences, University of Alberta, thank you for taking an awkward first year undergraduate as a summer student, look what happened.

**Table of Contents**


Chapter 1 ..... 1

Introduction ..... 1

Chapter 1 Introduction ..... 2

1.1 Introduction ..... 2

1.2 Cancer Therapy ..... 3

1.3 Liposomes ..... 5

1.4 Liposome Preparation ..... 8

1.5 Drug Loading ..... 11

1.6 Drug Release ..... 14

1.7 Bioavailability ..... 16

1.8 Liposomes *In Vivo* ..... 18

1.9 Long Circulating Liposomes ..... 20

1.10 Tissue and Tumor Biodistribution of SL ..... 23

1.11 Liposomal Doxorubicin ..... 26

1.12 Pilot Trial and Phase I Studies of STEALTH® Liposomal Doxorubicin ..... 29

1.13 Phase II and Phase III Studies of STEALTH® Liposomal Doxorubicin ..... 30

1.14 Toxicities of Caelyx® ..... 33

1.15 Palmar-Plantar Erythrodysesthesia ..... 33

1.16 Hypothesis for the Development of Palmar-Plantar Erythrodysesthesia ..... 37

1.17 Experimental Model ..... 38

1.18 Thesis Outline ..... 39

Chapter 2 ..... 42

Materials and Methods ..... 42

Chapter 2 Materials and Methods ..... 43

2.1 Materials ..... 43

2.2 Tumor Cell Line ..... 44

2.3 Liposome Preparation ..... 44

2.4 Mice ..... 46

2.5 Tumor Implantation ..... 46

2.6 Blood Content of the 4T1 Tumor ..... 46

2.7 *In vitro* Leakage of Doxorubicin ..... 47

2.8 Quantification of Doxorubicin ..... 48

2.9 Quantification of Liposomal Lipid ..... 50

2.10 Pharmacokinetic and Biodistribution Studies ..... 50

2.10.1 Pharmacokinetic and Biodistribution Using an Aqueous Space Marker. 50

2.10.2 Pharmacokinetic and Biodistribution Using Drug Fluorescence and a Radioactive Lipid Marker ..... 51

2.10.3 Pharmacokinetics of Repeat Administration of Caelyx® ..... 52

2.11 Pharmacokinetic Analysis ..... 52

2.12 Therapeutic Studies ..... 53

2.12.1 Influence of Liposome Size ..... 54

2.12.2 Influence of Doxorubicin Leakage Rate ..... 54

2.12.3 Influence of Caelyx® Dose Schedule and Dose Intensity ..... 54

2.13 Statistics ..... 55

Chapter 3. ..... 56

Rate of Biodistribution of STEALTH® Liposomes to Tumor and Skin: Influence of Liposome Diameter and Implications for Toxicity and Therapeutic Activity... 56

Chapter 3: Results and Discussion ..... 57

3.1 Biodistribution Experiments ..... 58

3.2 Therapeutic Experiments ..... 66

3.3 Conclusion ..... 70

Chapter 4 ..... 71

Influence of Drug Release Rates on the Pharmacokinetics, Biodistribution and Therapeutic Activity of STEALTH® Liposomal Doxorubicin ..... 71

Chapter 4: Results and Discussion ..... 72

4.1 *In vitro* Leakage of Doxorubicin From STEALTH® Liposomes..... 72

4.2 Development of an Extraction Procedure for Doxorubicin ..... 75

4.3 Plasma Doxorubicin Concentrations Four Hours After Injection..... 77

4.4 Pharmacokinetic and Biodistribution Experiments in Tumor-Bearing Mice ... 79

4.5 Therapeutic Experiments ..... 95

4.6 Toxicity of Liposomes Composed of POPC:CHOL:mPEG-DSPE..... 96

4.7 Conclusion ..... 99

Chapter 5 ..... 101

Multiple Injections of Pegylated Liposomal Doxorubicin: Pharmacokinetics, Toxicity and Therapeutic Activity ..... 101

Chapter 5: Results and Discussion ..... 102

5.1 Dose Schedules With Different Dose Intensities ..... 103

5.1.1 Pharmacokinetic and Biodistribution Experiments ..... 103

5.1.2 Therapeutic Experiments ..... 112

5.2 Dose Schedules With the Same Dose Intensity ..... 118

5.2.1 Pharmacokinetic and Biodistribution Experiments for the Same Dose Intensity ..... 118

5.2.2 Therapeutic Experiments ..... 124

5.3 Conclusion ..... 127

Chapter 6 ..... 128

Summarizing Discussion and Future Directions ..... 128

Chapter 6 Discussion ..... 129

6.1 Summary ..... 129

6.2 Reducing Cutaneous Toxicities of STEALTH® Liposomal Doxorubicin ..... 131

6.2.1 Altering the Dose Schedule to Reduce Cutaneous Toxicities ..... 131

6.2.2 Treating Cutaneous Lesions (Palmar-Plantar Erythrodysesthesia) ..... 132

6.3 Increasing the Therapeutic Activity of STEALTH® Liposomal Doxorubicin 135

6.3.1 Ligand Targeted Liposomes ..... 136

6.3.2 Combination Chemotherapy With STEALTH® Liposomal Doxorubicin ... 137

6.3.3 Combined Modality Therapy and Triggered Release Formulations ..... 140

6.4 Measuring Bioavailability of Drug From Liposomal Carriers ..... 143

6.5 Chemotherapy With Liposomal Antineoplastic Agents ..... 145

6.6 Conclusion ..... 146

References ..... 147

## List of Tables

**Table 1.1** Currently approved liposome-based antineoplastic drug delivery systems. 6

**Table 1.2** Clinical grading scale for toxicities of Caelyx® ..... 34

**Table 1.3.** Dose delay protocol for patients developing cutaneous toxicities with Caelyx® ..... 36

**Table 3.1A**. Tumor-to-skin ratios as a function of time after injection. ..... 62

**Table 3.1B**. Tumor-to-paw ratios as a function of time after injection..... 62

**Table 4.1**. *In vitro* leakage half-lives of DXR from liposomes..... 74

**Table 4.2.** Recovery of DXR from tissue samples spiked with $^{14}$C-DXR comparing radioactivity and fluorescence measurements ..... 76

**Table 4.3.** Plasma concentrations of total DXR from various formulations of liposomes 4 hours after injection ..... 78

**Table 4.4** Pharmacokinetic parameters for tumor-bearing mice receiving liposomal DXR ..... 82

**Table 4.5A** Tumor to skin ratios for DXR and liposomal lipid as a function of time post injection..... 89

**Table 4.5B.** Tumor to paw ratios for DXR and liposomal lipid as a function of time post injection..... 90

**Table 5.1.** Pharmacokinetic parameters for mice receiving i.v. Caelyx® at a dose of 9 mg/kg q1wk, q2wk, or q4wk ..... 106

**Table 5.2.** Numbers (percent) of mice developing PPE-like lesions as a function of dose schedule ..... 111

**Table 5.3.** Pharmacokinetic parameters for mice receiving Caelyx® at a dose intensity of 9 mg/kg/wk ..... 121

## List of Figures

**Figure 1.1.** General strucure of a 1st generation liposome (classical liposome). ..... 7

**Figure 1.2**. The structure of some common liposome-forming phospholipids. ..... 9

**Figure 1.3** Classification of liposomes based on size and lamellarity (15)..... 10

**Figure 1.4**. Doxorubicin loading with an ammonium sulfate gradient ..... 13

**Figure 1.5**. STEALTH® liposome and a STEALTH® liposomal doxorubicin ..... 21

**Figure 1.6.** Passive targeting of doxorubicin-loaded STEALTH® liposomes in a solid tumor ..... 24

**Figure 1.7**. Chemical structure of doxorubicin ..... 27

**Figure 3.1.** Accumulation of $^{125}$I-tyraminylinulin liposomes in mouse tissues as a function of time ..... 59

**Figure 3.2** 4T1 carcinoma blood content as a function of tumor weight ..... 67

**Figure 3.3**. Therapeutic activity of various sizes of SL-DXR against the 4T1 mouse mammary carcinoma ..... 69

**Figure 4.1.** Plasma concentrations of DXR, liposomal lipid and normalized drug to lipid ratios ..... 81

**Figure 4.2.** Tumor concentrations of DXR, liposomal lipid and normalized drug to lipid ratios ..... 84

**Figure 4.3.** Skin concentrations of DXR, liposomal lipid and normalized drug to lipid ratios ..... 86

**Figure 4.4**. Paw concentrations of DXR, liposomal lipid and normalized drug to lipid ratios ..... 87

**Figure 4.5.** Therapeutic activity of different formulations of SL-DXR against the 4T1 murine mammary carcinoma ..... 97

**Figure 5.1**. Tissue concentrations of DXR in mice given Caelyx® at a dose schedule of 9 mg/kg q1wk. ..... 104

**Figure 5.2**. Tissue concentrations of DXR in mice given Caelyx® at a dose schedule of 9 mg/kg q2wk. ..... 107

**Figure 5.3**. Tissue concentrations of DXR in mice given Caelyx® at a dose schedule of 9 mg/kg q4wk. ..... 109

**Figure 5.4.** Therapeutic activity of Caelyx® against the 4T1 murine mammary carcinoma using different dose schedules ..... 114

**Figure 5.5**. Tissue concentrations of DXR in mice given Caelyx® at the same dose intensity ..... 120

**Figure 5.6.** Therapeutic activity of Caelyx® against the 4T1 murine mammary carcinoma using dose schedules with the same dose intensity ..... 125

## List of Abbreviations

| | |
|---|---|
| ABS | adult bovine serum |
| ABV | adriamycin, bleomycin, vincristine |
| AIDS | human acquired immunodeficiency syndrome |
| Ara-C | 1-β-D-arabinofuranosylcytosine |
| AUC | area under the plasma/tissue concentration versus time curve |
| BD | biodistribution |
| BV | bleomycin, vincristine |
| $C_{ss}$ | tissue/plasma concentration at steady state |
| CHF | congestive heart failure |
| CHOL | cholesterol |
| CL | clearance |
| CLip | classical liposome |
| $C_{max}$ | maximal tissue drug concentration |
| D5W | dextrose, 5% in sterile water |
| DDS | drug delivery system |
| DXR | doxorubicin |
| DHM3 | Bi(3,5-dimethyl-5-hydroxylmethyl-2-oxomorpholin-3-yl) |
| DMPC | dimyristoylphosphatidylcholine |
| DOPC | dioleoylphosphatidylcholine |
| DPPC | dipalmitoylphosphatidylcholine |
| DSPC | distearoylphosphatidylcholine |

| | |
|---|---|
| eggPC | egg yolk phosphatidylcholine |
| 5-FU | 5-fluorouracil |
| FBS | fetal bovine serum |
| $GM_1$ | monosialoganglioside |
| Gray | Gy |
| $^{3}$H-CHE | $^{3}$H-cholesteryl hexadecylether |
| HBS | HEPES buffered saline |
| HEPES | 4-(2-hydroxyethyl)-1-piperazineethanesulfonic acid |
| HSPC | fully hydrogenated soy phosphatidylcholine |
| $^{111}$In-rbc | $^{111}$In-labeled red blood cells |
| $^{125}$I-TI | $^{125}$I-tyraminylinulin |
| kDa | kiloDalton |
| LDL | low density lipoproteins |
| LUV | large unilamellar vesicle |
| MEM | minimal essential medium |
| MLV | multilamellar vesicle |
| mPEG-DSPE | methoxypolyethyene glycol ($M_r$ 2000)-distearoylphosphatidylethanolamine |
| MPS | mononuclear phagocyte system |
| PEG | methyl-terminated polyethyene glycol, molecular wt. 2000 |
| PK | pharmacokinetics |
| PMPC | palmitoyl-myristoylphosphatidylcholine |
| POPC | palmitoyl-oleoylphosphatidylcholine |

| | |
|---|---|
| PPE | palmar-plantar erythrodysesthesia |
| p.s.i. | pounds per square inch |
| q3d | every third day |
| q1wk | once a week |
| q2wk | once every second week |
| q4wk | once every fourth week |
| RFU | relative fluorescence units |
| SL | Sterically stabilized (STEALTH®) liposome |
| SL-DXR | STEALTH® liposomal doxorubicin |
| SMPC | stearoyl-myristoylphosphatidylcholine |
| SPPC | stearoyl-palmitoylphosphatidylcholine |
| SUV | small unilamellar vesicle |
| $t_m$ | liquid to solid phase transition temperature for phospholipids |
| wt/wt | ratio of weight to weight |
| wt/vol | ratio of weight to volume |
| $V_d$ | volume of distribution |
| vol/vol | ratio of volume to volume |

# Chapter 1

# Introduction

## Chapter 1 Introduction

### 1.1 Introduction

Despite the clinical approval of several liposomal anticancer drugs, there are relatively few published in depth pharmacokinetic (PK) and biodistribution (BD) studies focusing on the accumulation of liposomes and their associated drug into tumor versus cutaneous tissues. These tissues are important as they respectively represent the sites of therapeutic activity and toxicity for Caelyx® (STEALTH® liposomal doxorubicin, SL-DXR; Doxil® in the United States)[1] (1). The objective of this thesis was to undertake detailed PK and BD studies using formulations of SL-DXR that vary in size, lipid composition and drug release characteristics using an orthotopically implanted murine mammary carcinoma model (4T1). Another objective was to study the influence of repeat administration of Caelyx®, using different dose schedules and dose intensities, on its PK and BD in the same tumor model. These experiments were performed because anticancer therapy is given in repeated cycles in the clinic, and the cutaneous toxicities of Caelyx® have been observed to develop after multiple injections (1). Further, few studies to date have examined, in detail, the PK and BD of repeat injections of Caelyx® in experimental models. A final objective was to examine the therapeutic implications of altering

[1] For the purposes of this thesis Caelyx® and Doxil® will be used synonymously (e.g., with respect to clinical trials). SL-DXR will refer to other STEALTH® liposomal formulations of doxorubicin. The liposomal bilayer of Caelyx® is composed of hydrogenated soy phosphatidylcholine, cholesterol and methoxypolyethyene glycol ($M_r$ 2000)-distearoylphosphatidylethanolamine at a 55:40:5 molar ratio. In the United States, Doxil® is manufactured by ALZA Corporation/Johnson&Johnson and outside the the United States Caelyx® is manufactured by Shering-Plough.

liposome properties as well as using different dose schedules and dose intensities for Caelyx® in the same 4T1 murine mammary carcinoma model.

Due to the mucocutaneous toxicities of SL-DXR, a specific goal of this thesis was to identify conditions that minimized the accumulation of SL-DXR into the cutaneous tissues of mice (skin and paws) while maximizing the accumulation into orthotopically implanted murine mammary tumors (4T1). The underlying assumption for these studies is that a decrease in cutaneous drug concentrations will decrease the likelihood of mice developing cutaneous toxicities and that this will have implications for the use of SL-DXR in humans.

**1.2 Cancer Therapy**

Cancer is one the leading causes of mortality in Westernized nations. In 2001 it was estimated that 65,300 Canadians died of cancer and 134,100 new diagnoses were made (2). Solid tumors of the lung, breast, prostate and colon/rectum presently account for over half of all cancer deaths and over half of all newly diagnosed tumors (2). Current therapies for solid tumors, like breast cancer, focus on the surgical removal of the primary tumor (if possible), and radiation therapy to increase local tumor control. Local therapy can be followed by chemotherapy or hormonal therapy to treat minimal residual, or disseminated (i.e., metastatic), disease. Combinations of therapy modalities and combination chemotherapy have resulted in increased life spans and disease-free survival, however treatments and cure rates remain inadequate for metastatic disease (3-5). Conventional chemotherapy is marginally selective for neoplastic tissues based on its preferential toxicity for rapidly proliferating cells.

Normal tissues with elevated levels of mitotic activity, as well as other susceptible tissues, incur high incidences of treatment-related toxicities. Toxicities to normal tissues such as bone marrow, the gastrointestinal tract, kidneys, neurons and heart are dose limiting, with the particular toxicities being drug-dependent. Further, many of these agents produce other toxicities such as alopecia that may not be life threatening, but which have a negative psychological impact on patients. Therefore, newer therapies that are less toxic and/or more selective for neoplastic cells are needed.

Several strategies have been used to achieve this goal. Newer drugs, such as the tyrosine kinase inhibitor imatinib (Glivec®) have been rationally designed using molecular techniques and are targeted toward the underlying pathology of certain cancers e.g., BCR-ABL kinase in chronic myeloid leukemia, or the cKIT receptor tyrosine kinase in gastrointestinal stromal tumors, (recently review by Capdville et al. (6)). Imatinib has shown good therapeutic activity with comparatively few side effects compared to conventional chemotherapy in chronic myeloid leukemia and gastrointestinal stromal tumors (7-9). As our technology and understanding of cancer pathobiology increases, more targeted therapies such as imatinib will undoubtedly be developed.

Another extensively developed approach to increasing the specificity of cancer therapy is the use of particulate drug delivery systems (DDS). One of the characteristics of DDS is their ability to alter the PK and BD of their associated drugs. Decreases in drug-related side effects are achieved by limiting systemic exposure or peak levels of cytotoxic drugs to sensitive tissues. For example, encapsulating

doxorubicin (DXR) within liposomes decreases peak cardiac drug levels and overall cardiac drug concentrations (10). Further, if DDS are able to increase drug concentrations in the tumor (site of therapeutic action) then the therapeutic activity of the formulation will increase compared to equivalent doses of free drug. The overall effect, therefore, is to increase the drug's therapeutic index.

Important criteria for ideal DDS include their ability to be formulated from biocompatible materials and their ability to entrap drugs of various chemical classes while protecting the entrapped drug from degradation *in vivo*. Liposomes, one of the most extensively developed drug delivery systems, fulfill these criteria. Their lipid components are biocompatible and they are able to encapsulate many types of drugs (see below). The development of liposomes as drug delivery systems has focused primarily, although not exclusively, on anticancer and anti-infective drugs. As previously mentioned, anticancer therapy (and the treatment of systemic infections) is associated with a high degree of morbidity. The application of liposomes as DDS for anticancer agents, like DXR, has increased their therapeutic index (11). To date, several liposome-based DDS are approved for use in humans for the treatment of cancer (**Table 1.1**).

**1.3 Liposomes**

Liposomes were first described by Bangham et al. in 1965 in a study examining the movement of ions across the lamella of swollen lipid bilayers (12). They are microscopic vesicles composed of a phospholipid bilayer surrounding an aqueous interior (**Figure 1.1**). A phospholipid bilayer is a thermodynamically stable

**Table 1.1** Currently approved liposome-based antineoplastic drug delivery systems.

| Product | Drug | Formulation | Indications | Manufacturer |
|---|---|---|---|---|
| Caelyx®/ Doxil® | Doxorubicin | STEALTH® liposome | Kaposi's sarcoma and Refractory ovarian cancer | ALZA Corporation/ Johnson & Johnson |
| DaunoXome® | Daunorubicin | Liposome | Kaposi's sarcoma | Gilead Sciences |
| Myocet™ | Doxorubicin | Liposome | Metastatic breast cancer | Elan Corporation |
| Depotcyt® | Cytosine arabinoside | Lipid spheres | Lymphomatous meningitis | Skye Pharma Inc. and Chiron Corp. |

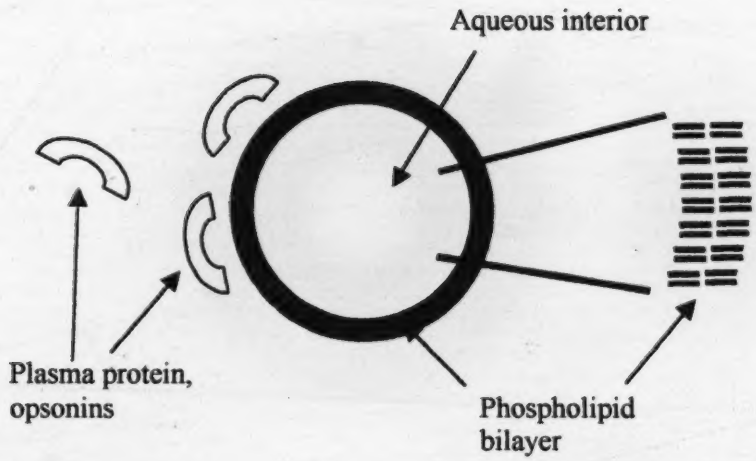


**Figure 1.1.** General strucure of a 1st generation liposome (classical liposome). Note the phospholipid bilayer surrounding and aqueous interior. Hydrophilic drugs can be associated with liposomes by encapsulation within this aqueous space, alternatively hydrophobic drugs will be carried within the inner portion of the bilayer. Amphipathic molecules reside at the interface of the hydrophobic and aqueous compartments. Plasma proteins and opsonins readily bind to classical liposomes, hastening their removal from circulation by the mononuclear phagocyte system.

structure in which the charged polar head groups of amphipathic phospholipids interact with the aqueous media on both sides of the bilayer, shielding the hydrophobic fatty acyl chains which self associate to form the inner portion of the bilayer (13). The structures of some common liposome forming lipids are seen in **Figure 1.2**.

**1.4 Liposome Preparation**

One of the most common procedures used to prepare liposomes is to hydrate dried lipid films with an aqueous solution; this is called thin film hydration (14). Homogeneous mixtures of lipids are prepared in an organic solvent that is evaporated before hydration (13). This procedure can be used to make liposomes of various compositions. When rigid phospholipids (i.e., high solid to liquid crystalline phase transition temperatures, $T_m$) are used, the lipid hydration step and other procedures are carried out at temperatures above the $T_m$ of the major phospholipid component. This ensures complete mixing during the hydration and sizing steps (see below). When a dried lipid film is hydrated, large multilamellar vesicles (MLV) are formed; these vesicles are composed of bilayers within bilayers (**Figure 1.3**). MLV have a low trapped aqueous volume and are very heterogeneous in size, which makes them sub-optimal for most *in vivo* applications requiring systemic administration (14). For MLV to be suitable carriers for anticancer drugs *in vivo* they must be reduced in size. Sonicating MLV, with either a probe or bath sonicator, yields small unilamellar vesicles (SUV) that are more homogeneous in size (**Figure 1.3**). The drawback to this method is that it yields small liposomes with a low trapped volume per unit lipid

**Common Phospholipids Structures**

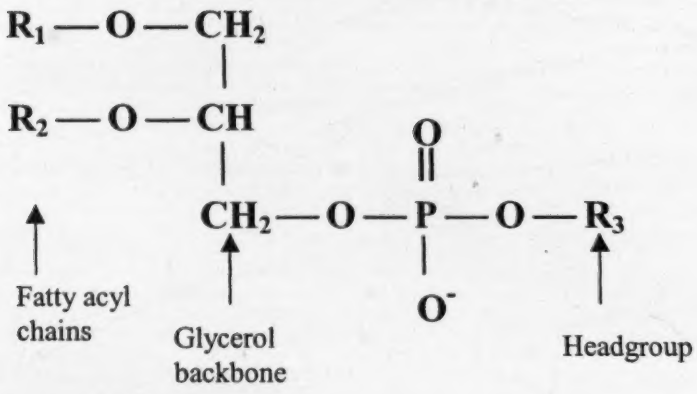


**Fatty Acyl chains ($R_1$ and $R_2$)**

*Saturated fatty acids*

| | | |
|---|---|---|
| Stearic acid | (C18:0) | $CH_3(CH_2)_{16}COOH$ |
| Palmitic acid | (C 16:0) | $CH_3(CH_2)_{14}COOH$ |
| Myristic acid | (C14:0) | $CH_3(CH_2)_{12}COOH$ |

*Unsaturated fatty acids*

| | | |
|---|---|---|
| Oleic acid | (C18:1) | $CH_3(CH_2)_7CH{=}CH(CH_2)_7COOH$ |

**Head Groups ($R_3$)**

| | |
|---|---|
| Choline | $-CH_2-CH_2-N^+-(CH_3)_3$ |
| Ethanolamine | $-CH_2-CH_2-NH_3^+$ |
| Inositol | |

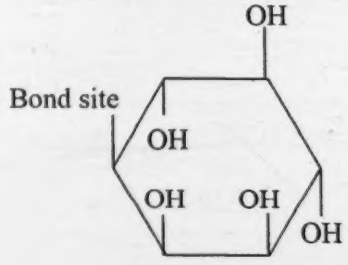


**Figure 1.2**. The structure of some common liposome-forming phospholipids.

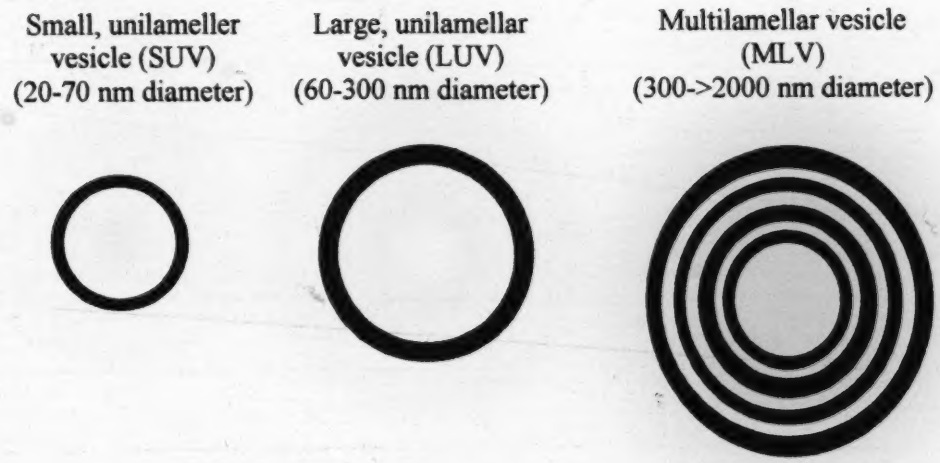
Small, unilameller vesicle (SUV) (20-70 nm diameter)
Large, unilamellar vesicle (LUV) (60-300 nm diameter)
Multilamellar vesicle (MLV) (300->2000 nm diameter)

**Figure 1.3** Classification of liposomes based on size and lamellarity (15).

and their small diameter (20-50 nm) results in a high degree of curvature to the membrane making them unstable and not optimal for *in vivo* applications (13, 14).

Alternatively, MLV can be sized by extrusion through polycarbonate filters of defined pore size (16, 17). Liposomes prepared by this technique are homogeneous, primarily unilamellar or oligolamellar, and will adopt a diameter close to the size of the pore (e.g., 80, 100, 200 nm) (16, 17). These large unilamellar vesicles (LUV) have higher trapped volumes than SUV and their diameter can be controlled so that they are appropriate for various parenteral applications *in vivo*. Extruders using moderate pressures (< 600 p.s.i.) are commercially available in a number of sizes and are temperature controlled to work with high phase transition temperature lipids (e.g. the extruder from Northern Lipids Inc, Vancouver B.C.).

Other methods, such as solvent injection and reverse phase evaporation can also be used for preparing liposomes (18, 19). All methods can generate liposomes of various compositions; the exact method will depend on the application and the volume of material required. In the experiments presented in this thesis, liposomes were prepared by thin film hydration and sized by extrusion through polycarbonate filters (17).

**1.5 Drug Loading**

Drugs can be associated with liposomes in a number of ways. Hydrophobic drugs (e.g., photosensitizers) can be co-dissolved with lipids in organic solvent before drying so that the drugs will associate with the hydrophobic interior of the liposome bilayer upon hydration (13, 20). Alternatively hydrophobic drugs can be loaded into

preformed liposomes using a solvent injection technique (21). Hydrophilic drugs (e.g., cisplatin and 1-β-D-arabinofuranosylcytosine) can be passively entrapped within the liposome interior during MLV formation; however, the major limitation to this method is the low loading efficiency (14, 15). This low entrapment efficiency can be overcome by using freeze-thaw techniques or other liposome preparation methods such as reverse phase evaporation (19, 22).

In contrast to these techniques where the drug is "passively" associated with the liposome, "active" or "remote" loading techniques were developed for drugs like DXR (an amphipathic weak base), which can be loaded into preformed liposomes in response to chemical or pH gradients. These techniques work by trapping the drug in its charged form within liposomes and complete incorporation of drugs at high drug to lipid ratios can be achieved (23-28). In the case of DXR, concentrations within the liposome interior can exceed its aqueous solubility, leading to the formation of a DXR precipitate (23, 25). These precipitates form stable fibers, which organize into fiber bundles when divalent anions like citrate are used to control the internal pH (29). The loading of DXR into Caelyx®, the clinical formulation of STEALTH® liposomal DXR, relies upon the generation of an ammonium sulfate gradient (**Figure 1.4**) (25, 26). Similar to citrate-mediated pH loading, ammonium sulfate loading results in the generation of a stable DXR precipitate within the liposome's interior (25). The ammonium sulfate loading procedure was used to prepare DXR-loaded liposomes in this thesis.

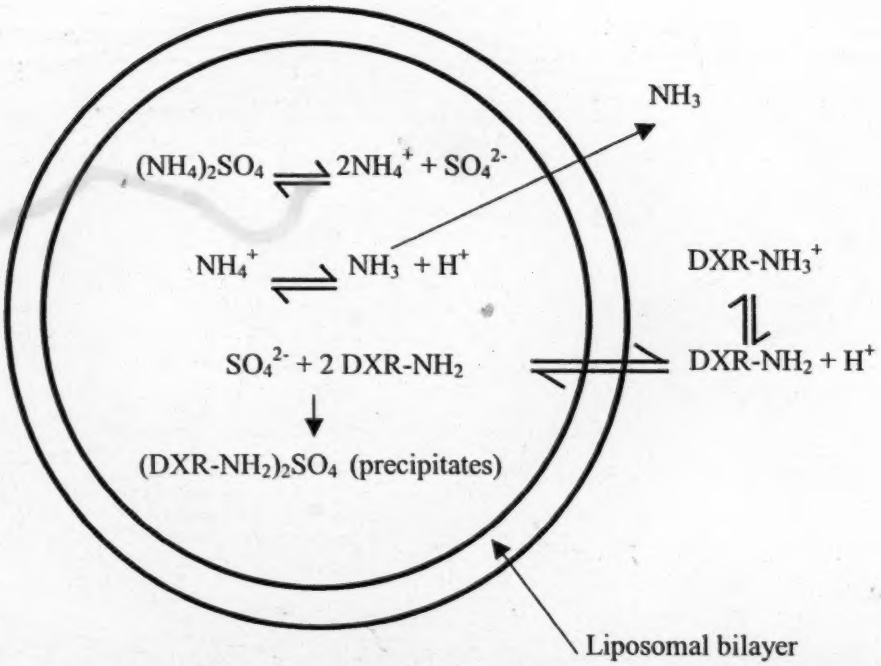


**Figure 1.4**. Doxorubicin loading with an ammonium sulfate gradient. Uncharged DXR will enter the liposome by passive diffusion where it will react with sulfate anions ($SO_4^{2-}$) to form a precipitate of $(DXR\text{-}NH_2)_2SO_4$. The production of $H^+$, and the diffusion of $NH_3$ out of the liposome creates a pH gradient across the liposome's membrane (inside acidic) favoring the influx of more uncharged DXR. The initial pH of the system is 5.5 on both sides of the bilayer. Adapted from (26).

**1.6 Drug Release**

The relationship between the rate of drug release and the therapeutic effect is a complex and unpredictable one and depends on a number of factors, including the growth rate of the tumor and the nature of the particular anticancer drug.

A number of factors influence the rate of drug release from liposomes. *In vivo*, lipids from the bilayer can exchange with, or be transferred to, plasma lipoproteins. This destabilizes the membranes and increases drug leakage (30). Therefore, factors that increase bilayer stability, such as the use of long chain, fully saturated lipids and cholesterol (CHOL) will reduce the actions of lipoproteins and increase drug retention (27, 28, 30-32). This is especially true of hydrophilic drugs that do not cross membranes, where drug release is dependent on membrane permeablization or disruption. For stable liposome preparations, drug release can be very slow and in extreme cases it can lead to low levels of therapeutic activity due to a lack of bioavailable drug. Such was the case for SPI-077, a STEALTH® liposomal formulation of the anticancer drug cisplatin (33, 34). This formulation produced a large area under concentration versus time curve (AUC) for tumor tissue, but there was not a concomitant increase in therapeutic activity due to low levels of bioavailable drug (33-35). Hydrophobic drugs, such as photosensitizers, on the other hand will quickly transfer to circulating lipoproteins *in vivo* (21). The drug-lipoprotein complex will then localize in some tumors, based on their overexpression of LDL receptors (36).

Amphipathic drugs, such as DXR, will be released when either the liposome is disrupted, leading to drug spillage, or by dissipation of the pH gradient, which will allow the uncharged form of the drug to cross the membrane and leak out of the liposome. This was demonstrated *in vivo* using experimental models for DXR loaded into STEALTH® liposomes (SL) (32). SL formulations containing low phase transition temperature lipids like egg yolk phosphatidylcholine had much lower 24 h plasma levels in mice compared to SL composed of more rigid high phase transition temperature lipids like fully hydrogenated soy phosphatidylcholine (0.7 μg/ml versus 37.4 μg/ml, respectively) (32).

Experimentally, the therapeutic activity of a formulation will depend upon several factors, including the mechanism of action and physical chemistry of the drug, the leakage rate of the drug, and the tumor model. For example, in a series of studies using the murine L1210 and P388 leukemia models, it was determined that the optimal liposomal formulation of vincristine was a rigid bilayer composed of sphingomyelin and cholesterol (55:45 mol/mol) (24, 27, 37). This formulation has a relatively slow rate of drug release, which should be optimal because of the cell cycle phase-specific mechanism of action of vincristine. The slow rate of drug release ensures that the tumor cells are exposed to cytotoxic drug concentrations long enough for the majority of cells to pass through the sensitive portion of the cell cycle. Similar results were seen for long-circulating liposomal formulations of cytosine arabinoside. It was determined that long circulating liposomes with a fairly rapid rate of drug

release were needed for optimal antitumor activity for this drug in the murine L1210 leukemia model (38).

In another series of experiments, drug release from liposomal formulations of mitoxantrone was tested in the L1210 murine leukemia model and in a human xenograft model (LS180 human colon carcinoma). In these experiments, "leaky" liposomes composed of DMPC:CHOL (55:45 mol/mol) had superior activity compared to a more solid formulation (DPSC:CHOL, 55:45 mol/mol) indicating that rapid drug release was preferable for these tumor models (28, 39). It must also be pointed out for the studies using the L1210 leukemia that the tumor cells were implanted intravenously where they will seed into the liver and spleen. The DMPC:CHOL liposomes are more likely to be taken out of circulation by the mononuclear phagocyte system (MPS) cells in liver and spleen than the DSPC:CHOL liposomes, which can increase tumor cell kill in these organs. However, the results for the LS180 tumor model demonstrated the beneficial effect of rapid drug release in this tumor model. These results contrast with those of mitoxantrone formulated into programmable fusogenic vesicles where increased stability of the liposomes resulted in superior therapeutics in the LS180 tumor model, so even in the same tumor model, the effects of different rates of drug release can be unpredictable, although differences in the two formulations make direct comparisons difficult (39, 40).

**1.7 Bioavailability**

The bioavailability of encapsulated drugs is a fundamental, and sometimes overlooked, concept in drug delivery. Both the therapeutic activity and toxicity of a

formulation will depend on the bioavailability of drug from the carrier. For example, if a drug is stably entrapped within liposomes and is released very slowly, its PK and BD will essentially be those of the carrier, and the location of its cytotoxic actions will be determined by the disposition of the carrier and by whether the rate of drug release from the carrier leads to drug levels above the minimal cytotoxic concentration in tissues where the carrier localizes. Toxicities associated with the free drug will be greatly reduced or eliminated when drug release is slow, but if the carrier distributed to normal tissues as well as target tissues, drug toxicities may become problematic. Alternatively, if the drug is rapidly released from the carrier then its PK and BD will not be substantially different from that of the free drug, and the carrier basically functions as a vehicle to solubilize the drug. In this case, the toxicity profile and therapeutic activity of the liposomal drug would parallel those of the free drug, but toxicity could be reduced since the lipid vehicle is generally less toxic than standard vehicles. For example, Cremophor® EL, the vehicle used to deliver paclitaxel is associated with hypersensitivity reactions (41, 42). The use of liposomes as an alternative vehicle for paclitaxel has shown promise in reducing vehicle-associated toxicities, and in some experimental models liposomes have increased the therapeutic activity of paclitaxel against xenograft models (43-45).

The relationship between bioavailability, drug release and drug PK is illustrated by two different liposomal formulations of DXR, Caelyx® and Myocet™. Caelyx® is a long-circulating (STEALTH®) formulation of DXR that is very stable *in vivo*, with a slow rate of drug release and a long circulation time ($t_{1/2}$ is > 48 hour in

humans), a low volume of distribution (4.1L) and slow clearance (0.08 L/min) (46). Myocet™ is a classical liposome formulation composed of egg yolk phosphatidylcholine and cholesterol (55:45 mole), it has a shorter $t_{1/2}$ (6.7 hours), larger volume of distribution (18.8 L), a faster clearance (23.3 L/h) and a faster rate of drug release (47). The side effect profile for both of these formulations reflects the differences in their PK and BD. Similar to conventionally administered DXR (free DXR), the dose-limiting toxicity of Myocet™ for single doses is leucopenia, whereas the dose limiting toxicities of Caelyx® for single and multiple doses are stomatitis and palmar-plantar erythrodysesthesia (PPE), respectively (see below) (1, 47). This toxicity for Caelyx® is thought to be dependent upon the localization of the carrier into the skin, where sustained release of the drug causes cell damage (48, 49).

**1.8 Liposomes *In Vivo***

In the early days of liposomes, there was much excitement regarding the potential use of liposomes as drug delivery systems due to their biocompatibility and their ability to increase the therapeutic index of many drugs (20, 50, 51) (reviewed by Gregoriadis (52, 53)). However, the early enthusiasm for liposomes as a DDS was tempered by problems associated with their *in vivo* disposition. Early formulations of liposomes (classical liposomes, CLip) were composed of a naked phospholipid bilayer, with or without cholesterol. CLip have dose-dependent, saturable, non-linear pharmacokinetics, so at high doses they were able to increase blood concentrations of various drugs in various experimental animals (or humans) compared to free drug after intravenous administration, but at low doses they were rapidly cleared from

circulation (20, 54, 55). The vesicles are rapidly opsonized by plasma proteins and are removed from circulation by the MPS, which includes fixed macrophages in the spleen and Kupffer cells in the liver (54). The rapid uptake of liposomes into the MPS was a barrier to their development as a drug delivery system for treating diseases outside these organs, i.e., systemic disease.

In order for liposomes to concentrate in tissues outside the MPS, especially tumor tissue, longer circulation times (i.e., reduced MPS uptake) were necessary. Several factors were identified as being important in controlling the *in vivo* PK and BD of liposomes (recently reviewed by Drummond et al. (56)). Vesicle size is important in determining the BD of liposomes, and a diameter of 100 nm was found to be optimal since liposomes of this diameter have a reasonable trapped volume but are small enough to extravasate across leaky tumor vasculature and localize to solid tumors (31, 57).

Lipid composition also influences the *in vivo* fate of liposomes. Formulations composed of long chain, saturated fatty acids with high phase transition temperatures (e.g., sphingomyelin or distearoylphosphatidylcholine), with the addition of cholesterol, have decreased interactions with plasma lipoproteins and other opsonins, which results in longer circulation times than more fluid liposomes (58, 59). Alternatively, long circulation times for CLip can also be achieved by the less desirable strategy of using large doses of liposomes or by predosing animals with empty liposomes to saturate MPS clearance mechanisms (57, 60-62).

**1.9 Long Circulating Liposomes**

It was not until the late 1980's and early 1990's that more efficient methods of decreasing the uptake of liposomes into the MPS were developed. Allen and Chonn first described a reduction of liposomes into the MPS by incorporating monosialoganglioside ($GM_1$) into liposomes composed of lipids with high phase transition temperatures (63). Other formulations of liposomes with extended circulation times were subsequently described that contained phoshatidylinositol, and increased accumulation into tumors of long-circulating liposomes was demonstrated (64). These original long circulating, STEALTH®, liposomes (SL) soon gave way to new formulations, as several groups published work demonstrating the long circulating effects of lipid conjugates of the hydrophilic polymer poly(ethylene glycol) (mPEG) (65-68). Liposomes containing mPEG-derivatized lipids (5-15%) have reduced uptake by the MPS and were shown to have dose-independent, log-linear pharmacokinetics (reviewed by Allen (55, 69)).

The decrease in MPS uptake and the long circulation times imparted by $GM_1$ and mPEG-DSPE is due to steric stabilization. These components increase liposome surface hydrophilicity and block the binding of protein opsonins, leading to decreased liposome clearance into liver and spleen **(Figure 1.5)** (59, 70). mPEG has several advantages over $GM_1$, including the ability to increase the circulation times of various compositions of liposomes, not just liposomes composed of rigid lipids (e.g. sphingomyelin) (71, 72). Further, mPEG-DSPE is inexpensive and easily purified to

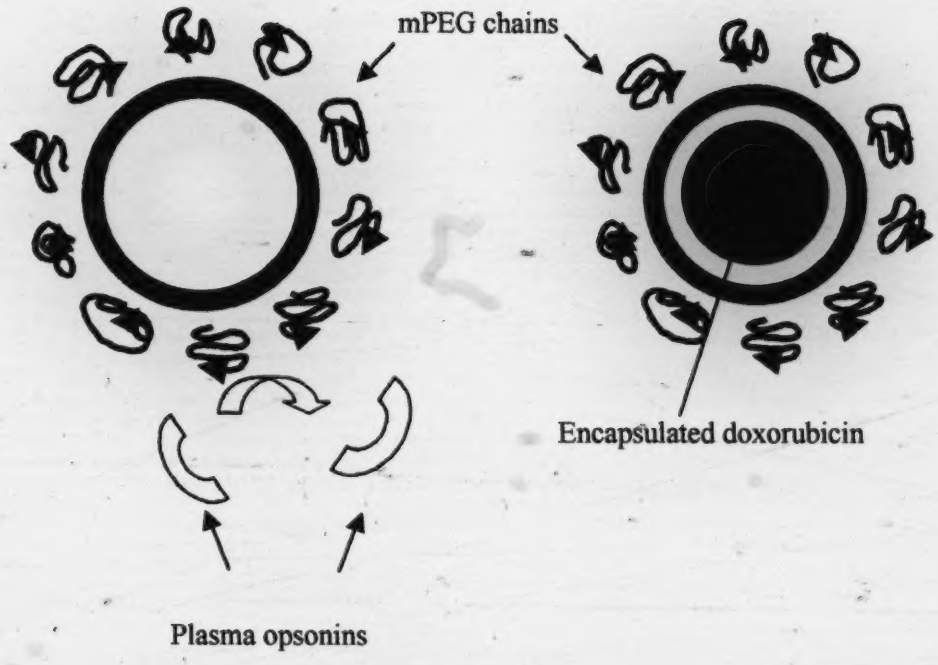


**Figure 1.5**. STEALTH® liposome and a STEALTH® liposomal doxorubicin. The mPEG chains increase surface hydration and inhibit the binding of plasma proteins and opsonins, resulting in longer circulation times.

pharmaceutical standards; it is currently the most used sterically stabilizing agent (69).

Although SL have long circulations *in vivo*, recent experiments have demonstrated that, when experimental animals receive multiple injections of SL (less than 4 weeks apart), the second dose is cleared rapidly from circulation into the liver and spleen (73-75). Dams and colleagues demonstrated that for weekly doses of SL in rats the second dose is removed from circulation quickly, but that this effect decreases for subsequent doses and the fourth dose has PK similar to the first dose. They also demonstrated that, if the second dose is administered 4 weeks after the first, the enhancement in clearance is of lower magnitude. It was further demonstrated that a heat-labile 150 kDa serum factor is responsible for this phenomenon in rats (73). This work was recently confirmed by the same group and other researchers (74, 75). It is important to point out that this was a species-dependent phenomenon, which occurred in rats and a rhesus monkey, but not in mice (73). Secondly, this phenomenon only occurs with "empty" SL and does not occur with SL containing the anticancer drug DXR. Thus, this effect may be a more relevant consideration for the use of SL as carriers for diagnostic imaging agents than for SL anticancer drugs (76). The failure to observe this effect for DXR-containing liposomes is most likely due to the toxicity of DXR toward the cells that produce this factor. Other groups have demonstrated MPS toxicity of liposomal DXR (i.e., the tissue responsible for the clearance of liposomal DXR) (77). However, the relevance of these studies to anticancer drug delivery is debatable, as they used large (200 nm diameter), leaky,

CLip (eggPC:CHOL, 55:45 mol/mol), which are more likely to be removed quickly from the circulation by the MPS and to dump their cytotoxic drugs. More recent studies, looking at blood bacterial clearance in rats, have demonstrated a lack of substantial MPS toxicity when SL-DXR is given at clinically relevant doses (78).

**1.10 Tissue and Tumor Biodistribution of SL**

Soon after the description of $GM_1$, it was demonstrated that the long circulation time of sterically stabilized liposomes allowed them to accumulate in non-MPS tissues that had enhanced vascular permeability (e.g., tumor tissue) to a greater extent than CLip (64, 79). This was followed by studies demonstrating that drug-loaded SL were capable of delivering increased levels of drug (e.g., DXR) to tumors and that this resulted in increased therapeutic activity for these formulations (80-82).

Unlike normal tissues that have tight junctions in their endothelial linings, tumors have defective endothelial linings with openings and gaps that can range in size from 380-780 nm for most subcutaneously implanted tumors (83). The actual size of these openings is dependent upon the particular tumor model and the anatomical location of tumor implantation, and in some cases can be as large as 4.7 μm (83-87). These gaps allow the extravasation of liposomes and macromolecules of appropriate sizes, and along with the impaired lymphatic drainage of solid tumors form the basis for the enhanced permeability and retention effect (EPR) originally described for the drug-polymer conjugate SMANCS (recently reviewed by Maeda et al, (88, 89)).

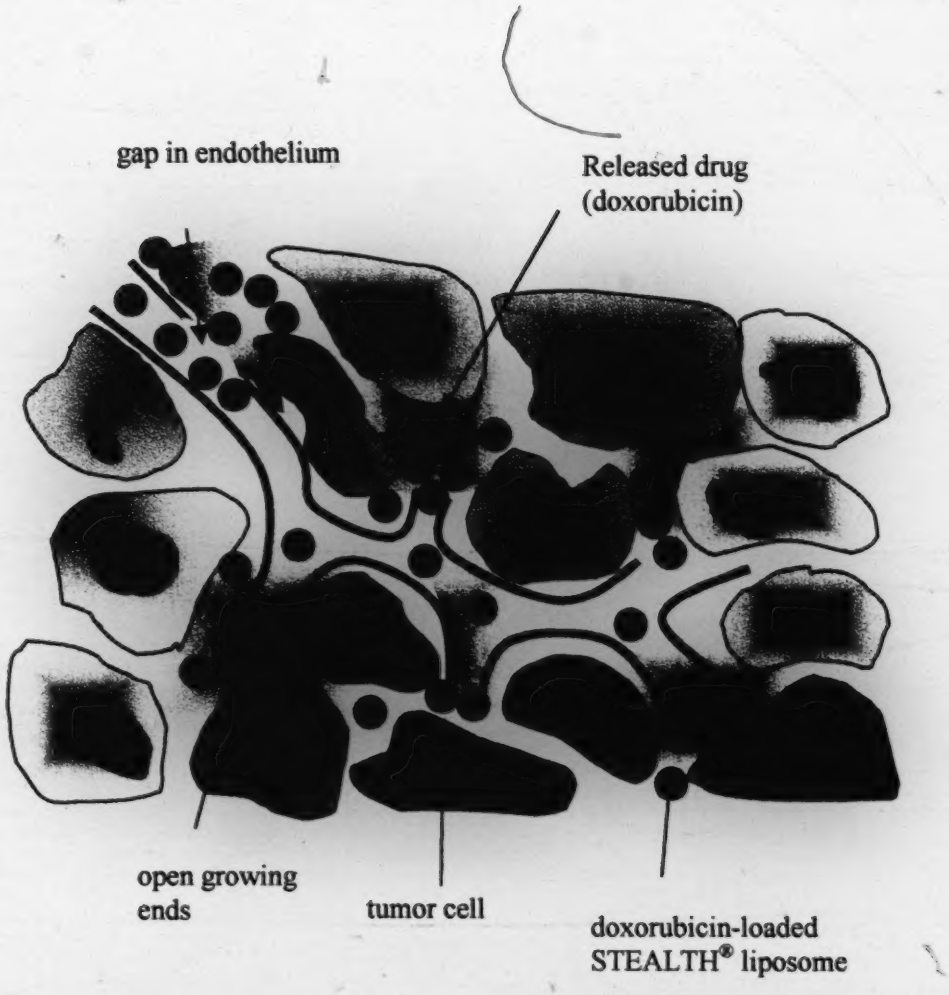


**Figure 1.6.** Passive targeting of doxorubicin-loaded STEALTH® liposomes in a solid tumor. The endothelial lining of most subcutaneously implanted tumors contains gaps (380-780 nm) and open growing ends that allow for the extravasation of liposomes. Due to their long circulation time, STEALTH® liposomes will accumulate in the tumor's interstitial space through these gaps. After localizing in tumor, they will slowly release their contents, in this case doxorubicin, by diffusion down their concentration gradients.

Thus, as liposomes circulate through the vasculature of solid tumors they are able to extravasate into the tumor's interstitial space in a process called passive targeting (**Figure 1.6**) (90, 91). Liposomes are large particles and their diffusion is limited once they localize in solid tumors (86, 92), although in experimental models the extent of diffusion is dependent on tumor type and location (93). Current thinking regarding the mechanism of liposomal drug action is that the drug (e.g., DXR) is slowly released from liposomes as the carrier degrades in the tumor's interstitial space.

Although large gaps exist in tumor endothelium, the extravasation of liposomes is still size-dependent. A study by Ishida *et al.* demonstrated that, for equivalent blood concentrations, small SL (~120 nm diameter) reached higher concentrations in tumor than larger SL (~ 400 nm) (91). Thus the odds of any particle passing through a tumor's endothelial pore increases as the particle size decreases relative to the diameter of the pore.

Although there have been no systematic studies of the phenomenon, it has been noted that long circulating liposomes localize in skin to a greater extent than CLip (64, 68, 80, 94-96). The long circulation time and small size of SL is thought to facilitate extravasation in cutaneous tissues, especially in areas of the skin subjected to pressure (e.g. flexure creases of the hands) (49). As pointed out by Gabizon and co-workers, although liposome concentrations in skin are generally lower than in tumor, the skin's mass makes it the largest depot for liposome localization (in mice) (96). Despite the fact that the importance of cutaneous tissues has previously been

alluded to in the literature, there is relatively little data exploring factors that govern the accumulation of liposomes or liposomal drugs into the skin, even though the dose-limiting cutaneous toxicities of SL-DXR have been known for several years (1, 46).

**1.11 Liposomal Doxorubicin**

DXR is one of the most widely used anticancer drugs; it has anticancer activity in a wide range of tumors including cancer of the breast, lung, thyroid, ovary, stomach and soft-tissue sarcomas (97). The structure of DXR is seen in **Figure 1.7**. Proposed mechanisms for the cytotoxicity of DXR include: topoisomerase II inhibition, intercalation into and cross-linking of DNA, the formation of DNA adducts, oxidative damage via the formation of free radicals, and induction of apoptosis through the generation of ceramide (97-99). In humans, although conventionally administered DXR (i.e., bolus, non-liposomal) binds to plasma proteins, it is extensively distributed to tissues (volume of distribution, $V_d$ 20-30 L/kg); its elimination can be described using triexponential models ($t_{1/2\alpha}$ 12 minutes, $t_{1/2\beta}$ 3.3 hours, $t_{1/2\gamma}$ 30 hours) (97, 100). The toxicities of DXR include nausea, vomiting, alopecia, infusion reactions, extravasation injuries, myelosuppression and cardiomyopathy (97). Acutely, DXR therapy is limited by myelosuppression, with leucopenia being predominant; onset is within two weeks with recovery by four weeks after administration. Cumulative doses of DXR should not exceed 550 mg/m$^2$, as the incidence of DXR-associated cardiomyopathy, manifesting as congestive heart failure (CHF), increases once this dose is exceeded (100). The mechanism of this toxicity is thought to be mediated by free radical damage to cardiac myocytes and is

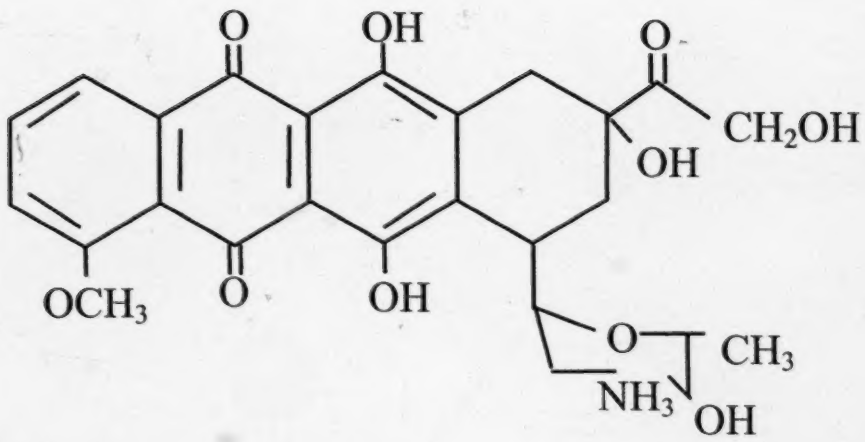


**Figure 1.7.** Chemical structure of doxorubicin

related to peak DXR levels in the heart (97). It is important to emphasize that therapy with DXR must be stopped when this threshold is reached, even if patients are responding to therapy.

Changing the method of administration can alter the toxicities of DXR. Delivering DXR as a prolonged infusion, over several days to weeks, reduces peak drug levels in the heart and decreases cardiac toxicity, but it results in the development of cutaneous toxicities such as PPE (see below) (101, 102). This method of delivery is not routinely used due to practical aspects, the dangers of DXR extravasation injury, and the need for prolonged central venous access in an ambulatory setting.

Therefore, due to its broad spectrum of antitumor activity and the need to reduce its toxicity, DXR was an ideal candidate to formulate into liposomes for clinical use. Further, as previously mentioned (**1.5 Drug Loading**), its chemistry allowed for the development of stable formulations having efficient drug loading. Experimental and clinical data have demonstrated that encapsulating DXR within liposomes reduces its cardiac toxicities by lowering peak drug concentrations in the heart (10, 103, 104). Specifically, the use of SL as a drug delivery system has allowed cumulative doses exceeding 1000 $mg/m^2$ to be administered without clinical evidence of heart failure; the incidence of other toxicities associated with conventionally administered DXR has also been reduced (105-107).

In pre-clinical models, the prolonged circulation time and increased tumor accumulation of SL-DXR translated into increased therapeutic activity in a variety of

tumor models (recently reviewed by Drummond et al. (56)). The tumor models tested included primary (108), syngeneic (80, 82, 109) and human xenograft (110, 111) models in mice as well as rat tumors (112, 113). Due to the high degree of therapeutic activity and improved toxicity profile, clinical trials were then undertaken.

**1.12 Pilot Trial and Phase I Studies of STEALTH® Liposomal Doxorubicin**

In a pilot clinical study comparing free DXR and SL-DXR, patients with various malignancies were administered either 25 or 50 mg/m$^2$ DXR as either free drug or SL-DXR (46). For SL-DXR, stomatitis was the most serious toxicity, occurring in 5/15 patients at 50 mg/m$^2$; other toxicities were mild (grade 1-2) and included nausea with sporadic vomiting. PPE also occurred in two patients after three doses, and resolved with a two-week treatment delay. No clinically relevant cardiac toxicity was observed. Liposomal delivery resulted in a 4-16 fold increased accumulation of drug into the malignant exudates of patients compared to free drug. Patients receiving conventional DXR developed myelosuppression (grade 1-3). There were two responses in this study; however, the design of the trial (cross-over) made it difficult to determine if the response could be attributed to SL-DXR therapy. Pharmacokinetic parameters were determined for the patients receiving SL-DXR and were $t_{1/2\alpha}$ 2 hours, $t_{1/2\beta}$ 45 hours, CL 0.08 L/h and a $V_d$ of 4.1 L (approximately 0.058 L/kg for a hypothetical 70 kg person).

Another pilot study in patients with AIDS-related Kaposi's sarcoma was performed comparing Caelyx® to conventional DXR at doses of 10, 20 and 40 mg/m$^2$ (114). The nine patients receiving Caelyx® had a median $t_{1/2\beta}$ of 41.3 hours, which is

consistent with the above study. Caelyx® also delivered between 5.2-11.4 times as much DXR to Kaposi's sarcoma lesions as conventional DXR. The most common toxicity seen in these patients was neutropenia, with 3/9 patients experiencing greater than grade 2 toxicity. The hematological toxicity seen in this study was likely due to the co-morbidities in these patients.

The results of two larger Phase I dose escalation studies in patients with various malignancies were published together (1). They demonstrated that stomatitis was the dose-limiting toxicity for a single dose of Caelyx® (>70 mg/m$^2$), and that an increased incidence of PPE was associated with dose intensities exceeding 12.5 mg/m$^2$/wk (1). In these studies myelosuppression was mild and cardiac toxicity, as measured by left ventricular ejection fractions, did not change from baseline (except for one patient whose baseline was not determined at the study site). Interestingly, out of 45 assessable patients there were 8 confirmed partial responses, 7 patients experienced improvements and 4 patients had stable disease. Based on these trials Phase II studies were undertaken in patients with AIDS-related Kaposi's sarcoma and solid tumors.

**1.13 Phase II and Phase III Studies of STEALTH® Liposomal Doxorubicin**

Caelyx® has been tested in several Phase II and Phase III trials. For the treatment of AIDS-related Kaposi's sarcoma, it demonstrated superior therapeutic activity in two Phase III trials comparing it to then standard therapy of bleomycin and vincristine (BV) with or without conventional DXR (ABV) (115, 116). In these studies single agent Caelyx® (20 mg/m$^2$ q2wk or 20 mg/m$^2$ q3wk) demonstrated

overall response rates of 45.9% and 58.7% compared to 24.8% (ABV) and 23.3% (BV), respectively. In the study comparing Caelyx® to BV, the former was more myelosuppressive, but was well tolerated overall (116). These studies led to the clinical approval of Caelyx® for the treatment of Kaposi's sarcoma in 1995.

Caelyx® demonstrated activity in refractory ovarian cancer (disease progression <6 months following therapy regimes utilizing platinum-based compounds or taxanes) in two Phase II and one Phase III trial (117-119). Initial trials demonstrated that Caelyx® was active at a dose of 40 mg/m$^2$ every three or four weeks, and the response rate was 25.7% (117). Grade 3/4 toxicities included PPE (see below) in 10/35 patients, neutropenia (7/35) and stomatitis (5/35). Reducing the dose or increasing the dose interval reduced PPE severity. In another Phase II study Caelyx® achieved an overall response rate of 15/82 (18.3%), at a dose of 50 mg/m$^2$ q4wk, in tumors refractory to paclitaxel and platinum compound-based therapy (118). In this study PPE was again the dose limiting toxicity and dose adjustment was necessary for 38/82 patients (43.8%). A Phase III study was then undertaken comparing Caelyx® to topotecan in patients with ovarian cancer refractory to platinum compound-based chemotherapy (119). In this study Caelyx® (50 mg/m$^2$ q4wk) showed comparable levels of efficacy to topotecan with an overall decrease in grade 3/4 toxicities. For example, the most common grade 3/4 toxicity in the Caelyx® arm was PPE in 55/239 (23%) patients compared to the topotecan arm where 180/235 (76.6%) patients had grade 3/4 neutropenia. Caelyx® has since received approval for

use in treating ovarian cancer that is refractory to treatment with platinum-based compounds and taxanes.

For patients with metastatic breast cancer (71 patients, 257 cycles of therapy) Caelyx® was administered at 45-60 mg/m$^2$ every 3 to 4 weeks and had an overall response rate of 31% with a further 31% of patients having stable disease during treatment (120). Similar to the ovarian cancer studies, skin reactions were the dose limiting toxicity. The incidence of PPE in patients receiving 60 mg/m$^2$ q3wk was 54% (7/13); four patients developed PPE after cycle 2, two after cycle 3 and one after cycle 5. The incidence of PPE dropped to 16% (5/32) when the dose was reduced to 45 mg/m$^2$ q4wk. Myelosuppression was generally mild and was ≥ grade 3 in only 10% of cycles (27% of patients). Since this study, several other trials have been undertaken examining the use of Caelyx® to treat breast cancer in combination with other chemotherapeutic agents including vinorelbine, gemcitabine, and docetaxel (121-123).

Further clinical trials have confirmed the therapeutic activity and altered DXR toxicity profile of Caelyx® in a number of tumors including: mesothelioma, colorectal cancer, soft tissue and bone sarcoma, cutaneous T-cell lymphoma, small-cell lung cancer, malignant gliomas, gastric cancer and head and neck cancers (124-131). Although Caelyx® has shown reasonable therapeutic activity in a wide range of tumors, like all anticancer therapies its activity was limited in pretreated patients with resistant tumors (132).

### 1.14 Toxicities of Caelyx®

As previously mentioned, myelosuppression was a common toxicity of Caelyx® for AIDS-patients with Kaposi's sarcoma, but in other studies the incidence of PPE and mucositis overshadowed myelosuppression. This is likely due to co-morbidities in patients with AIDS (115-117, 120). The fact that PPE was rare in the Kaposi's sarcoma trials was due to the use of relatively low doses and dose intensities of 6.67 mg/m$^2$/wk (115) and 10 mg/m$^2$/wk (116). Trials of Caelyx® in solid tumors (ovarian and breast cancer) used higher dose intensities (10-15 mg/m$^2$/wk; 45-60 mg/m$^2$ q3wks or q4wk) and PPE was defined as the dose-limiting toxicity (117, 118, 120). As clinical experience with Caelyx® grew, it was recognized that the dose intensity of ~10-12 mg/m$^2$/wk limited adverse skin reactions (106, 117, 120, 133).

### 1.15 Palmar-Plantar Erythrodysesthesia

Although PPE is the dose limiting toxicity of Caelyx®, it was originally described by Lokich and Moore in patients receiving prolonged infusions of 5-flurouracil (5-FU) or DXR (134). Clinically, PPE starts with dysesthesia that leads to edema, and erythema; if left unchecked, blistering and cracking of the skin will occur (134-136). High-grade lesions are extremely painful and patients have described the syndrome as feeling as though their hands or feet are "on fire". Histological evaluation of PPE lesions shows an inflammatory infiltration with hyperkeratosis; necrotic and pycnotic cells are also seen in the basal layers of the skin, suggesting drug-associated toxicity to basal keratinocytes (48, 135, 137). Discontinuation of therapy results in desquamation and re-epithelization of affected areas, usually within

**Table 1.2** Clinical grading scale for toxicities of Caelyx®. Stomatitis is dose dependent and PPE is schedule dependent (from reference (118)).

| Grade | Stomatitis | PPE |
|---|---|---|
| 1 | Painless ulcers or mild soreness | Mild erythema, swelling or desquamation not interfering with activities of daily living |
| 2 | Painful erythema, edema, or ulcers, but can eat | Erythema, desquamation or swelling interfering with, but not precluding, normal physical activities; small blisters or ulcerations less than 2 cm in diameter |
| 3 | Painful erythema, edema or ulcers but cannot eat | Blistering, ulceration or swelling interfering with walking or normal daily activities; cannot wear regular clothing |
| 4 | Requires parenteral or enteral support | Diffuse or local process causing infectious complications, or a bedridden state or hospitalization |

four weeks; reinstatement of treatment, without dose reduction, results in a recurrence of symptoms (134, 136). Clinically, PPE and stomatitis/mucositis are graded on a scale from 1-4 based on the increasing severity of toxicity (**Table 1.2**).

Gabizon and co-workers described PPE resulting from STEALTH® liposomal DXR as being indistinguishable from PPE induced by non-liposomal drugs (138), and, as previously mentioned, more reports followed as clinical experience with Caelyx® grew (1, 117-119, 137, 139). For Caelyx®-associated PPE, clinical and experimental data have demonstrated that the likelihood of developing the syndrome is related to the dose intensity of Caelyx® therapy, and increases with dose intensities exceeding 10-12 $mg/m^2/wk$ (106, 117, 120, 133, 140). In addition to the palms of the hands and soles of the feet, Caelyx®-induced lesions also occur with increased frequency in areas of skin that are subjected to pressure or irritation, such as belt lines or where tight clothing rests upon the skin (48).

Clinically, dose delay and dose reduction are the most effective interventions for PPE once lesions start to develop (**Table 1.3**). To try and reduce lesion severity, patients receiving Caelyx® are counseled to avoid situations that increase vasodilation (e.g., hot baths or showers) and pressure on the skin (e.g., leaning on one's elbows or wearing tight clothes) as these activities increase the number of liposomes localizing to the skin as evidenced by the anatomical distribution of PPE lesions (48). Attempts have been made to treat PPE lesions once they develop. Treatments showing some efficacy include topical DMSO and oral pyridoxine (vitamin $B_6$); topical corticosteroids had no effect (135, 141-143). With the exception of the study by Vail

**Table 1.3.** Dose delay protocol for patients developing cutaneous toxicities with Caelyx®, from reference (118).

| Stomatitis or PPE Grade | Week after dose | | |
|---|---|---|---|
| | 4 | 5 | 6 |
| 1 | Redose unless patient has experienced a previous grade 3 or 4 toxicity, in which case wait an additional week | Redose unless patient has experienced a previous grade 3 or 4 toxicity, in which case wait an additional week | Redose at 25% dose reduction; return to 4-week interval or withdraw patient at investigator's assessment |
| 2 | Wait an additional week | Wait an additional week | Redose at 25% dose reduction; return to 4-week interval or withdraw patient at investigator's assessment |
| 3 | Wait an additional week | Wait an additional week | Withdraw patient |
| 4 | Wait an additional week | Wait an additional week | Withdraw patient |

and co-workers in companion dogs, most of these reports are case studies with a small number of patients, and larger prospective studies are needed to determine the best intervention to reduce the symptoms of PPE (142).

A recent clinical study addressed the issue of reducing PPE by altering the dose and dose schedule (144). In this study, patients with refractory gynecological malignancies received Caelyx® at a dose intensity of 10 mg/m$^2$/wk (40 mg/m$^2$ q4wk) instead of 12.5 mg/m$^2$/wk (50 mg/m$^2$ q4wk) in a palliative setting. Some antitumor responses (4/49) were seen in these previously treated patients, and the severity of PPE was reduced with no grade 3/4 lesions (144).

**1.16 Hypothesis for the Development of Palmar-Plantar Erythrodysesthesia**

The current hypothesis for the development of PPE is that the small size (100 nm diameter) and long circulation time of Caelyx® ($t_{1/2}$ is approximately 48-90 hours in humans) allows liposomes to accumulate in the skin (46, 48, 106). The accumulation of liposomes is thought to be greatest in skin that experiences vasodilation resulting from pressure or irritation due to the anatomical distribution of lesions, such as the flexure creases of the hands or soles of the feet. PPE lesions then develop as the basal layers of the skin are damaged after prolonged exposed to DXR as the liposomes slowly release their contents and/or are cleared. In other words, the slow rate of drug release in the skin mimics a prolonged infusion.

Clinical and laboratory data support this hypothesis. First, PPE lesions in humans develop primarily on the hands, feet or around areas where tight clothes or belts rest against the skin (pressure is exerted on these surfaces during activities of

daily living) (48, 137). Secondly, liposomes with long circulating properties are known to localize in the skin of experimental animals to a greater extent than liposomes with shorter circulation times (64, 68, 145). As already mentioned, Myocet™, which has a different PK profile than Caelyx®, does not produce PPE.

**1.17 Experimental Model**

A murine model (BALB/c mice) was used to test the effects of a number of parameters on the development of PPE. The tumor model selected was the 4T1 murine mammary carcinoma originally described by Aslakson and Miller (146). The cell line was derived from a spontaneously arising mammary tumor from a BALB/cfC$_3$H mouse and the cell line is a thioguanine-resistant, metastatic adenocarcinoma. The authors did not determine the mechanism of drug resistance, but they used the phenotype as a means to quantify occult metastatic tumor cells in various organs (146-148). *In vivo*, the 4T1 cell line grows optimally when implanted orthotopically into the mammary fat pad of mice and it will spontaneously metastasize to the lungs (146, 149).

The 4T1 murine mammary carcinoma is a good model for several reasons. This tumor has previously been shown to grow well in BALB/c mice obtained from the breeding colony at the University of Alberta Health Sciences Laboratory Animal Services (>99% tumor take rate). Orthotopic implantation mimics the physiological milieu of the tumor's original anatomical location, and the tumor is sensitive to SL-DXR *in vivo* (150). Since Caelyx® is currently being evaluated for the treatment of metastatic breast cancer in humans (at dose intensities that are likely to produce PPE),

an orthotopically implanted murine mammary tumor is an excellent choice as it more closely mimics the natural history of breast cancer compared to subcutaneously implanted tumor models. Lastly, this tumor model grows in conventional inbred mice, which negates the need for the special housing required when using human xenograft models in immunodeficient mice.

The studies in this thesis focus on the PK, BD and therapeutic activity of SL. Particular attention is given to the cutaneous and tumor localization of liposomes. Two "cutaneous tissues" from mice were studied: dorsal skin and paws. Paws were selected because PPE lesions occur primarily on the hands and feet of humans, and similar to human hands and feet, the paws of mice are exposed to pressure as mice move about their cages, groom, feed, etc. Skin from the back of mice was also collected to determine the accumulation of liposome/liposomal DXR in cutaneous tissues that were not subjected to pressure. Lastly, tumor and plasma (or blood) were also assayed for liposomes and/or liposomal drug.

**1.18 Thesis Outline**

The studies presented in the following chapters of this thesis explore the importance of liposome size, drug release rate, dose and dose intensity for the development of PPE. These studies also attempt to reduce the cutaneous accumulation of liposomal DXR, while maintaining high levels of antitumor activity. Chapter 3 examines how the BD of liposomes to 4T1 tumors and cutaneous tissues of mice is altered by increasing the liposome diameter of Caelyx®-like formulations. The rationale for these experiments was that the biodistribution of liposomes is size

dependent, and since tumors have endothelial gaps that range in size from 380-780 nm (151), it may be possible to decrease the accumulation of liposomes into cutaneous tissues, which lack these gaps, while still having good localization of liposomes into tumors. Therapeutic experiments were performed to determine the therapeutic implications of the PK and BD experiments.

Chapter 4 explores the possibility of reducing the accumulation of DXR (from SL) into murine cutaneous tissues by altering DXR leakage rates. Various formulations of liposomal DXR were prepared and tested both *in vitro* and *in vivo*. Data from Chapter 3 determined that there are differences in the time course of liposome accumulation between tumor and cutaneous tissues, with the former accumulating liposomes faster and to a higher extent than the latter. Therefore, the rationale for the experiments in Chapter 4 was that the cutaneous toxicities of liposomal DXR may be reduced if a liposome DDS can be developed that will release the majority of its DXR soon after liposome concentrations peak in tumor, but before cutaneous concentrations peak. DXR leakage rate was manipulated by altering the fatty acyl chain length and degree of saturation, as well as the cholesterol content of the lipid bilayers. Again, experiments were performed to determine the therapeutic significance of changes in the rate of DXR leakage from liposomes.

The data in Chapter 5 examine the relationship between the PK and BD of Caelyx® and its dose schedule and dose intensity with repeat intravenous administration. Two different sets of experiments were performed in this Chapter. First, the influence of dose delay (i.e., reducing the dose intensity) on the PK and BD

of DXR (from Caelyx®) into the skin and paws of non-tumor-bearing mice were studied at a constant total dose. This was done because dose delay is the first intervention used when PPE lesions develop in the clinic. Next, the PK and BD of DXR (from Caelyx®) into tumors and cutaneous tissues of mice was studied for different dose schedules with the same dose intensity. These experiments were performed because cutaneous toxicities limit the dose intensity of Caelyx® therapy in humans, and recent data suggests that for a given dose intensity it is better to administer larger doses less often than small doses more often (152). The therapeutic activity of these dose regimes was then tested in 4T1 murine mammary carcinoma models. These latter experiments are important as they mimic the clinical use of Caelyx® by using repeat administration.

Lastly, Chapter 6 provides a summarizing discussion and future directions for reducing the incidence and severity of the cutaneous toxicities of Caelyx® and for increasing the therapeutic index of liposomal DXR by increasing its therapeutic activity.

# Chapter 2

## Materials and Methods

## Chapter 2 Materials and Methods

### 2.1 Materials

Hydrogenated soy phosphatidylcholine (HSPC), methoxypolyethyene glycol ($M_r$ 2000)-distearoylphosphatidylethanolamine (mPEG-DSPE), doxorubicin hydrochloride (DXR) and Caelyx® (STEALTH® liposomal DXR, composed of HSPC:CHOL:mPEG-DSPE at 55:40:5 molar ratio), were generous gifts from ALZA Corporation (Mountain View, CA). Dimyristoylphosphatidylcholine (DMPC), dioleoylphosphatidylcholine (DOPC), dipalmitoylphosphatidylcholine (DPPC), distearoylphosphatidylcholine (DSPC), egg yolk phosphatidylcholine (eggPC), palmitoyl-myristoylphosphatidylcholine (PMPC), palmitoyl-oleoylphosphatidylcholine (POPC), stearoyl-myristoylphosphatidylcholine (SMPC), stearoyl-palmitoylphosphatidylcholine (SPPC) and cholesterol (CHOL) were purchased from Avanti Polar Lipids (Alabaster, AL). Dialysis cassettes (Slide-a-lyzer®) with a molecular weight cuff-off of 10 kDa were from Pierce (via MJS Biolynx Inc., Brockville ON). Sephadex-G50 and Sepharose CL-4B were from Amersham-Pharmacia Biotech (Baie d'Urfe, PQ). Minimal essential medium (MEM) and adult bovine serum (ABS) were from Sigma Chemical Company (St. Louis, MO). Fetal bovine serum (FBS), penicillin and streptomycin were from Life Technologies Inc. (Burlington, ON). Methoxyflurane (Metafane) was from Janssen (Toronto, ON) and halothane was from MTC Pharmaceuticals (Cambridge, ON). Sterile, pyrogen-free saline and dextrose 5% in water (D5W; UPS) was purchased from the University of Alberta Hospitals' outpatient pharmacy (Baxter, Toronto,

ON). Sterile saline was supplemented with 25 mM (4-(2-hydroxyethyl)-1-piperazineethanesulfonic acid (HEPES), pH 7.4 (HBS). $^{14}$C-doxorubicin was from Amersham Biosciences (Baie d'Urfe, PQ). $^{3}$H-cholesteryl hexadecylether ($^{3}$H-CHE) was from Perkin-Elmer Biosciences (Boston, MA). Solvable (tissue solubilzer) and Ultima Gold (scintillation fluor) were from PerkinElmer Lifesciences (Mississauga, ON). Na$^{125}$I was purchased from Amersham (Oakville, ON) and $^{125}$I-tyraminylinulin ($^{125}$I-TI; an aqueous space marker for liposomes) was prepared as previously described (153). $^{111}$In-oxine was from Nycomed Amersham (Oakville, ON). All other chemicals were of the highest grade possible.

**2.2 Tumor Cell Line**

The 4T1 mouse mammary carcinoma cell line is a metastatic, thioguanine-resistant cell line, and was a generous gift from Dr. Fred Miller (Barbara Ann Karmanlos Cancer Institute, Detroit, MI) (146). The cell line was maintained in MEM supplemented with 10 % FBS, penicillin (100 units/ml) and streptomycin (100 μg/ml) at 37°C in a humidified incubator with a 5% $CO_2$ atmosphere. Cells were harvested for passage with the use of phosphate buffered-saline containing EDTA (PBS-EDTA; 0.54 mM EDTA, 137 mM NaCl, 3 mM KCl, 8 mM $Na_2HPO_4$, 1.5 mM $KH_2PO_4$, pH 7.4) followed by trypsin-EDTA (0.05% trypsin in 137 mM NaCl, 5.4 mM KCl, 7 mM $NaHCO_3$, 0.34 mM EDTA).

**2.3 Liposome Preparation**

Liposomes were prepared by thin film hydration. For the PK, BD and therapeutic experiments described in Chapter 3, all liposomes were composed of

HSPC:CHOL:mPEG-DSPE (55:40:5 mole). For these BD experiments liposomes were prepared by hydrating dried lipid films with HEPES-buffered saline (HBS) containing $^{125}$I-TI. Liposomes were sized by sequential extrusion through stacked Nuclepore polycarbonate filters (0.4 μm down to 0.080 μm) using an extrusion device (Lipex Biomembranes, Vancouver, BC) at 65°C. Free $^{125}$I-TI was separated from liposome-encapsulated $^{125}$I-TI by size exclusion chromatography on a Sepharose CL-4B column eluted with HBS. Mean liposome diameters for preparations used for biodistribution experiments in Chapter 3 were as follows: 82, 101, 154 or 241 nm. The diameter of liposomes in Chapter 4 were typically 100 ± 10 nm, and had low polydispersities.

For therapeutic experiments in Chapter 3, and all experiments in Chapter 4, DXR was remote-loaded with an ammonium sulfate gradient, as previously described and illustrated in **Figure 1.4** (26). Briefly, lipid films were hydrated in 250 mM ammonium sulfate and preparations with low polydispersity were made by extrusion through Nuclepore filters with appropriate pore sizes. The external buffer was changed to sodium acetate (pH 5.5) by passage over a Sephadex G-50 column, and then DXR, dissolved in 10% sucrose (wt/vol), was incubated with the liposomes at a 0.2:1 drug:lipid ratio for 15-60 minutes at 65°C. Unencapsulated DXR was separated by passage over a Sephadex G-50 column equilibrated with HBS, pH 7.4. Lipid concentrations were determined by the method of Bartlett or by the specific activity of the non-metabolizable, non-exchangeable lipid marker $^{3}$H-CHE (154, 155).

Liposomes were sized by dynamic light scattering using a Brookhaven BI-90 particle sizer (Brookhaven Instruments, Holtsville, NY). DXR concentrations were determined spectrophotometrically from a standard curve in methanol extracts at 480 nm.

**2.4 Mice**

Female BALB/c mice (6-8 weeks) were purchased from the breeding colony at Health Sciences Laboratory Animal Services. Mice were housed under standard conditions and had access to food and water *ad libitum*. All animal protocols were approved by the Health Sciences Animal Policy and Welfare Committee, University of Alberta and are in accordance with the Guide to the Care and Use of Experimental Animals set forth by the Canadian Council on Animal Care.

**2.5 Tumor Implantation**

Tumors were implanted as previous described (150). Female BALB/c mice (6-8 weeks) were anesthetized with either methoxyflurane or halothane. The lower abdomen was shaved and a 6-8 mm incision was made adjacent to the mid-line to expose the right #4 mammary fat pad where $10^5$ 4T1 cells were injected in 10 μL of full media. The incision was then closed with a surgical wound clip, which was removed 7 days later.

**2.6 Blood Content of the 4T1 Tumor**

Murine erythrocytes (rbc) were radiolabeled using $^{111}$In-oxine in order to determine the tumor blood volume of the 4T1 tumor. Female BALB/c mice (6-8 weeks) were euthanized and whole blood was collected via cardiac puncture with a

heparinized syringe. The collected blood (approximately 0.5 mL) was diluted with 1 mL of HBS pH 7.4, and red cells were pelleted by centrifugation at 560 x g for 5 minutes. The pellet was washed twice in a similar manner with 1 mL of HBS. $^{111}$In-oxine (50 μL) was then incubated for 15 minutes with the washed rbc. The pellet was again washed three times with 1 mL HBS before final resuspension with 0.5 mL of HBS. For each day of experiments, fresh rbc were collected and labeled.

Mice were implanted with 4T1 tumors as described above. On days 5-15 after injection, mice (n=3, except day 15 where n=2) were injected intravenously (i.v.) with 50 μL of $^{111}$In-rbc; ten minutes after injection the mice were euthanized and tumors were removed, weighed and counted (Beckman 8000 gamma counter). Data are presented as c.p.m. per mg tumor weight normalized to $10^6$ c.p.m. injected.

**2.7 *In vitro* Leakage of Doxorubicin**

The *in vitro* leakage of DXR was measured using a dialysis method. In these experiments, liposomes (mean diameter of 100 ± 15 nm) were incubated in 50% v/v adult bovine serum (ABS):HBS (pH 7.4). Plasma lipoproteins are important in inducing drug leakage from liposomes, and due to difficulties in attaining human plasma ABS was used as a source of plasma lipoproteins. Solutions of liposomes, 0.5 mM lipid, were diluted in 50% ABS, placed in a dialysis cassette with a molecular weight cutoff of 10 kDa, and dialyzed against 200 ml of 50% ABS containing penicillin (100 units/ml) and streptomycin (100 μg/ml) at 37°C (28). This concentration of lipid approximates a 20 g mouse receiving a Caelyx® dose of 5-6 mg/kg of DXR. At various time points, aliquots were withdrawn from the cassette

and stored at 4°C until analysis. DXR fluorescence ($\lambda_{ex}$ 470 nm, $\lambda_{em}$ 590 nm) in acidified methanol (0.075 M HCl) was measured (SLM-AMINCO Model 8100 Series 2 Spectrometer, Spectronics Instruments Inc., Rochester, NY). The results were plotted on a semi log scale (percent remaining fluorescence versus time) and the $t_{1/2}$ was calculated using the regression line from the linear portion of the curve; $r^2$ values for these lines were greater than 0.926 (range 0.926-0.994).

**2.8 Quantification of Doxorubicin**

DXR was quantified in a manner similar to previously published methods (156, 157). This method has the advantages of allowing for the processing of large numbers of samples with high efficiency and allowing for the parallel quantification of liposomal lipid using liquid scintillation counting techniques.

To quantify DXR, tissue homogenates (10%, wt/vol) were prepared in water. Skin and paws were frozen in liquid nitrogen and crushed with a mortar and pestle before homogenization with a Polytron homogenizer (Brinkmann Instruments, Inc., Mississauga, ON). Blood was collected via cardiac puncture with a heparinized syringe and plasma was isolated by centrifugation at 3000 x g for 5 minutes. Homogenate or 25% plasma (200 µl) were placed in a 2 ml micro-centrifuge tube and 100 µl of 10% (vol/vol) Triton X-100, 200 µl of water and 1500 µl acidified isopropanol (0.075 M HCl) were added. The tubes were mixed thoroughly and DXR was allowed to extract from the tissues overnight at -25°C. The next day, the tubes were warmed to room temperature, vortexed for 5 minutes, centrifuged at 15000 x g for 20 min to pellet any particulates, and stored at -80°C until analysis. DXR was

quantified fluorometrically ($\lambda_{ex}$ 470 nm, $\lambda_{em}$ 590 nm) using an SLM-AMINCO Model 8100 Series 2 Spectrometer (Spectronics Instruments Inc., Rochester, NY) against a standard curve. To correct for the background fluorescence of each tissue, standard curves were generated in the presence of tissue homogenate extracts from naïve mice; for these curves $r^2$ >0.97. The data represent the mean ± S.D. of triplicate aliquots from 4-5 mice.

To validate this assay, the fluorescence properties of DXR were used in conjunction with $^{14}$C-DXR. Tissue homogenates were prepared from untreated BALB/c mice, DXR (150 ng or 300 ng) spiked with $^{14}$C-DXR was added to aliquots of the homogenates and incubated overnight at 37°C. The next day, the tissues were extracted as described above and DXR fluorescence was compared against equivalent amounts of $^{14}$C-DXR (150 ng or 300 ng) added to blank homogenates. Afterwards, the samples were taken for liquid scintillation counting. The results were expressed as percent recovered relative fluorescence units (RFU) and percent-recovered c.p.m. The limits of detection using this assay were 0.1 RFU/g of tumor, 0.05 RFU/g of skin and paws and 0.04 RFU/ml plasma were determined from the lowest DXR concentration used for the standard curve. Results are expressed as RFU as this assay does not discriminate between DXR and any fluorescent metabolites that may have similar excitation and emission profiles. The results obtained were in agreement with the previously published results, and this assay was used in subsequent experiments (see Section 4.2: Development of an Extraction Procedure for Doxorubicin) (28, 156-158).

**2.9 Quantification of Liposomal Lipid**

Liposomal lipid was quantified using a method similar to that of Mayer and co-workers using the non-exchangeable, non-metabolizeable lipid marker $^{3}$H-CHE (156). For lipid quantification, 500 µl of Solvable was added to 50 µl of plasma or 200 µl of a 10 % (wt/vol) tissue homogenate (as above). The tissues were allowed to digest at 60°C for 2 hours. After the vials cooled to room temperature, 50 µl of 200 mM EDTA was added before overnight bleaching with 200 µL of hydrogen peroxide (30% vol/vol). Next, 100 µl of 1 M HCl was added, followed by 5 ml Ultima Gold. After mixing thoroughly, the samples were counted in a Beckman LS 6500 liquid scintillation counter. The data represent the mean ± S.D. of triplicate aliquots from 4-5 mice, and are expressed as total lipid µg per ml of plasma or per gram of tissue.

**2.10 Pharmacokinetic and Biodistribution Studies**

PK and BD studies were performed using either $^{125}$I-tyraminylinulin ($^{125}$I-TI), which is a liposomal aqueous space marker, or by measuring the fluorescence of the drug DXR in conjunction with a radiolabeled lipid marker. Mice were dosed based on mg of DXR in the liposomal formulation per kg body weight.

**2.10.1 Pharmacokinetic and Biodistribution Using an Aqueous Space Marker**

For the PK and BD experiments performed in Chapter 3, female BALB/c mice were implanted with the 4T1 mammary carcinoma as described above. Ten days after tumor inoculation mice were injected i.v., via the lateral tail vein, with 200 µl HBS containing 0.5 µmoles of lipid, i.e., $^{125}$I-TI-labeled liposomes (1.5-2.5 x $10^{5}$

c.p.m. per mouse) with mean diameters (polydispersities) of 82 (0.111), 101 (0.122), 154 (0.073) or 241 (0.081) nm. At various times post-injection (24, 48, 72 or 96 h), groups of mice (n=10) were euthanized and organs (tumor, skin and paws) were taken for radioactive counting (Beckman 8000 gamma counter). The skin was washed and shaved to remove hair and contaminating blood, and data from all four paws were pooled. Results are expressed as c.p.m. per mg tissue normalized to $10^6$ injected c.p.m. The data were corrected for the blood volume of organs as previously described (72). Tumor-to-skin and tumor-to-paw ratios were calculated from the data.

### 2.10.2 Pharmacokinetic and Biodistribution Using Drug Fluorescence and a Radioactive Lipid Marker

PK experiments were performed where DXR and liposomal lipid were quantified (Chapter 4). In these experiments DXR was measured fluorometrically ($\lambda_{em}$ 470 nm and $\lambda_{em}$ 590 nm) and liposomal lipid was quantified using the non-exchangeable, non-metabolizable lipid marker $^3$H-CHE (2 μCi/μmole total lipid) (155). Mice were implanted with the 4T1 murine mammary carcinoma as described above. Ten days later they were injected i.v., via the lateral tail vein, with 6 mg/kg (18 mg/m$^2$) liposomal DXR of various compositions. At various time points after injection (1, 12, 24, 48, 72, 168 hours) mice (n=5) were euthanized and tissues and plasma were processed to quantify DXR and lipid as described in Sections 2.8 and 2.9 respectively. PK parameters were calculated as in Section 2.11.

### 2.10.3 Pharmacokinetics of Repeat Administration of Caelyx®

Experiments studying the PK and BD of repeat injections of Caelyx® were undertaken in either naïve mice or mice bearing the 4T1 murine mammary carcinoma (Chapter 5). Caelyx® (used as supplied) was diluted in D5W and 200 µl was injected i.v. via the lateral tail vain. In tumor-free mice, 9 mg/kg (27 mg/m$^2$) of Caelyx® was administered either weekly for a total of 4 doses (q1wk x 4), every two weeks (q2wk x 4), or every 4 weeks (q4wk x 4), for a total dose of 36 mg/kg (108 mg/m$^2$). The dose intensities for these schedules are 9 mg/kg/wk (27 mg/m$^2$/wk), 4.5 mg/kg/wk (13.5 mg/m$^2$/wk) and 2.25 mg/kg/wk (6.75 mg/m$^2$/wk), respectively (159). In another set of experiments, mice bearing the 4T1 murine mammary carcinoma received i.v. injections (via the lateral tail vein) of Caelyx®, starting 10 days after tumor implantation, at a DXR dose intensity of 9 mg/kg/wk (27 mg/m$^2$/wk) given as either 4.5 mg/kg every three days (q3d) for 4 doses, 9 mg/kg q1wk for 2 doses, or 18 mg/kg for one dose. For all these experiments mice (n=4-5 per group) were euthanized at various time points post injection. Organs were removed and DXR quantified as described in Section 2.8. PK parameters were calculated as in Section 2.11.

### 2.11 Pharmacokinetic Analysis

For experiments in Chapters 4 and 5, PK parameters were calculated for total DXR and liposomal lipid (where appropriate). Area under the plasma/tissue concentration versus time curve (AUC) was calculated using the trapezoidal rule with extrapolation to infinity (where appropriate), and $t_{1/2}$ was calculated using the formula $t_{1/2}=0.693/k_{elm}$ where $k_{elm}$ is the elimination constant derived from the best-fit line of

the data using an exponential curve fitter; $r^2$ was also calculated for these curves (160). CL was calculated using the formula CL=dose/$AUC_{0-\infty}$ and $V_d$ was calculated with the formula $V_d$=CL/$k_{elm}$ (160). Tissue elimination $t_{1/2}$'s were calculated in a similar manner, using the terminal slope of the tissue concentration versus time curve. In Chapter 5, tissue elimination $t_{1/2}$'s were not calculated for q1wk dosing as there were not sufficient time points on the terminal portion of the curves. The average steady state concentration ($C_{ss}$) was calculated by taking the $4^{th}$ dose AUC (taken as steady state) as determined by the trapezoidal rule and dividing by the dose interval in hours.

**2.12 Therapeutic Studies**

For all therapeutic studies, mice were implanted with the 4T1 tumor as described above; treatment was started four days after tumor implantation when tumors were just palpable. All injections were i.v. via the lateral tail vein and drug doses are based on mg of DXR for the liposomal formulation per kg of body weight. Tumor volume was monitored and volume was calculated using the formula $v=0.4ab^2$ where a and b are perpendicular diameters and a>b, and are expressed and the mean ± S.D. for (n) mice (161). In all therapeutic experiments mice were euthanized if at any time they showed signs of distress, when tumors started to ulcerate, or when tumors reached greater than 10 mm in both diameters. Results from these experiments are given with a range of n (e.g. n = 6-10 mice); unless stated, this is due to premature ulceration of the lesions and subsequent euthanasia of these animals, with continued monitoring of the remaining mice.

### 2.12.1 Influence of Liposome Size

For therapeutic experiments examining the effect of liposome diameter, groups of five mice were injected i.v. with liposomal DXR (6 mg/kg, 18 mg/m$^2$) of various diameters (polydispersity): 102 (0.152), 156 (0.077), or 254 (0.086) nm. The experiment was repeated once with liposomes having similar mean diameters (polydispersity): 98 (0.140), 159 (0.078), or 256 (0.054) nm. The results at each liposome size were pooled as follows: 100 nm (98 and 102 nm), 157 nm (156 and 159 nm) and 255 nm (254 and 256 nm). All control mice received 200 μL of sterile saline. Results are presented as the mean tumor volume ± S.D. with n= 6-10.

### 2.12.2 Influence of Doxorubicin Leakage Rate

For therapeutic experiments examining the therapeutic activity of liposomes that leak DXR at different rates, groups of six mice were injected i.v. with 6 mg/kg (18 mg/m$^2$) liposomal DXR composed of DSPC:CHOL:mPEG-DSPE, POPC:CHOL:mPEG-DSPE or DOPC:CHOL:mPEG-DPSE. Controls received 200 μL of sterile saline. The experiment was repeated once and the results of the two experiments were pooled. Results are presented as the mean tumor volume ± S.D. with n=5-12, except for mice receiving POPC:CHOL:mPEG liposomes, where n=4-6.

### 2.12.3 Influence of Caelyx® Dose Schedule and Dose Intensity

For therapeutic experiments examining the influence of altering dose schedule and dose intensity, mice received DXR as Caelyx® at a dose schedule of 9 mg/kg (27 mg/m$^2$) q1wk, 9 mg/kg q2wk or 9 mg/kg q4wk for a total of two doses. For

experiments where the dose intensity was kept constant, mice (n=5) received Caelyx® as either one i.v. injection of 18 mg/kg (54 mg/m$^2$), two i.v. injections at 9 mg/kg (27 mg/m$^2$) q1wk or four i.v. injections at 4.5 mg/mg (13.5 mg/m$^2$) q3d to a total drug dose of 18 mg/kg. Both experiments were repeated once, and the results were pooled. Results are expressed as the mean tumor volume ± S.D. for n=4-10.

**2.13 Statistics**

Statistical comparisons were performed using a one-way ANOVA with a Tukey-Krammer post test or Student t-test (as appropriate) on Graph Pad InStat version 3.01 for Windows 95/NT (GraphPad Software, San Diego CA).

# Chapter 3.

## Rate of Biodistribution of STEALTH® Liposomes to Tumor and Skin: Influence of Liposome Diameter and Implications for Toxicity and Therapeutic Activity

**Chapter 3: Results and Discussion**

The experiments in this chapter examine the influence of liposome diameter on the PK and BD of SL with the same lipid composition as Caelyx® (HSPC:CHOL:mPEG-DSPE, 55:40:5 mole) and were published in Charrois and Allen, 2003 (49). The objectives of these experiments were to ascertain the time course of liposome accumulation into the tumor (4T1 murine mammary carcinoma), skin and paws of mice and to determine if a relative increase in liposome accumulation into tumor over skin or paws could be affected by increasing liposome diameter. The rationale for these experiments is that the PK and BD of liposomes are size dependent (57, 91, 94). Tumors have leaky blood vessels with gaps that range in size from 380-780 nm, rendering them permeable to appropriate diameters of liposomes and macromolecules as part of the enhanced retention and permeability effect (88), whereas the capillaries of normal tissues are lined with tight junctions that do not allow for the substantial extravasation of liposomes (83, 92). Thus, an increase in liposome diameter (e.g. 150-250 nm versus the 100 nm of Caelyx®) may reduce liposome accumulation in normal tissues (e.g. skin) without having substantial effects on tumor uptake. In addition to PK and BD experiments, therapeutic experiments were also performed in the same tumor model, using DXR-loaded SL of various diameters, to determine the therapeutic significance of any size-dependent alterations in tissue distribution.

**3.1 Biodistribution Experiments**

For biodistribution experiments, mice were orthotopically implanted with the 4T1 murine mammary carcinoma, and 10 days later they were injected i.v. with $^{125}$I-TI-labelled liposomes (HSPC:CHOL:mPEG, 55:40:5 mole). $^{125}$I-TI is a non-metabolizeable aqueous space label for liposomes and its localization to a tissue represents the accumulation of intact liposomes (153). The mean diameter (polydispersity) of the various preparations was: 82 (0.111), 101 (0.122), 154 (0.073) and 241 (0.081) nm. At 24, 48, 72 or 96 hours after injection, groups of 10 mice were euthanized, and organs (tumor, skin, and paws) were weighed and taken for radioactive counting. The skin was washed and shaved to remove hair and contaminating blood, and data from all four paws were pooled. The results are expressed as c.p.m. per mg tissue, normalized to $10^6$ injected c.p.m. Tumor-to-skin and tumor-to-paw ratios were calculated from the data.

Tumor uptake of $^{125}$I-TI liposomes is shown in **Figure 3.1A**. Tumor accumulation of liposomes was highest at 24 hours for all sizes tested. The largest liposomes (241 nm) had substantially lower tumor levels than the smaller sizes at all time points ($p<0.001$). Some statistically significant differences also occurred among the tumor uptakes of the smaller liposomes, although these may not be therapeutically significant (see results of therapeutic experiments below). For example, the 101 nm liposomes had higher accumulation in tumor than the 82 nm liposomes at 24 and 48

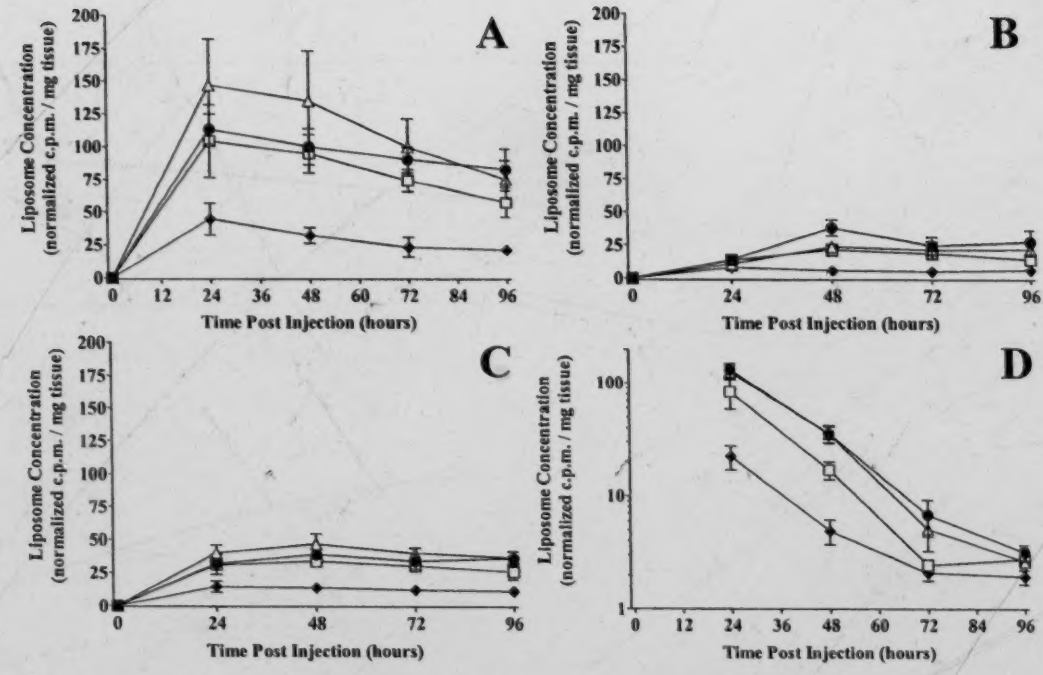


**Figure 3.1.** Accumulation of $^{125}$I-tyraminylinulin liposomes in mouse tissues as a function of time. BALB/c mice were implanted in the #4 mammary fat pad with the 4T1 tumor and injected i.v. 10 days later with $^{125}$I-tyraminylinulin-labelled liposomes of various mean diameters: ●, 82 nm; △, 101 nm; □, 154 nm; ◆, 241 nm. Data are expressed as c.p.m /mg tissue normalized to $10^6$ c.p.m- injected. (A) 4T1 mouse mammary carcinomas, (B) mouse skin, (C) mouse paws (D) blood. Data represent the mean ± S.D., n=10. See text for results of statistical comparisons.

hours after injection ($p<0.05$-$0.01$) and had significantly higher accumulation than the 154 nm liposomes at all time points ($p<0.05$-$0.001$). Also, the 82 nm liposomes had higher tumor levels than the 154 nm liposomes at 72 and 96 hours after injection ($p<0.05$ and $p<0.001$).

Skin accumulation of liposomes is shown in **Figure 3.1B**. Skin levels of liposomes were significantly lower than tumor levels, and, with a few exceptions (154 nm at 24 hours, 101 nm at 48 hours, and 82 nm at 96 hours), were also significantly lower than paw levels ($p<0.05$ to $p<0.001$). Skin levels of the largest liposomes were highest at 24 hours after injection, whereas the smaller sizes had peak levels at 48 hours. For the 48, 72, and 96 hour time points, the largest liposomes had significantly lower skin accumulation than the smaller liposomes ($p< 0.01$ to $p<0.001$). Again these data show that the three smaller sizes of liposomes accumulate to a greater extent in tissue than the largest size of liposomes.

Results of the uptake of liposomes into paws are shown in **Figure 3.1C**. Liposome levels in paws were significantly lower than tumor levels. The level of liposomes in paws was highest at 48 hours, except for the 241 nm liposomes, which plateaued at 24 hours. The largest (241 nm) liposomes attained lower levels in paws than the smaller sizes of liposomes ($p<0.01$ to $p<0.001$). Other statistically significant differences between the paw uptake of the other liposomes were as follows: 101 nm liposomes had higher paw accumulation than the 154 nm liposomes at all time points ($p< 0.01$ to $p<0.001$) and had higher accumulation than the 82 nm

liposomes at 24, 48, and 72 hours ($p<0.05$ to $p<0.01$). The 82 nm liposomes had higher paw levels at 72 and 96 hours than the 154 nm liposomes ($p<0.001$).

Blood levels of liposomes are presented in **Figure 3.1D**. The blood concentrations of the two smallest liposomes (82 nm and 101 nm) are equivalent, and significantly higher than the 241 nm liposomes at all time points ($p<0.05$-$0.001$) and than the 154 nm liposomes, except at 96 hours ($p<0.01$-$0.001$). The 154 nm liposomes achieved higher blood levels than the largest liposomes for 24, 48 and 96 hours ($p<0.001$). These blood levels are consistent with other data showing that liposomal diameter influences circulation times (91, 162).

Tumor-to-skin ratios are presented in **Table 3.1A**. At the 24 hour time point, only the 101 nm liposomes had a significantly higher ratio than the other three sizes of liposomes. ($p<0.01$ to $p<0.001$). There were no other significant differences in the tumor-to-skin ratios for the different sizes of liposomes at all other time points. However, for any given size of liposome, the tumor to skin ratios decreased over time. The three smaller liposome sizes had approximately 8- to 17-fold higher levels in tumor than in skin at 24 hours and this decreased significantly with time to approximately 3- to 4-fold by 96 hours after injection ($p<0.01$ to 0.001). The tumor-to-skin ratios for the largest liposomes (241 nm) also decreased over time, with the ratio at 24 hours being significantly higher than the ratio at 96 hours ($p<0.01$).

Tumor-to-paw ratios are presented in **Table 3.1B**. There were no significant differences within the data columns, i.e., altering liposome size did not produce a

**Table 3.1A.** Tumor-to-skin ratios as a function of time after injection.
Data represent the ratios of liposome levels in tumor and skin (cpm/mg tissue) for the mean ± SD of 10 mice. Ratios were calculated from the data in **Figures 1A** and **1B**.

| Liposome Diameter | 24 hrs | 48 hrs | 72 hrs | 96 hrs |
|---|---|---|---|---|
| 82 nm | 8.8 ± 2.3 | 4.5 ± 1.2 | 4.0 ± 1.6 | 3.3 ± 1.1 |
| 101 nm | 17.0 ± 9.6 | 5.9 ± 2.2 | 5.1 ± 1.9 | 3.7 ± 1.3 |
| 154 nm | 8.4 ± 3.2 | 4.8 ± 1.9 | 4.1 ± 1.0 | 4.1 ± 0.7 |
| 241 nm | 6.3 ± 2.6 | 5.5 ± 1.4 | 5.0 ± 1.8 | 3.6 ± 1.1 |

**Table 3.1B.** Tumor-to-paw ratios as a function of time after injection.
Data represent the ratios of liposome levels in tumor to paw (cpm/mg tissue) for the mean ± SD of 10 mice. Ratios were calculated from the data in **Figures 1A** and **1C**.

| Liposome Diameter | 24 hrs | 48 hrs | 72 hrs | 96 hrs |
|---|---|---|---|---|
| 82 nm | 3.6 ± 0.5 | 2.6 ± 0.4 | 2.8 ± 0.7 | 2.3 ± 0.5 |
| 101 nm | 3.7 ± 0.9 | 3.0 ± 1.2 | 2.6 ± 0.8 | 2.1 ± 0.6 |
| 154 nm | 3.6 ± 1.4 | 2.8 ± 0.5 | 2.5 ± 0.5 | 2.3 ± 0.6 |
| 241 nm | 3.3 ± 1.0 | 2.5 ± 0.7 | 2.1 ± 0.8 | 2.0 ± 0.4 |

preferential accumulation of liposomes into tumor versus paws. However, for a given size of liposome, the tumor-to-paw ratios decreased significantly over time. At 24 hours after injection, regardless of liposome size, almost four times as many liposomes accumulated in tumor than in paws and this decreased to approximately two-fold by 96 hours after injection ($p<0.01$). The ratios at the 24 hour time point for all liposome diameters were significantly higher than the other time points ($p<0.05$ to $p<0.001$).

The biodistribution of STEALTH® liposomes has long been known to be size dependent, and the dermal localization of long-circulating liposomes has been previously described (64, 68, 94-96). These data represent the first systematic investigation to compare the accumulation of liposomes in tumors versus cutaneous tissues (skin and paws). These experiments indicate that time to peak levels of liposome accumulation was delayed in cutaneous tissues relative to tumor tissue, and time to peak levels was not dependent on liposome size.

Liposome levels peaked in tumor tissue at or before 24 hours, whereas levels in skin and paws peaked at 48 hours. If a liposome system can be engineered that leaks its drug contents after tumor levels peak, but before skin levels peak, it might lead to lower levels of drug in the skin, potentially reducing the likelihood of PPE. The higher uptake of liposomes into paws compared to skin suggests that there may be a pressure-dependent extravasation of liposomes into paws. Pressure would be exerted on the paws as the mice walk around the cage, feed, groom, etc. Pressure was not applied to the mice's skin to mimic human skin under pressure (e.g. belt lines) for

ethical and technical reasons; however, the data for paws may reflect the human condition where PPE lesions are found on the hands and feet. Thus, following the clinical administration of long-circulating liposomal DXR, it may be necessary to limit activity in order to avoid this pressure-dependent accumulation of liposomes. Indeed, some clinicians prescribe bed rest for patients on Caelyx® therapy for a short period of time following drug administration. Additionally, patients on Caelyx® are counseled to avoid situations that will increase blood flow to the skin, (e.g. hot baths), in an effort to reduce the number of liposomes localizing in the skin.

Tumor-to-skin and tumor to paw ratios did not change for the various sizes of liposomes. This demonstrates that altering liposome diameter does not decrease liposome accumulation into skin or paws without a proportional decrease in tumor accumulation. This is a surprising finding given that tumor blood vessels are reported to be "leakier" than normal capillaries (skin and paws), due to fenestrations and gaps in the endothelium (83, 87). This would suggest that, even though there are large gaps in the tumor's vasculature, there is also a size cutoff for particles that can pass through these gaps. Recent work by Hobbs and colleagues demonstrated that the pore sizes in tumor blood vessels were dependent upon the tumor model used and on the anatomical location of tumor implantation (83). Most tumors implanted subcutaneously exhibited a pore size range of 380-780 nm (as large as 0.3-4.7 μm in some tumor models); pore size was smaller in the cranial microenvironment (83, 87). The authors also identified that pore size range is heterogeneous in any given tumor, and that, for a particle or liposome to penetrate the pore, its diameter should be much

smaller than that of the pore. Because pore size is dependent upon tumor type and location (an orthotopically implanted breast tumor was used for these experiments), using a "leakier" tumor may have produced a difference in the tumor to skin ratios for the various sizes of liposomes. Ishida and colleagues further demonstrated the concept of pore size cutoff in recent experiments with the murine C26 colon carcinoma implanted subcutaneously. The authors showed a size-dependent accumulation of SL that was independent of blood liposome concentrations (163). This was inferred from the observation that increasing the blood levels of 400 nm diameter SL (achieved following splenectomy) did not increase liposome accumulation into tumors. In other words, for a particle to pass through a pore, the smaller it is in relation to the pore, the more likely it is to extravasate.

In the current study, it can be hypothesized that the 4T1 tumor may have a pore size cutoff of approximately 250 nm, as liposome accumulation dropped off significantly for the largest size of liposomes, this may also be partly due to reduced blood concentrations of these liposomes. Skin and paws accumulated substantially lower concentrations of liposomes than did tumors and also exhibited a similar fall-off in accumulation for the larger liposomes. The lower levels of liposome accumulation in skin and paws are consistent with the explanation that blood vessels in these tissues are "tighter" than those found in solid tumors.

Several factors are likely responsible for the decrease over time in tumor-to-skin and tumor-to-paw ratios. First, the concentrations of liposomes in skin and paws peak later than in tumors. As skin and paw concentrations increase, their ratios to

tumor concentrations will decrease if they are accumulating liposomes to a greater degree than tumors at later time points. Secondly, tumors continue to grow over the course of the study, with weights ranging from 0.20 g at 24 hours after injection to 0.34 g at 96 hours after injection. If the tumor grows faster than the rate of accumulation of liposomes in the tumor, the concentration of liposomes (c.p.m. per mg tissue) will decrease.

**3.2 Therapeutic Experiments**

Therapeutic experiments were performed to determine the influence of liposome size on the therapeutic activity of SL-DXR. The 4T1 tumor grows rapidly, therefore therapeutic experiments were started 4 days after tumor implantation when the tumors were just palpable, even though biodistribution experiments were carried out ten days after tumor implantation, when the tumors were large enough to excise.

To ensure that starting the therapeutic experiments earlier than the PK/BD experiments did not affect the delivery of liposomes to the tumor, the blood content of 4T1 tumors was measured using $^{111}$In-labeled murine red blood cells ($^{111}$In-rbc). Mice bearing the 4T1 murine mammary carcinoma were injected with $^{111}$In-rbc from 5 to 15 days after tumor implantation. Ten minutes later they were euthanized and their tumors were dissected, weighed and taken for radioactive counting. Tumor blood content (measured by the accumulation of $^{111}$In-rbc) as a function of tumor weight is seen in **Figure 3.2**. The results show that tumor blood content is proportional to tumor weight. Thus, starting therapeutic experiments when tumors are smaller should not bias the results of the experiments due to a lack of blood content.

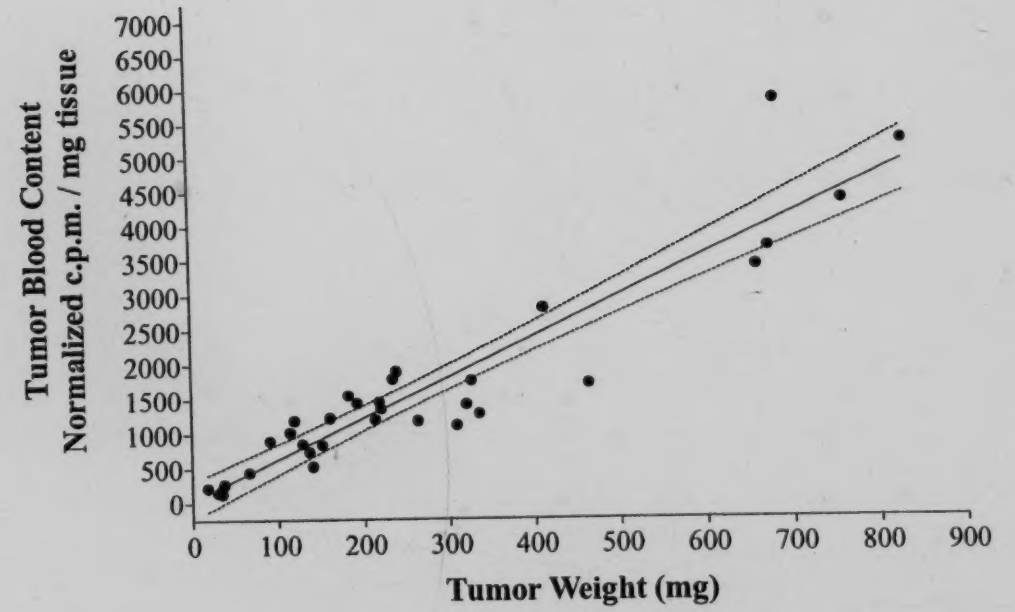


**Figure 3.2** 4T1 carcinoma blood content as a function of tumor weight. Mice were implanted with the 4T1 murine mammary carcinoma. From day 5 to 15 after tumor implantation mice were injected with $^{111}$In-labeled murine red blood cells ($^{111}$In-rbc). Ten minutes after injection of $^{111}$In-rbc, mice were euthanized and tumors were weighed and taken for radioactive counting. Each point represents the c.p.m. per mg tissues normalized to $10^6$ c.p.m. for an individual tumor. The best-fit line was generated using the least squares method for linear regression (Graphpad Prism); the coefficient of correlation ($r^2$) is 0.880. Dotted lines represent the 95% confidence intervals of the line.

For therapeutic experiments, groups of five mice were implanted with the 4T1 tumor and four days later were injected intravenously with liposomal DXR (6 mg/kg) of various diameters (polydispersity): 102 (0.152), 156 (0.077), or 254 (0.086) nm. Tumor growth was monitored by measuring perpendicular diameters (a and b), and volume was calculated with the formula $v=0.4ab^2$ where a>b (150). The experiment was repeated once with liposomes having similar mean diameters (polydispersity): 98 (0.140), 159 (0.078), or 256 (0.054) nm. The results at each liposome size were pooled as follows: 100 nm (98 and 102 nm), 157 nm (156 and159 nm) and 255 nm (254 and 256 nm). All control mice received 200 μl sterile saline. Results are presented as the mean ± S.D. with n= 6-10. There were no statistically significant differences between the end tumor volumes of the replicates as determined by a one-way ANOVA. Liposomes of approximately 82 nm diameter were not used for the therapeutic studies since their PK and BD were similar to the 101 nm liposomes. All three tested sizes of liposomal DXR delayed tumor growth (**Figure 3.3**). The smaller liposomes (100 and 157 nm) had almost equivalent anticancer activity, which was greater than that seen for the larger liposomes (255 nm). These data are consistent with the data from the biodistribution experiments, which showed greater tumor accumulation of the smaller liposomes compared with the largest ones. It is reasonable to expect that higher tumor levels of drug for the smaller liposomes would result in greater therapeutic activity. The small differences seen in the level of tumor accumulation for the smaller liposomes (101 and 154 nm), although statistically significant, resulted in no measurable differences in therapeutic activity.

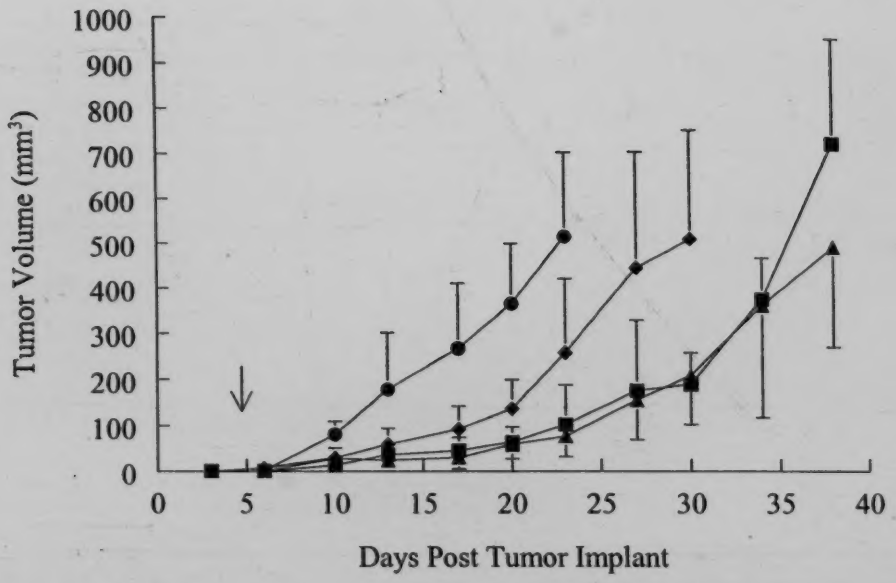


**Figure 3.3**. Therapeutic activity of various sizes of SL-DXR against the 4T1 mouse mammary carcinoma. BALB/c mice were implanted with the #4 mammary fat pad with the 4T1 tumor and 4 days later (arrow) were treated with a single treatment of 6 mg/kg SL- DXR of various mean diameters: ●, saline control; ▲, 100 nm; ■, 157 nm; ◆, 255 nm. Tumor volume was calculated using the formula $v=0.4ab^2$ where a and b are perpendicular diameters and a>b. The results represent the mean ± SD of 6-10 mice from two pooled experiments.

These experiments show a dependence of therapeutic activity on liposome size, with smaller liposomes (100 and 157 nm) being more efficacious than larger liposomes (255 nm). This is consistent with work from other laboratories using DXR or annamycin (164, 165). Although the 100 nm size of Caelyx® is considered optimal for therapeutic activity, based on our data, a modest increase in size would probably not result in a decrease in therapeutic activity, and may also not reduce the incidence of cutaneous toxicities such as PPE. However, a small increase to 150 nm would result in higher drug to lipid ratios, which may offer a cost saving in liposome preparation.

**3.3 Conclusion**

In conclusion, these data confirm that size plays an important role in the PK, BD and therapeutic activity of SL and SL-DXR. Cutaneous tissues accumulated liposomes slower than tumor tissue, but the kinetics of liposome accumulation for a given tissue were independent of liposome size. There was a preferential accumulation of liposomes into tumor over skin and paws, as evidenced by the tumor-to-skin and tumor-to-paw ratios. However, it was not possible to increase these ratios by increasing liposome diameter. The differential rates of liposome accumulation offer a potential strategy to decrease the amount of liposomal drug that accumulates in cutaneous tissues versus tumor, if a system can be engineered to release its encapsulated drug after tumor levels reach maximal values but before skin and paw concentrations plateau. This is the subject of experiments presented in Chapter 4.

# Chapter 4

## Influence of Drug Release Rates on the Pharmacokinetics, Biodistribution and Therapeutic Activity of STEALTH® Liposomal Doxorubicin

## Chapter 4: Results and Discussion

This chapter explores the relationship between the rate of release of DXR from SL and its PK, BD and therapeutic activity in the 4T1 murine mammary carcinoma model. Specifically, the accumulation of SL-DXR into the tumor, skin and paws of mice was studied as a function of time and drug leakage rate. The rationale for this study comes from Chapter 3, where it was demonstrated that the 4T1 murine mammary carcinoma accumulates smaller liposomes (82-154 nm diameter) faster than the skin and paws of mice. Therefore, it may be possible to reduce the accumulation of DXR in cutaneous tissues by altering the rate of DXR leakage. This would potentially reduce the incidence and severity of the cutaneous toxicities of SL-DXR, without adversely affecting its therapeutic activity. This may be accomplished if SL are formulated so that they release the majority of their DXR after tumor liposome concentrations have peaked, but before liposome levels in cutaneous tissues peak. This rationale is supported by the fact that Myocet™, a classical liposomal formulation of DXR, which has a much faster rate of drug release than Caelyx®, does not produce cutaneous toxicities (47).

### 4.1 *In vitro* Leakage of Doxorubicin From STEALTH® Liposomes

Before *in vivo* experiments could be performed it was necessary to identify liposomal formulations that release DXR at different rates. Liposomes that leak DXR at different rates were prepared by maintaining a constant amount of mPEG-DSPE (5 mole percent) in the formulation while altering the cholesterol (CHOL) content as well as the fatty acyl chain length and/or the degree of saturation of the

phosphatidylcholine component. These parameters were chosen because they influence the rigidity of the liposome's bilayer, which in turn significantly influences the retention of DXR (25, 32). DXR leakage was examined *in vitro* in the presence of serum, using a dialysis method. Liposomes were composed of CHOL and mPEG-DSPE in combination with the following phosphatidylcholines: egg yolk phosphatidylcholine (eggPC, $T_m$ 5°C), hydrogenated soy phosphatidylcholine (HSPC, which is similar in phase transition to DSPC, C18:0, $T_m$ 55°C), dimyristoyl-phosphatidylcholine (DMPC, C:14:0, $T_m$ 23°C), dioleoylphosphatidylcholine (DOPC, C18:1, $T_m$ -20°C), dipalmitoylphosphatidylcholine (DPPC, C16:0, $T_m$ 41°C), palmitoyl-oleoylphosphatidylcholine (POPC, C16:0, C18:1, $T_m$ -2°C), and stearoyl-palmitoyl phosphatidylcholine (SPPC, C18:0, C16:0, $T_m$ 44°C). Experiments were performed as described in Section 2.7 (*In vitro* leakage of Doxorubicin).

Results of these experiments are presented in **Table 4.1**. Incorporating phosphatidylcholines with a low phase transition temperature into the liposomal membrane (i.e., shorter fatty acyl chains and/or unsaturated fatty acyl chains) and reducing the proportion of CHOL increased drug leakage rates. This is consistent with data for DXR and other drugs, which demonstrated that the fluidity of the membrane plays an important role in the release of liposomal contents (23, 28, 38). For the purpose of this thesis, these data provide a range of formulations for performing *in vivo* studies.

**Table 4.1**. *In vitro* leakage half-lives of DXR from liposomes. Liposomes (0.5 mM phospholipid) were placed inside a dialysis cassette (MW cutoff 10 kDa) and incubated at 37°C in adult bovine serum in HBS, pH 7.4 (50% v/v). At various time points, aliquots were withdrawn and the DXR was extracted in acidified methanol and measured fluorometrically. Data were then plotted on a semi-log scale as percent remaining fluorescence vs. time. Half-lives were determined using regression of the linear portion of each curve. Half-lives represent the mean ± S.D. of n experiments; for n<3 the individual half-lives are given for each experiment.

| Lipid Composition | Ratio (mole) | n | $t_{1/2}$ (h) |
|---|---|---|---|
| Caelyx (HSPC:CHOL:mPEG) | 55:40:5 | 5 | 118.4 ± 18.8 |
| HSPC:CHOL:PEG | 2:1:0.1 | 5 | 91.8 ± 11.2 |
| | 2:0.25:0.1 | 1 | 110 |
| DPPC:CHOL:PEG | 2:1:0.1 | 1 | 53.9 |
| | 2:0.5:0.1 | 1 | 25.9 |
| | 2:0.25:0.1 | 1 | 14.8 |
| DMPC:CHOL:PEG | 2:1:0.1 | 4 | 23.0 ± 6.4 |
| SPPC:CHOL:mPEG | 2:1:0.1 | 1 | 82.2 |
| | 2:0.5:0.1 | 1 | 71.2 |
| | 2:0.25:0.1 | 1 | 47.4 |
| POPC:CHOL:PEG | 2:1:0.1 | 2 | 14.6, 11.9 |
| | 2:0.5:0.1 | 1 | 11.3 |
| | 2:0.25:0.1 | 1 | 8.82 |
| DOPC:CHOL:PEG | 2:1:0.1 | 2 | 14.9, 10.2 |
| | 2:0.5:0.1 | 1 | 8.48 |
| eggPC:CHOL:PEG | 2:1:0.1 | 1 | 10.1 |

**4.2 Development of an Extraction Procedure for Doxorubicin**

For the experiments presented in this Chapter, it was essential to distinguish between the PK and BD of the liposomal carrier and that of the pharmacologically active agent, DXR. Therefore, it was necessary to select a procedure to extract total DXR from tissue homogenates and plasma. The procedure chosen for quantifying DXR was based on previous work and is described in Section 2.8 (Quantification of Doxorubicin) (156-158). To validate this assay, tissue homogenates were spiked with known amounts of $^{14}$C-DXR. The spiked samples were extracted in acidified isopropanol to determine total DXR recovery using fluorescence and the extracts were also taken for liquid scintillation counting to determine the recovery of $^{14}$C-DXR (see Section 2.8: Quantification of Doxorubicin). The results are presented in **Table 4.2**. The recovery of radioactive counts was high (>90%, with one exception), and with the exception of preparation 2 for paws, this assay recovered on average >85% of DXR measured by fluorescence assays. These data are in agreement with previously published data, and this fluorescence assay was then used in subsequent experiments (156-158). Results are expressed as relative fluorescence units (RFU) of total DXR as this assay does not discriminate between doxorubicin and any fluorescent metabolites that may have similar excitation and emission profiles; as well, this assay does not distinguish between liposomal DXR and released DXR (discussed further in Section 4.4 and Section 6.4).

**Table 4.2.** Recovery of DXR from tissue samples spiked with $^{14}$C-DXR comparing radioactivity and fluorescence measurements. DXR spiked with $^{14}$C-DXR was added to 200 µl aliquots of 10% w/v tissue homogenates and the samples were allowed to incubate overnight at 37°C. The next day, samples were extracted as described in the text. Data represent one or two readings from two tissue preparations (1 and 2) and are expressed as % of recovered radioactivity or % of recovered relative fluorescence units.

| | | Radioactivity | | Fluorescence | |
|---|---|---|---|---|---|
| | | Preparation | | Preparation | |
| Tissue | DXR added (ng) | 1 | 2 | 1 | 2 |
| Skin | 150 | 98.9, 97.0 | 99.3, 80.6 | 86.7, 91.9 | 89.1, 78.6 |
| Skin | 300 | 91.8, 94.7 | 93.7, 94.6 | 90.8, 101.4 | 92.3, 93.7 |
| Paws | 150 | 97.3, 99.2 | 103, 100 | 76.8, 76.4 | 90.1, 101.9 |
| Paws | 300 | 98.8, 92.1 | 96.6, 94.8 | 81.9, 118 | 96.2, 96.1 |
| Tumor | 150 | 102, 104 | 102, 99.0 | 93.7, 107 | 99.5, 99.5 |
| Tumor | 300 | 99.1, 100 | 95.6, 95.0 | 104, 98.9 | 98.8, 99.9 |
| Plasma | 150 | 94.5, 96.4 | 98.6, 94.4 | 97.5, 95.9 | 95.9, 97.0 |
| Plasma | 300 | 98.9 | 96.1 | 106 | 93.8 |

### 4.3 Plasma Doxorubicin Concentrations Four Hours After Injection

From the data presented in **Table 4.1**, several liposome compositions were selected for *in vivo* testing. DSPC was selected instead of HSPC because DSPC is a synthetic lipid with a similar phase transition temperature to HSPC.

Plasma DXR concentrations were determined in naïve female BALB/c (6-8 weeks) mice in order to identify formulations for further study. Mice (n=3 per formulation) were injected with 6 mg/kg of SL-DXR. Four hours after injection, the mice were euthanized and plasma DXR concentrations were determined as in Section 2.8 (Quantification of Doxorubicin). All liposome formulations were composed of a phosphatidylcholine, CHOL and mPEG-DSPE at a 2:1:0.1 ratio and had a mean diameter of 100 ± 20 nm. Liposomes with lower CHOL contents were not studied further as altering the phosphatidylcholine acyl chain length or saturation provided an adequate number of formulations with desirable *in vivo* characteristics. The phosphatidylcholines used were DSPC, SMPC, POPC, DOPC, and DMPC; Caelyx® was tested as well.

The plasma concentrations of DXR four hours after injection are presented in **Table 4.3**. When DXR is released from liposomes it is quickly redistributed and eliminated. Thus, plasma drug concentrations reflect the retention of DXR within the liposomes. In agreement with the above *in vitro* data, and other *in vivo* studies (32), liposomes composed of phosphatidylcholines with long, saturated fatty acyl chains (i.e., more rigid bilayer) retained DXR longer and resulted in higher plasma concentrations at four hours after injection than more fluid liposomes (**Table 4.3**).

**Table 4.3.** Plasma concentrations of total DXR from various formulations of liposomes 4 hours after injection. Mice were injected with SL-DXR at a dose of 6 mg/kg (18 mg/m$^2$). HSPC: hydrogenated soy phosphatidylcholine; for all other abbreviations see text. Values represent the mean ± S.D. of triplicate aliquots from three mice.

| Formulation | Composition (molar ratios) | Phase transition temperature of phosphatidylcholine | Plasma concentration (RFU/ml) |
|---|---|---|---|
| Caelyx® (HSPC:CHOL:mPEG) | 55:40:5 | 55 °C | 97.4 ± 11.4 |
| DSPC:CHOL:mPEG | 2:1:0.1 | 55 °C | 91.7 ± 5.8 |
| SMPC:CHOL:mPEG | 2:1:0.1 | 30 °C | 80.4 ± 4.1 |
| POPC:CHOL:mPEG | 2:1:0.1 | -2 °C | 63.5 ± 9.7 |
| PMPC:CHOL:mPEG | 2:1:0.1 | 27 °C | 43.2 ± 4.9 |
| DOPC:CHOL:mPEG | 2:1:0.1 | -20 °C | 18.4 ± 2.7 |
| DMPC:CHOL:mPEG | 2:1:0.1 | 23 °C | 14.2 ± 1.6 |

Plasma levels provide a good measure of drug retention since drug released in plasma rapidly redistributes to other tissues. In fact, it has been observed that >95% of circulating DXR is entrapped within liposomes (79). The only liposomes where the *in vivo* leakage results were not similar to the *in vitro* results were for liposomes containing POPC. These liposomes had a short *in vitro* $t_{1/2}$ but produced a higher than expected 4-hour plasma DXR concentrations. This may be due to the differences in the composition of the adult bovine serum versus mouse blood or other unidentified factors. Further, other investigators have found discrepancies between *in vitro* and *in vivo* leakage results for other drugs such as vincristine (24). From these preliminary experiments, more weight was placed on the *in vivo* data for directing the course of future experiments. Based on these data, formulations were chosen with slower (DSPC:CHOL:mPEG-DSPE), intermediate (POPC:CHOL:mPEG-DSPE) and faster (DOPC:CHOL:mPEG-DSPE) rates of DXR leakage for further study in tumor-bearing mice.

**4.4 Pharmacokinetic and Biodistribution Experiments in Tumor-Bearing Mice**

Female BALB/c mice (6-8 weeks) were implanted with the 4T1 murine mammary carcinoma and ten days later were injected with 6 mg/kg of liposomal DXR composed of either DSPC:CHOL:mPEG-DSPE, POPC:CHOL:mPEG-DSPE, or DOPC:CHOL:mPEG-DSPE (2:1:0.1 mole; mean diameter 100 ± 10 nm). The liposomes contained the non-exchanged, non-metabolized lipid marker $^{3}$H-CHE (28, 156-158). At 1, 12, 24, 48, 72 and 168 hours after injection mice were euthanized, organs were removed, weighed and processed to determine DXR and $^{3}$H-CHE as

described in Section 2.8 (Quantification of Doxorubicin) and Section 2.9 (Quantification of Liposomal Lipid), respectively.

Plasma concentrations of DXR, liposomal lipid and their respective drug to lipid ratios are presented in **Figure 4.1**. Liposomes composed of DSPC:CHOL:mPEG-DSPE (slower release) achieved the highest plasma concentration of DXR (**Figure 4.1A**), followed by liposomes composed of POPC:CHOL:mPEG-DSPE (intermediate release), then DOPC:CHOL:mPEG-DSPE (faster release). Pharmakokinetic parameters are given in **Table 4.4** and demonstrate that the DSPC-containing liposomes had the longest plasma $t_{1/2}$, which approximated that of the liposomal carrier. Further, the DSPC liposomes had the slowest rate of clearance compared to the other formulations, which is consistent with the drug being stably retained within the liposomes.

Although the PK parameters for the drug differed for each formulation, the PK parameters for the liposomes, as measured using a lipid label ($^3$H-CHE), were similar for each formulation (**Figure 4.1B**), and they have comparable values for AUC, $t_{1/2}$, CL and $V_d$ (**Table 4.4**). In other words, the liposomes behaved the same *in vivo* and were long circulating whether or not they still contain drug. This is consistent with data demonstrating that mPEG-DPSE can impart long circulating times to liposomes composed of fluid as well as solid lipids (68, 71). Drug to lipid ratios decreased as liposome contents were lost; the more fluid formulations had the lowest ratios (**Figure 4.1C**).

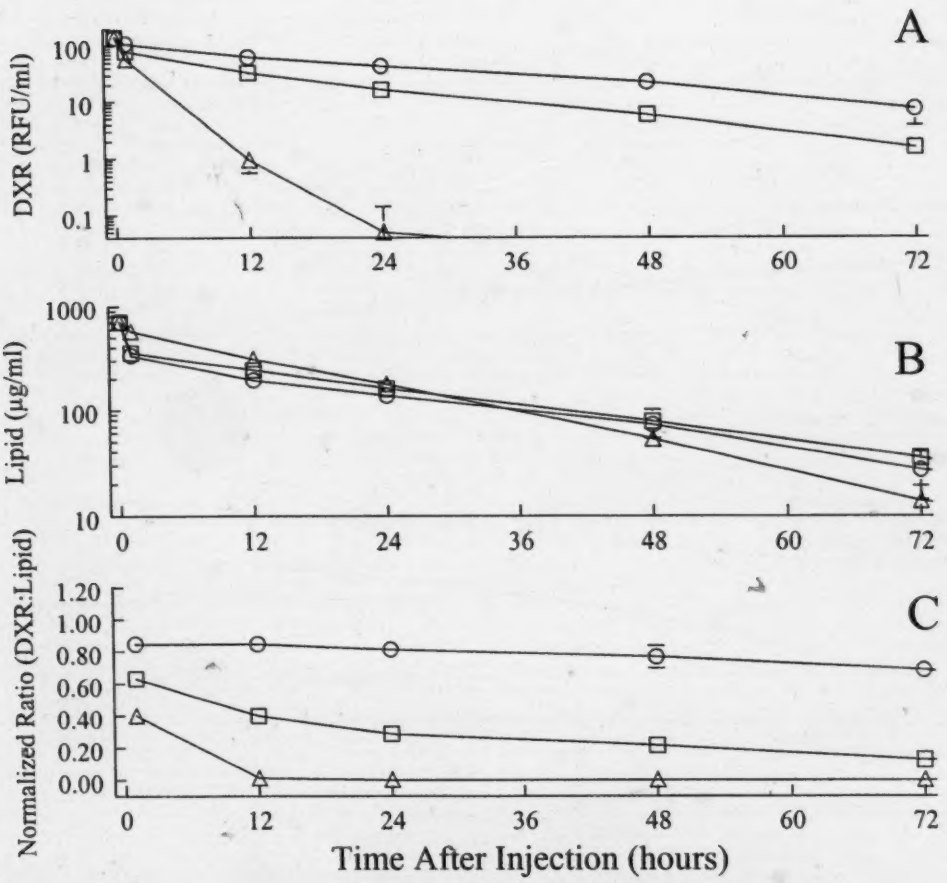


**Figure 4.1.** Plasma concentrations of DXR (panel A), liposomal lipid (panel B) and normalized drug to lipid ratios (panel C). BALB/c mice bearing the 4T1 murine mammary carcinoma were injected with 6 mg/kg liposomal DXR (○, DSPC:CHOL:mPEG-DSPE; □, POPC:CHOL:mPEG-DSPE, △; DOPC:CHOL:mPEG-DSPE at a molar ratio of 2:1:0.1) ten days after tumor implantation. Drug and lipid were quantified as detailed in the text. The results represent the mean ± S.D. from triplicate aliquots of 5 mice per time point. Drug to lipid ratios in plasma were normalized to the drug to lipid ratio of the injected liposomes.

**Table 4.4** Pharmacokinetic parameters for tumor-bearing mice receiving liposomal DXR (6 mg/kg) of either DSPC:CHOL:mPEG (DSPC) , POPC:CHOL:mPEG (POPC) or DOPC:CHOL:mPEG (DOPC). All formulations were 2:1:0.1 (mol). AUC were calculated using the trapezoidal rule and plasma and tissue $t_{1/2}$'s were calculated using the formula $t_{1/2}=0.693/k_{elm}$ where $k_{elm}$ is the elimination constant derived from the plasma or tissue concentration versus time curve; $r^2$ represents the coefficient of determination for this equation. (For the purposes of AUC, calculation 1 RFU is assumed to equal to 1 μg of DXR and/or metabolites).

| Plasma | | | | | | |
|---|---|---|---|---|---|---|
| | DSPC | | POPC | | DOPC | |
| | DXR | $^3$H-CHE | DXR | $^3$H-CHE | DXR | $^3$H-CHE |
| $k_{elm}$ | 0.0380 | 0.0339 | 0.0581 | 0.0365 | 0.3266 | 0.0398 |
| $r^2$ | 0.983 | 0.977 | 0.971 | 0.989 | 0.981 | 0.974 |
| $t_{1/2}$ (h) | 18.2 | 20.4 | 11.9 | 19.0 | 2.1 | 17.4 |
| AUC[a] | 3020 | 10600 | 1410 | 12200 | 430 | 12700 |
| CL[b] | 0.0020 | 0.0028 | 0.0043 | 0.0025 | 0.014 | 0.0024 |
| $V_d$[c] | 0.054 | 0.088 | 0.081 | 0.070 | 0.046 | 0.061 |
| **Tumor** | | | | | | |
| | DSPC | | POPC | | DOPC | |
| | DXR | $^3$H-CHE | DXR | $^3$H-CHE | DXR | $^3$H-CHE |
| $k_{elm}$ | 0.0097 | N/A | 0.0163 | N/A | 0.0280 | N/A |
| $r^2$ | 0.994 | N/A | 0.985 | N/A | 0.968 | N/A |
| $t_{1/2}$ (h) | 71.4 | N/A | 42.5 | N/A | 24.8 | N/A |
| AUC[d] | 1640 | 20200 | 432 | 20100 | 193 | 24800 |
| $C_{max}$[e] | 18.2 | 150.2 | 6.8 | 182.5 | 4.3 | 132.2 |
| **Skin** | | | | | | |
| | DSPC | | POPC | | DOPC | |
| | DXR | $^3$H-CHE | DXR | $^3$H-CHE | DXR | $^3$H-CHE |
| $k_{elm}$ | 0.0087 | N/A | 0.0083 | N/A | 0.0063 | N/A |
| $r^2$ | 0.936 | N/A | 0.996 | N/A | 0.811 | N/A |
| $t_{1/2}$ (h) | 79.6 | N/A | 83.5 | N/A | 110 | N/A |
| AUC[d] | 183 | 2300 | 89 | 3370 | 107 | 2700 |
| $C_{max}$[e] | 1.7 | 23.3 | 0.81 | 23.3 | 1.0 | 30.0 |
| **Paws** | | | | | | |
| | DSPC | | POPC | | DOPC | |
| | DXR | $^3$H-CHE | DXR | $^3$H-CHE | DXR | $^3$H-CHE |
| $k_{elm}$ | 0.0084 | N/A | 0.0092 | N/A | 0.0115 | N/A |
| $r^2$ | 0.997 | N/A | 0.986 | N/A | 0.969 | N/A |
| $t_{1/2}$ (h) | 82.5 | N/A | 75.3 | N/A | 60.2 | N/A |
| AUC[b] | 588 | 7060 | 200 | 6560 | 108 | 6750 |
| $C_{max}$[e] | 5.3 | 50.2 | 2.0 | 47.7 | 1.2 | 47.3 |

[a] units for plasma $AUC_{0-\infty}$s are (μg·h/ml)
[b] units for CL are ml/h/g
[c] units for $V_d$ are ml/g
[d] units for tissue AUC are (μg·g/g)
[e] units for $C_{max}$ are RFU/g tissue for DXR and μg lipid/g tissue for liposomal lipid

The decrease in drug to lipid ratios parallels the decrease in plasma concentrations of DXR for each formulation, suggesting that empty liposomes or liposomes with low contents levels remain in circulation. $^{3}$H-CHE is reported to be non-exchangeable and non-metabolizeable and the results for at least the first few hours in circulation reflect contents release. The low drug to lipid ratios, particularly at long time points, could be an artifact of the lipid label ($^{3}$H-CHE) transferring to circulating lipoproteins.

The accumulation of DXR and liposomal lipid into 4T1 mammary tumors is presented in **Figure 4.2**. The most stable liposomes, composed of DSPC:CHOL:mPEG-DSPE, achieved the highest total DXR concentrations in tumor, far exceeding tumor DXR concentrations from POPC:CHOL:mPEG-DPSE, and DOPC:CHOL:mPEG-DPSE liposomes (**Figure 4.2A**). This is reflected in their respective AUCs (**Table 4.4**).

The time course for DXR accumulation in tumor was different for all three formulations. Liposomes composed of DSPC:CHOL:mPEG-DSPE reached peak tumor concentrations ($C_{max}$) at 24 hours, while $C_{max}$ was reached at 12 hours for POPC:CHOL:mPEG and DOPC:CHOL:mPEG-DSPE liposomes. The accumulation of liposomal lipid was similar for all three formulations, with tumor concentrations of lipid plateauing between 12 and 24 hours (**Figure 4.2B**), indicating that drug-depleted liposomes were accumulating in tumor. Lipid concentrations reached plateau levels in tumor at around 24 h and lipid did not appear to be substantially cleared over the time course of the experiments; this is consistent with data from Chapter 3 and is

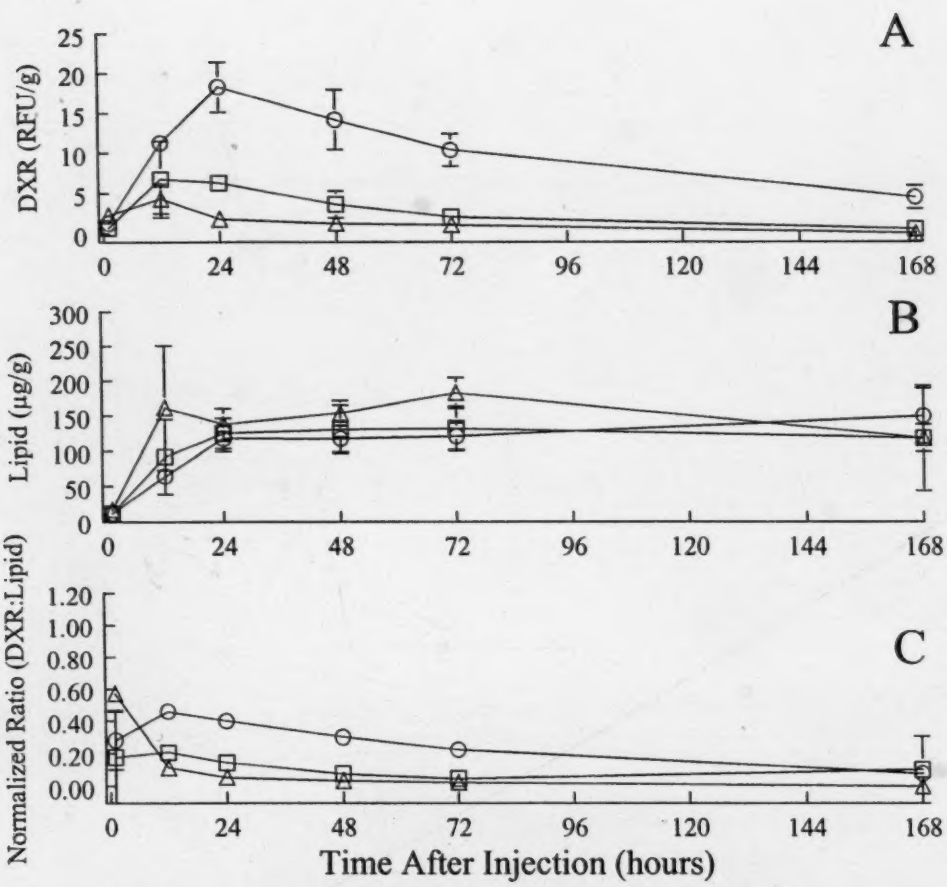


**Figure 4.2.** Tumor concentrations of DXR (panel A), liposomal lipid (panel B) and normalized drug to lipid ratios (panel C). BALB/c mice bearing the 4T1 murine mammary carcinoma were injected with 6 mg/kg liposomal DXR of various compositions (○ DSPC:CHOL:mPEG-DSPE; □ POPC:CHOL:mPEG-DSPE; △ DOPC:CHOL:mPEG-DSPE at a molar ratio of 2:1:0.1) ten days after tumor implantation. Drug and lipid were quantified as in the text. The results represent the mean ± S.D. from triplicate aliquots of 5 mice per time point. Drug to lipid ratios in tumor were normalized to the drug to lipid ratio of the injected liposomes.

expected for a non-metabolized label. DXR was gradually cleared from the tumor over the time course of the experiment, which is particularly apparent for liposomes composed of DSPC:CHOL:mPEG-DSPE, since this formulation resulted in higher tumor levels of drug. The gradual decrease in tumor drug levels suggests that the drug was released over several days from this formulation and the released drug was either metabolized to a non-fluorescent form or cleared from the liposomes. The elimination $t_{1/2}$'s for DXR from tumor demonstrate that DSPC:CHOL:mPEG-DSPE were the most stable as they had the slowest rates of DXR elimination from tumor, followed by the POPC and DOPC formulations (**Table 4.4**). This is consistent with the DOPC-liposomes having the fastest rate of drug leakage and is also supported by the decrease in the drug to lipid ratios (**Figure 4.2C**).

Similar results for the accumulation of total DXR and lipid into skin and paws are seen in **Figures 4.3** and **4.4** respectively, with the exception that tissue levels peaked later and at lower levels than in tumor, and lipid levels continued to increase over several days. The lipid data suggests that drug-depleted liposomes were accumulating in skin and paws for the fluid formulations that had more rapid drug release. PK parameters are given in **Table 4.4** and again demonstrate that the accumulation of liposomal lipid was independent of composition for the formulations used. DXR tissue clearance $t_{1/2}$s are presented in **Table 4.4**. Values for skin and paws are of a similar magnitude for all three formulations, while the DOPC-containing liposomes had the shortest $t_{1/2}$ for tumor, followed by the POPC and DSPC-based formulations. The faster rate of DXR elimination for the DOPC-

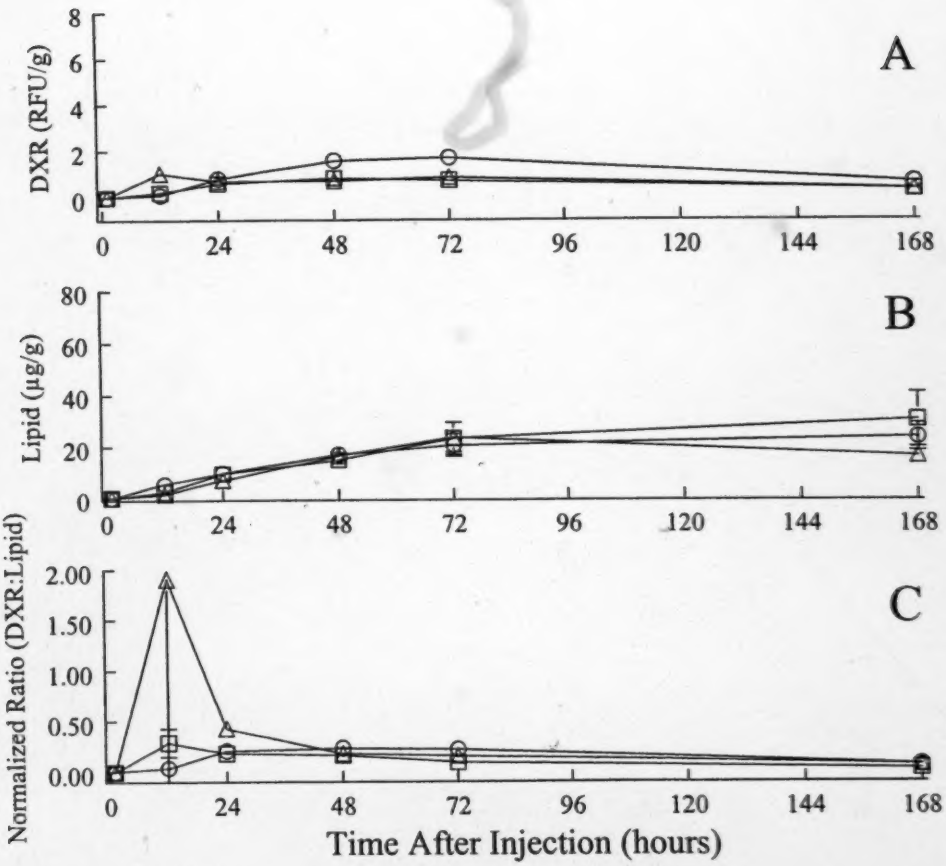


**Figure 4.3.** Skin concentrations of DXR (panel A), liposomal lipid (panel B) and normalized drug to lipid ratios (panel C). BALB/c mice bearing the 4T1 murine mammary carcinoma were injected with 6 mg/kg liposomal DXR of various compositions (○ DSPC:CHOL:mPEG-DSPE; □ POPC:CHOL:mPEG-DSPE; △ DOPC:CHOL:mPEG-DSPE at a molar ratio of 2:1:0.1) ten days after tumor implantation. Drug and lipid were quantified as in the text. The results represent the mean ± S.D. from triplicate aliquots of 5 mice per time point. Drug to lipid ratios in skin were normalized to the drug to lipid ratio of the injected liposomes.

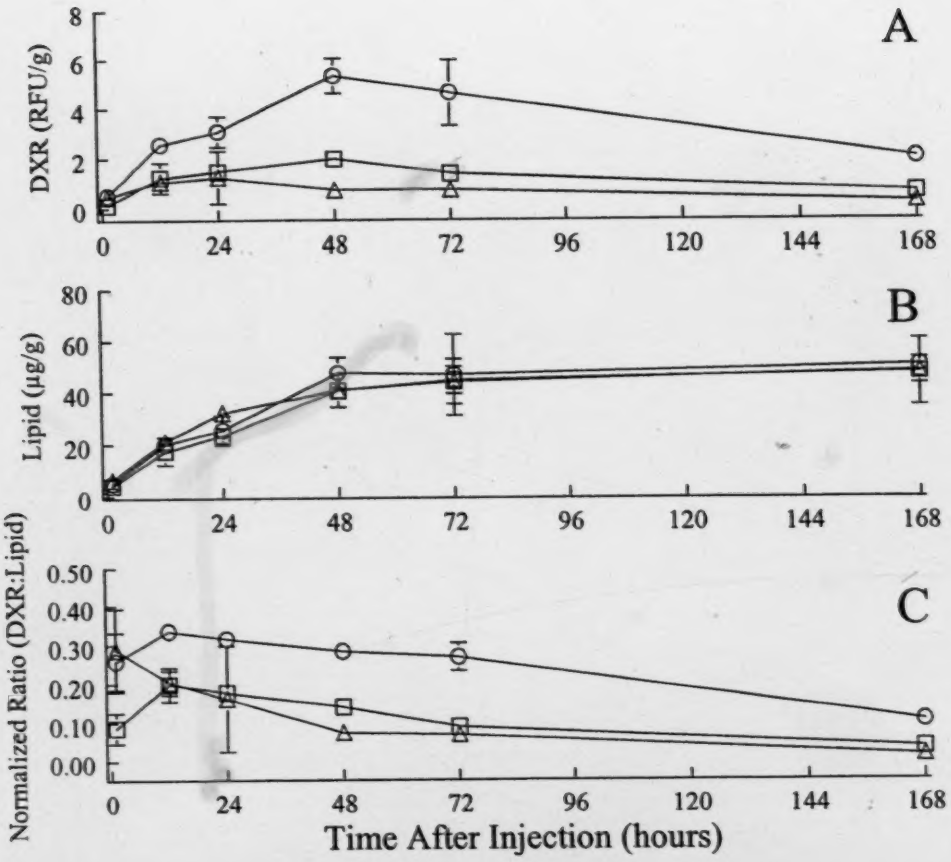


**Figure 4.4**. Paw concentrations of DXR (panel A), liposomal lipid (panel B) and normalized drug to lipid ratios (panel C). BALB/c mice bearing the 4T1 murine mammary carcinoma were injected with 6 mg/kg liposomal DXR of various compositions (○ DSPC:CHOL:mPEG-DSPE; □ POPC:CHOL:mPEG-DSPE; △ DOPC:CHOL:mPEG-DSPE at a molar ratio of 2:1:0.1) ten days after tumor implantation. Drug and lipid were quantified as in the text. The results represent the mean ±S.D. from triplicate aliquots of 5 mice per time point. Drug to lipid ratios in paws were normalized to the drug to lipid ratio of the injected liposomes.

containing liposomes could be due to differences in the tumor microenvironment, such as a slightly lower pH or metabolic byproducts, that favor drug release and elimination for the less stable formulations. Overall, the data presented in **Table 4.4** demonstrate that more solid liposomes delivered more DXR to all tissues of interest even though equal amounts of lipid were delivered by each formulation.

Tumor-to-skin and tumor-to-paw ratios for DXR and liposomal lipid are given in **Tables 4.5A** and **4.5B**, respectively. For the first 24 hours after injection the concentration of DXR and lipid in skin was near the limit of detection. As such, the mean and S.D. are very large and not interpretable. However, after approximately 24 hours, when tissue concentrations were higher, there is a trend for both the tumor-to-skin and tumor-to-paw ratios to decrease with time. These data are consistent with results presented in Chapter 3, and are likely due to skin and paw concentrations of DXR and lipid peaking later than tumor concentrations.

The DXR tumor-to-skin ratios for liposomes composed of DSPC:CHOL:mPEG are significantly higher than the corresponding ratios for the other two liposomal formulations from 24 hours post injection onward, i.e., at or around the time that drug levels from DSPC-containing liposomes peak in tumor ($p < 0.05$-$0.001$; ANOVA). This demonstrates that the DSPC:CHOL:mPEG-DSPE formulation is delivering more DXR to tumor than to skin compared to the other formulations. A comparison of the relative efficiency of each formulation in delivering drug to tumor relative to skin and paws can be obtained from the tissue AUCs (**Table 4.5A** and **4.5B**). DSPC:CHOL:mPEG-DSPE liposomes delivered 9-

**Table 4.5A** Tumor to skin ratios for DXR and liposomal lipid as a function of time post injection. Data represent the mean ± S.D. for 5 mice. Ratios were calculated from data in Figure 4.2 and 4.3.

| Doxorubicin | | | |
|---|---|---|---|
| Time (h) | DSPC | POPC | DOPC |
| 1 | ND | ND | ND |
| 12 | 96.2 ± 201.5 | 36.3 ± 19.9 | 4.2 ± 1.9 |
| 24 | 27.1 ± 12.7 | 10.8 ± 2.1 | 2.7 ± 0.9 |
| 48 | 9.3 ± 3.4 | 4.5 ± 1.9 | 1.8 ± 0.3 |
| 72 | 6.2 ± 1.5 | 3.0 ± 1.2 | 1.3 ± 0.3 |
| 168 | 6.8 ± 4.8 | 1.9 ± 1.1 | 0.1 ± 0.2 |
| [a]AUCs | 9.0 | 4.8 | 1.8 |
| Lipid | | | |
| Time (h) | DSPC | POPC | DOPC |
| 1 | ND | ND | ND |
| 12 | 12.7 ± 2.5 | 58.3 ± 60.8 | 53.7 ± 62.7 |
| 24 | 13.0 ± 3.9 | 14.1 ± 5.1 | 21.2 ± 6.5 |
| 48 | 7.1 ± 1.5 | 9.7 ± 4.5 | 9.8 ± 2.4 |
| 72 | 6.2 ± 2.0 | 6.2 ± 2.2 | 8.3 ± 2.6 |
| 168 | 6.1 ± 4.8 | 4.4 ± 3.5 | 7.6 ± 2.0 |
| [a]AUCs | 6.8 | 6.0 | 9.2 |

[a] Tumor-to-skin ratios calculated using AUC values from Table 4.4.
ND not determined since the concentration of DXR and lipid was below detectable limits

**Table 4.5B.** Tumor to paw ratios for DXR and liposomal lipid as a function of time post injection. Data represent the mean ± S.D. for 5 mice. Ratios were calculated from data in Figure 4.2 and 4.4.

| Doxorubicin | | | |
|---|---|---|---|
| Time (h) | DSPC | POPC | DOPC |
| 1 | 2.7 ± 2.0 | 7.8 ± 13.8 | 5.8 ± 1.9 |
| 12 | 4.4 ± 0.2 | 7.9 ± 8.9 | 4.2 ± 2.3 |
| 24 | 6.0 ± 0.8 | 4.4 ± 0.6 | 2.0 ± 1.1 |
| 48 | 2.7 ± 0.8 | 1.9 ± 1.1 | 1.8 ± 0.5 |
| 72 | 2.4 ± 0.9 | 1.6 ± 0.8 | 1.5 ± 0.5 |
| 168 | 1.9 ± 1.2 | 1.0 ± 0.5 | 0.1 ± 0.3 |
| [a]AUCs | 2.8 | 2.2 | 1.8 |
| Lipid | | | |
| Time (h) | DSPC | POPC | DOPC |
| 1 | 2.3 ± 0.3 | 2.8 ± 0.5 | 2.7 ± 0.5 |
| 12 | 3.2 ± 0.2 | 5.9 ± 4.5 | 7.6 ± 4.1 |
| 24 | 4.7 ± 0.8 | 5.4 ± 0.7 | 4.3 ± 0.7 |
| 48 | 2.5 ± 0.6 | 3.4 ± 1.3 | 3.8 ± 0.3 |
| 72 | 3.0 ± 1.3 | 3.0 ± 0.8 | 4.1 ± 1.1 |
| 168 | 3.0 ± 0.9 | 2.4 ± 1.3 | 2.5 ± 0.4 |
| [a]AUCs | 2.9 | 3.1 | 3.7 |

[a] Tumor-to-skin ratios calculated using AUC values from Table 4.4.

fold more DXR to tumor than skin, compared to 4.8 times more for the POPC:CHOL:mPEG liposomes or only 1.8 more for the DOPC:CHOL:mPEG liposomes. These ratios were lower for paws, i.e., 2.8, 2.2 and 1.8 for the DSPC, POPC and DOPC-containing liposomes respectively, because paws accumulated more drug and liposomal lipid than skin (**Table 4.4B**).

When the tissue AUCs for the various formulations were compared, the DSPC liposomes delivered 3.8 and 8.5 times as much total DXR to tumor as the POPC and DOPC-containing liposomes, respectively, while the POPC-containing liposomes delivered 2.2 times as much drug to tumor as liposomes composed of DOPC:CHOL:mPEG-DSPE. These ratios calculated for skin were 2.0 and 1.7 for the DSPC:CHOL:mPEG-DSPE formulation versus the POPC and DOPC-containing liposomes, respectively, and 0.83 for liposomes containing POPC compared to the DOPC-containing liposomes. The ratios for paws were slightly higher than the skin ratios; the DSPC-containing liposomes delivering 2.9 and 5.4 times as much total DXR to paws as the POPC and DOPC-containing liposomes, respectively. Finally the POPC:CHOL:mPEG-DSPE liposomes delivered 1.8 times as much total DXR to paws than the liposomes composed of DOPC:CHOL:mPEG-DSPE. These ratios demonstrate that the more solid liposomes delivered proportionally more total DXR to tumor than to cutaneous tissues. Therefore, for a given tumor DXR concentration, the DSPC:CHOL:mPEG-DSPE liposomes would actually deliver proportionally less DXR to cutaneous tissues.

In these experiments, the PK and BD of DXR and liposomal lipid were studied for liposomes with varying rates of DXR leakage. The PK and BD were examined for both entrapped drug (fluorescence) and liposomal lipid (a non-exchanged, non-metabolized lipid marker). The results show that the PK and BD of the liposomal carrier were the same regardless of the formulation and whether or not drug was still present in the liposomes; this is consistent with other studies examining the effects of mPEG-DSPE on liposome PK (68, 71). The most solid liposome formulation tested had the best drug retention and produced the highest tumor DXR AUC; unfortunately it also produced the highest drug AUC in cutaneous tissues. The therapeutic implications of this are examined in the proceeding section.

There were differences between the PK and BD of DXR and liposomal lipid, and these were most pronounced for liposome formulations with faster rates of drug release. For example, all the tested formulations of liposomes had tumor AUCs for liposomal lipid in excess of $2.0 \times 10^4$ μg·h/g whereas the DXR AUC is only 196 μg·h/g for the DOPC:CHOL:mPEG liposomes compared to 1640 μg·h/g for the DSPC-containing liposomes (assuming that 1 RFU is equal to 1 μg of DXR and/or metabolites). Thus, for similar liposome profiles the drug AUCs are almost an order of magnitude different, which will impair the interpretation of the results if the AUC for the drug is not determined and one relies only on data from the distribution of liposomal lipid. When comparing the results obtained in these experiments for the DSPC-containing liposomes with those in Chapter 3 for the 101 nm diameter liposomes (both formulations had similar compositions), the plasma PK were not

fundamentally different. The plasma $t_{1/2}$ using $^{125}$I-TI as a label was 13.0 hours while the DXR had a $t_{1/2}$ of 19.1 hours in these experiments; this is in comparison to a $t_{1/2}$ of 21.6 hours for the liposomal lipid as determined using a lipid marker. Thus, while $^{125}$I-TI is not a perfect surrogate, it is a reasonable marker to use in liposome PK studies. The difference in PK and BD parameters for DXR versus liposomal lipid is more pronounced for liposomes containing POPC and DOPC due to drug leakage.

Discrepancies for different PK labels (e.g., $t_{1/2}$ and $k_{elm}$) are a result of different clearance and excretion mechanisms once liposomes have disintegrated. Many studies, including those in Chapter 3, use surrogate markers for liposomes. This is often a matter of convenience, especially when gamma ray-emitting labels such as $^{125}$I-TI and $^{67}$Ga-desferoxime are used. These are aqueous space labels for intact liposomes; these labels are quickly excreted in the urine when liposomes disintegrate in the circulation (153, 166, 167). Lipid labels, on the other hand, will transfer to lipoproteins, albeit at a slow rate for metabolically stable ones like $^{3}$H-CHE (155). Thus, studies following only a lipid label and not the pharmacologically active agent should be interpreted with caution if the results are to be extrapolated to the encapsulated drug (73, 75, 76).

The bioavailability of the encapsulated drug is another important concept to consider when interpreting the therapeutic impact of these data. Current thinking regarding the mechanism of action of Caelyx® is that the liposomes accumulate in tumor and slowly release their contents. This released, i.e., bioavailable, drug then is able to exert its cytotoxic activity. If the concentration of bioavailable drug does not

reach minimum cytotoxic concentrations in tissues, then no appreciable therapeutic response will be seen. This problem was encountered with a STEALTH® liposomal formulation of cisplatin (SPI-077). This formulation produced high tumor drug AUCs in experimental tumor models, but failed to produce corresponding high antitumor responses in animal models and later in humans, and its development was stopped in Phase II clinical trials (33-35).

Another concept that complements drug bioavailability is that of mechanism of drug action. If the drug is cell cycle phase specific, cytotoxic drug concentrations need to be maintained for extended periods of time to allow for a substantial number of cells to pass through the sensitive phase of the cell cycle. In this case, the characteristics of the liposome must be tailored to the properties of the drug, and a slow release preparation may be desirable. This was demonstrated for liposomal formulations of 1-β- D-arabinofuranosylcytosine (ara-C) and the Vinca alkaloid vincristine, which are cell cycle phase specific agents (24, 27, 37, 38). Ara-C is a nucleoside analogue that is cytotoxic in S-phase of the cell cycle (42). When SL-ara-C was tested in the murine L1210 tumor model, optimal therapeutic responses were seen with SL (sphingomyelin:eggPC:CHOL: mPEG-DSPE, 1:1:1:0.1 mol/mol) having a long circulation time and a rate of drug release that was not slower than the doubling time of the target cells (38). The authors attributed the optimal therapeutic activity of this formulation to the ability of SL to mimic a prolonged infusion that allowed for the sustained release of cytotoxic concentrations of bioavailable drug. Vincristine acts by destabilizing microtubules and expresses its cytoxcity in M-phase

of the cell cycle (42). It produces superior therapeutic responses when encapsulated in solid liposomal formulations (e.g., composed of sphingomyelin:CHOL, 55:45 mol/mol) compared to more fluid formulations (e.g., eggPC:CHOL, 55:45 mol/mol) in murine L1210, P388 and human xenograft (A431 human squamous cell carcinoma) models (24, 27, 37). The authors attributed the improved therapeutic activity of the more solid formulation (sphingomyelin:CHOL) to its slower rate of drug release relative to the growth of the cells. This increases the time that tumor cells are exposed to cytotoxic drug concentrations, and allows more cells to pass through the sensitive portions of the cell cycle, resulting in increased therapeutic activity. A liposomal formulation of vincristine is currently being evaluated in Phase III clinical trials for the treatment of non-Hodgkin's lymphoma (Onco-TCS, INEX Pharmaceutics, Vancouver, B.C.) (168). In the current study, DXR is not a cell cycle phase specific drug. Therefore it is reasonable to hypothesize that its therapeutic action may be more dependent on peak drug levels. The question then presents itself as to whether or not the total drug AUCs measured here correlate with the amount of bioavailable DXR. If so, are the more solid DSPC:CHOL:mPEG-DSPE liposomes expected to have superior therapeutic activity compared to more rapid release formulations? This question is addressed in the next section.

**4.5 Therapeutic Experiments**

Experiments were carried out to determine the influence of drug release rate on the therapeutic activity of SL-DXR in the 4T1 tumor model. Female BALB/c mice were implanted in the right #4 mammary fat pad with the 4T1 murine mammary

carcinoma. Four days later mice were treated with 6 mg/kg of SL-DXR composed of DSPC:CHOL:mPEG, POPC:CHOL:mPEG or DOPC:CHOL:mPEG (2:1:0.1 mole) with a mean diameter of 100 ± 10 nm. Similar to the experiments presented in Chapter 3, tumor growth was followed by measuring perpendicular tumor diameters (a and b) using calipers, and tumor volume was calculated using the formula $v=0.4ab^2$ where a>b. The experiment was repeated once and the results were pooled. The data represent the mean tumor volume ± S.D. of 5-12 mice, except for liposomes composed of POPC:CHOL:mPEG where n=4-6 mice. There were fewer mice in the POPC:CHOL:mPEG group due to toxicity encountered with this formulation (see below). The results of the pooled experiments are seen in **Figure 4.5**.

All three liposomal formulations delayed tumor growth. The DSPC-containing liposomes appeared to have the highest therapeutic activity. Overall, these data demonstrate that the more solid liposomes appeared to have superior therapeutic activity compared to more fluid formulations having more rapid contents release. Thus, for the formulations tested, the higher total tumor DXR concentrations achieved with DSPC:CHOL:mPEG-DSPE liposomes resulted in sufficient concentrations of bioavailable DXR to achieve good therapeutic responses.

**4.6 Toxicity of Liposomes Composed of POPC:CHOL:mPEG-DSPE**

Liposomes composed of POPC:CHOL:mPEG-DSPE displayed unexpected toxicity during these therapeutic experiments. In the initial therapeutic experiment, all of the mice in the group were euthanized due to severe weight loss within one week of treatment. Gross post mortem exam (performed by the staff veterinary

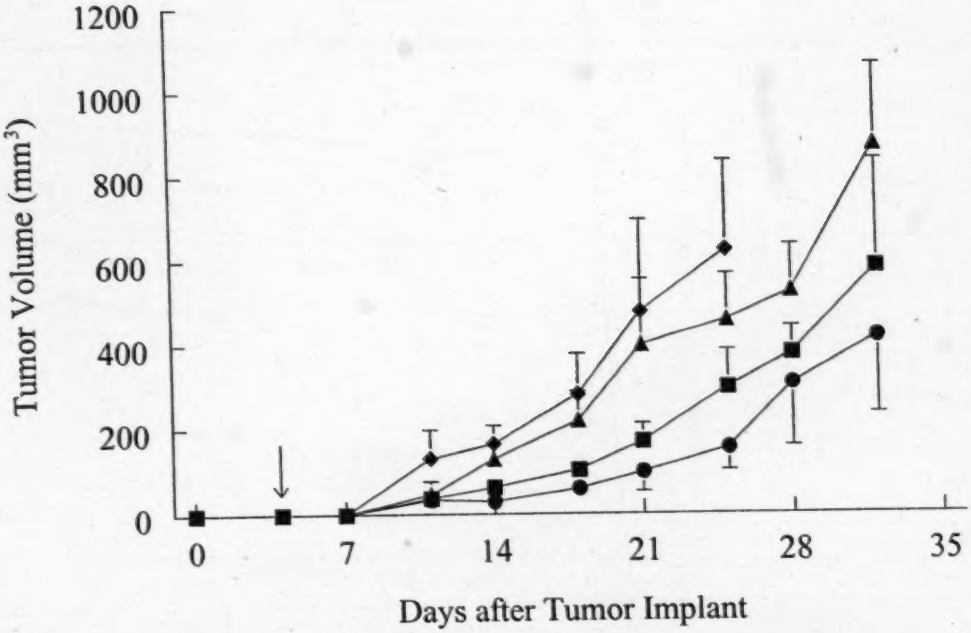


**Figure 4.5.** Therapeutic activity of different formulations of SL-DXR against the 4T1 murine mammary carcinoma. BALB/c mice were implanted in the #4 mammary fat pad with the 4T1 murine mammary carcinoma. Four days later (arrow) mice were treated with SL-DXR at a DXR dose of 6 mg/kg. Liposomes (2:1:0.1 mole) were composed of DSPC:CHOL:mPEG (●), POPC:CHOL:mPEG (■), DOPC:CHOL:mPEG (▲) or saline control (◆). Data represent the mean ± S.D. from 5-12 mice from two pooled experiments, except for POPC:CHOL:mPEG liposomes, which represent the mean ± S.D. from 4-6 mice from one experiment.

pathologist, University of Alberta Health Sciences Laboratory Animal Services) revealed blood congestion of organs, consistent with cardiovascular toxicity. When the experiment was repeated, the mice were followed very closely and only two of six were euthanized due to severe weight loss, one mouse had myocardial necrosis and the other had hepatic necrosis.

This toxicity was unexpected, as the biodistribution experiments performed at the same dose and over similar time frame did not result in the need to euthanized animals due to overt toxicity (Section 4.4). One possibility is that the larger tumors (10 days post implant for PK/BD experiments versus 4 days for therapeutic experiments) acted to enhance the elimination of liposomes and reduce the plasma levels, and the toxicity, of the formulation. These results highlight how altering drug release rates may influence not only the therapeutic activity of a formulation, but its toxicity as well. A likely reason for cardiac damage in these mice was that the rate of drug leakage was sufficient to cause prolonged cardiac exposure to bioavailable drug levels that were above the minimal cardio-toxic concentration. The more solid liposomes composed of DSPC:CHOL:mPEG-DSPE have a slower rate of drug release and are less likely to produce cardio-toxicity (**Table 4.4**). The leakiest liposomes composed of DOPC:CHOL:mPEG-DSPE would release their contents quickly, and cardiotixic drug concentrations would not be reached in the heart due to the rapid redistributin of the released DXR. However, there is the possibility that this formulation may produce cardiotoxic drug concentrations that could result in chronic toxicity with repeat administration. Thus the importance of understanding the

relationship between total and bioavailable drug levels relates not only to the therapeutic activity, but to drug toxicities as well.

**4.7 Conclusion**

Overall these experiments confirm that stable formulations of SL-DXR (e.g., similar to Caelyx®) achieve the highest $C_{max}$ and AUC for total DXR in tumors and that this translated into the best therapeutic activity of the formulations tested. Further, unlike formulations with intermediate release characteristics, they did not exhibit acute toxicities. If these murine data can be extrapolated to humans, then the current solid formulation of Caelyx® would be expected to have improved antitumor activity over a faster release formulation (but not necessarily over a triggered release formulation, see Section 6.3.3). These studies also point to the need to measure, and perhaps increase, the concentrations of bioavailable drug in tumor tissue if the therapeutic activity of a given formulation at a given dose is to be increased. For example, if it is possible to increase the concentration of bioavailable drug in tumor from a given dose of SL-DXR, its therapeutic activity should increase as well.

With respect to cutaneous toxicities, solid liposome formulations also achieved high concentrations of DXR in the cutaneous tissues of mice. If these results can be extrapolated to humans, we would expect to see a higher incidence of PPE in patients receiving these slow release formulations. Clinically, cancer chemotherapy is given in repeated cycles. If the dose interval is not long enough to allow for complete clearance of DXR from sensitive cutaneous tissues, then repeat administration is likely to lead to an accumulation of DXR, resulting in the

development of PPE and other cutaneous toxicities, as seen for Caelyx®. This is the basis for experiments performed in Chapter 5.

# Chapter 5

## Multiple Injections of Pegylated Liposomal Doxorubicin: Pharmacokinetics, Toxicity and Therapeutic Activity

**Chapter 5: Results and Discussion**

The experiments presented in this Chapter focus on the PK, BD and therapeutic activity of Caelyx® with repeat i.v. administration in a murine model. If the data presented in Chapters 3 and 4 can be extrapolated to humans, then the current formulation of Caelyx® has near optimal therapeutic activity for SL-DXR, but it also has the highest probability of producing cutaneous toxicities. For the single dose experiments presented in Chapter 4, DXR had a long $t_{1/2}$ of drug clearance from cutaneous tissues. If the dose interval is shorter than the time needed to completely clear DXR from the skin, the drug will accumulate and toxicity is likely to develop. In humans, PPE lesions develop after multiple doses of Caelyx® and dose delay is used to reduce the severity of PPE lesions once they develop (120). Therefore, the influence of dose delay (i.e., reducing the dose intensity) on the accumulation of DXR into the cutaneous tissues (skin and paws) of naïve BALB/c mice was studied for a given dose (9 mg/kg, 27 mg/m$^2$) of Caelyx®. As well, different dose schedules with the same dose intensity (9 mg/kg/wk, 27 mg/m$^2$ wk) were studied in mice bearing the orthotopically implanted 4T1 murine mammary carcinoma. The rationale for these latter experiments was that, in humans, the recommended dose intensity of Caelyx® therapy is 10-12 mg/m$^2$/wk, and that the most efficient manner to deliver this dose intensity has yet to be determined (140). Further, recent data suggests that for a given dose intensity of Caelyx®, larger infrequent doses are therapeutically superior to smaller frequent doses (152). Therapeutic experiments were also performed to

determine both the influence of dose intensity and dose schedule on the 4T1 murine mammary carcinoma.

**5.1 Dose Schedules With Different Dose Intensities**

Dose schedules with different dose intensities were achieved by lengthening the dose interval for a given dose of Caelyx® (9 mg/kg); both PK/BD and therapeutic experiments were performed.

**5.1.1 Pharmacokinetic and Biodistribution Experiments**

PK and BD experiments were performed in naïve female BALB/c mice (6-8 weeks). Mice received i.v. injections of 9 mg/kg (27 mg/m$^2$) weekly (q1wk), every second week (q2wk) or every fourth week (q4wk) for a total of four doses. At various time points after injection, mice were euthanized and DXR concentrations in plasma, skin and paws were determined (see Section 2.8 Quantification of Doxorubicin). The results are expressed as DXR RFU/ g of tissue or RFU / ml of plasma. These doses delivered dose intensities of 9 mg/kg/wk (27 mg/m$^2$/wk), 4.5 mg/kg/wk (13.5 mg/m$^2$/wk) and 2.25 mg/kg/wk (6.75 mg/m$^2$/wk). The 13.5 mg/m$^2$/wk dose intensity is similar to the currently recommended dose intensity for humans (10 to 12 mg/m$^2$/wk) and the other two schedules bracket this therapeutically relevant dose intensity (106).

**Figure 5.1** presents the plasma, skin, and paw DXR profiles for mice receiving weekly i.v. doses of 9 mg/kg (27 mg/m$^2$, q1wk x 4). Results shown in **Figure 5.1A** indicate that the drug was not completely cleared from the plasma before administration of subsequent doses. Plasma $t_{1/2}$ values were on the order of 40 hours,

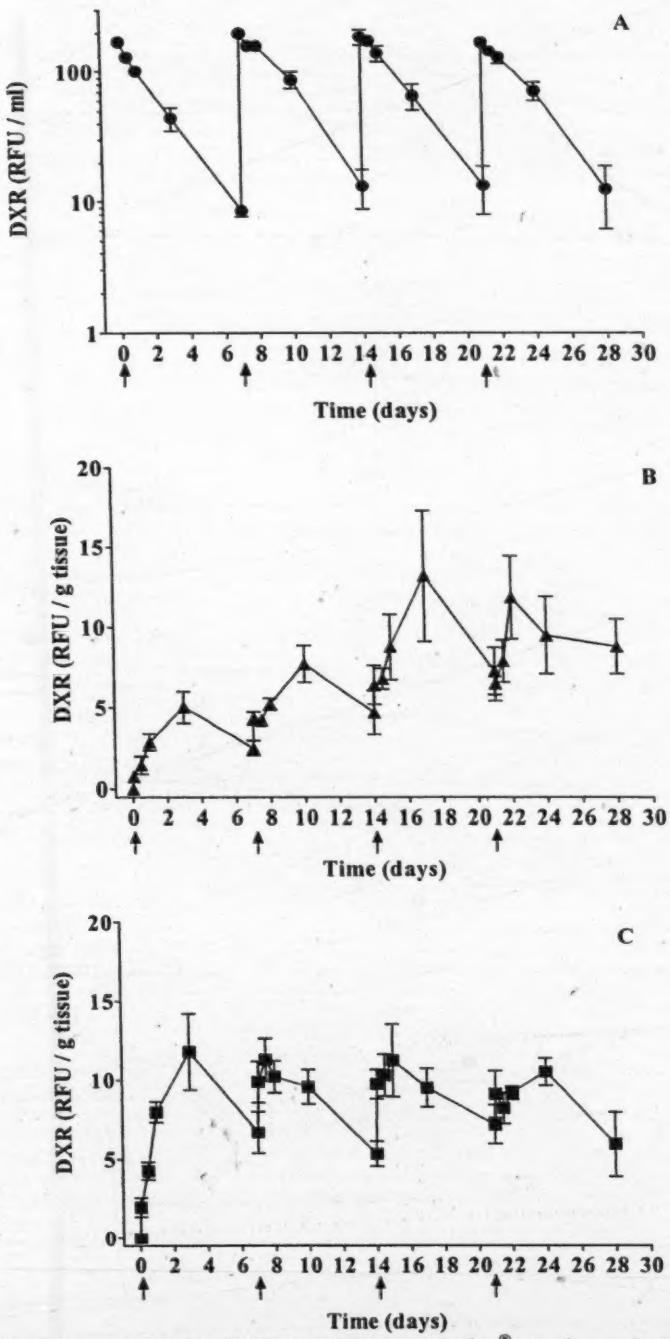


**Figure 5.1**. Tissue concentrations of DXR in mice given Caelyx® at a dose schedule of 9 mg/kg q1wk. Mice were injected i.v. via the lateral tail vein q1wk (arrows). Data represent the mean ± S.D. of triplicate aliquots from 4 to 5 mice and are reported as DXR RFU. A) plasma, B) skin, C) paws.

and plasma concentrations for each dose peaked at approximately the same values. Plasma AUC values plateaued after the second dose, suggesting that steady state was reached (**Table 5. 1**).

Skin and paw drug concentrations for a dose schedule of q1wk x 4 are seen in **Figures 5.1B** and **5.1C**, respectively. For the first 3 doses of Caelyx®, skin $C_{max}$ was reached 72 hours post-injection ($p<0.001$-$0.05$) and at 24 hours after injection for the fourth dose. The nadir occurred at increasing drug levels with each subsequent dose. Skin AUCs increased 3-fold between the first and third doses and then appeared to reach steady state (**Table 5.1**).

$C_{max}$ for total DXR was reached in paws 72 hours after the first dose, but was earlier for subsequent doses ($p<0.01$-$0.001$). Paws achieved higher drug concentrations than skin for the first two doses, as reflected in their higher AUC levels, but were similar to skin for the next two doses (**Figure 5.1**, **Table 5.1**). The nadir drug levels for paws remained high throughout the study and paw levels appeared to reach steady state after the first dose (the AUCs for paws did not change with subsequent doses). The higher drug levels in paws than in skin may be due to the pressure-dependent extravasation of liposomes as the mice walk around the cage, groom, feed, etc. and it is consistent with data presented in Chapters 3 and 4.

DXR levels in plasma, skin, and paws of mice receiving intravenous Caelyx® at a dose of 9 mg/kg q2wk are presented in **Figure 5.2**. Extending the dose interval allowed plasma drug levels to fall to below detectable limits before the next dose of

**Table 5.1.** Pharmacokinetic parameters for mice receiving i.v. Caelyx® at a dose of 9 mg/kg q1wk, q2wk, or q4wk. AUC values were calculated using the trapezoidal rule. Plasma and tissue $t_{1/2}$ values were calculated using the formula $t_{1/2}=0.693/k_{elm}$, where $k_{elm}$ is the elimination constant derived from the plasma or tissue concentration versus time curve; $r^2$ was determined for each curve and was >0.92. **(A)** 9 mg/kg q1wk. **(B)** 9 mg/kg q2wk. **(C)** 9 mg/kg q4wk. For the purpose of AUC calculation 1RFU is assumed to equal 1 μg of DXR and/or metabolites.

| A | Plasma | | | | | Skin | | | Paws | | |
|---|---|---|---|---|---|---|---|---|---|---|---|
| Dose | $t_{1/2}$ (h) | $k_{elm}$ | AUC[a] | CL[b] | $V_d$[c] | $t_{1/2}$ (h) | AUC[a] | $C_{max}$[d] | $t_{1/2}$ (h) | AUC[c] | $C_{max}$[d] |
| 1 | 39.4 | 0.0176 | 9140 | 0.00098 | 0.055 | ND | 589 | 5.0 | ND | 1470 | 11.8 |
| 2 | 43.0 | 0.0161 | 14600 | 0.00058 | 0.036 | ND | 1010 | 7.7 | ND | 1450 | 11.3 |
| 3 | 43.0 | 0.0161 | 12600 | 0.00067 | 0.042 | ND | 1680 | 13.2 | ND | 1550 | 11.3 |
| 4 | 44.7 | 0.0155 | 12200 | 0.00069 | 0.044 | ND | 1600 | 11.8 | ND | 1480 | 10.5 |
| $C_{ss}$ | n/a | n/a | 72.9 | n/a | n/a | n/a | 9.48 | n/a | N/a | 8.78 | n/a |

| B | Plasma | | | | | Skin | | | | Paws | | |
|---|---|---|---|---|---|---|---|---|---|---|---|---|
| Dose | $t_{1/2}$ (h) | $k_{elm}$ | AUC[a] | CL[b] | $V_d$[c] | $t_{1/2}$ (h) | $k_{elm}$ | AUC[a] | $C_{max}$[d] | $t_{1/2}$ (h) | $k_{elm}$ | AUC[c] | $C_{max}$[d] |
| 1 | 28.6 | 0.0242 | 9270 | 0.00097 | 0.040 | 58.2 | 0.0119 | 865 | 6.0 | 81.5 | 0.0085 | 2310 | 13.9 |
| 2 | 35.2 | 0.0197 | 12400 | 0.00073 | 0.037 | 37.9 | 0.0183 | 1280 | 6.8 | 100 | 0.0069 | 2070 | 10.3 |
| 3 | 41.5 | 0.0167 | 12500 | 0.00072 | 0.043 | 139 | 0.0050 | 1790 | 8.5 | 157 | 0.0040 | 1450 | 6.4 |
| 4 | 44.4 | 0.0156 | 12300 | 0.00073 | 0.047 | 218 | 0.0054 | 1960 | 8.5 | 178 | 0.0039 | 1380 | 6.0 |
| $C_{ss}$ | n/a | n/a | 33.2 | n/a | n/a | n/a | n/a | 5.84 | n/a | N/a | n/a | 4.11 | n/a |

| C | Plasma | | | | | Skin | | | | Paws | | |
|---|---|---|---|---|---|---|---|---|---|---|---|---|
| Dose | $t_{1/2}$ (h) | $k_{elm}$ | AUC[a] | CL[b] | $V_d$[c] | $t_{1/2}$ (h) | $k_{elm}$ | AUC[a] | $C_{max}$[d] | $t_{1/2}$ (h) | $k_{elm}$ | AUC[c] | $C_{max}$[d] |
| 1 | 41.5 | 0.0167 | 9810 | 0.00077 | 0.044 | 136 | 0.0051 | 800 | 3.9 | 103 | 0.0067 | 3210 | 14.4 |
| 2 | 33.2 | 0.0209 | 9960 | 0.00081 | 0.050 | 103 | 0.0067 | 1140 | 6.5 | 147 | 0.0047 | 1720 | 7.1 |
| 3 | 31.6 | 0.0221 | 11000 | 0.00076 | 0.047 | 147 | 0.0047 | 1340 | 5.9 | 198 | 0.0035 | 1460 | 4.9 |
| 4 | 46.8 | 0.0148 | 10700 | 0.00069 | 0.045 | 105 | 0.0066 | 1600 | 6.8 | 192 | 0.0036 | 1650 | 5.7 |
| $C_{ss}$ | n/a | n/a | 14.6 | n/a | n/a | n/a | n/a | 2.37 | n/a | N/a | n/a | 2.45 | n/a |

ND, not determined; [a] units for AUC are DXR μg·h/ml or μg·h/g; [b] units for CL are ml/h/g; [c] units for $V_d$ are ml/g; [d] units for $C_{max}$ are RFU/g tissue.

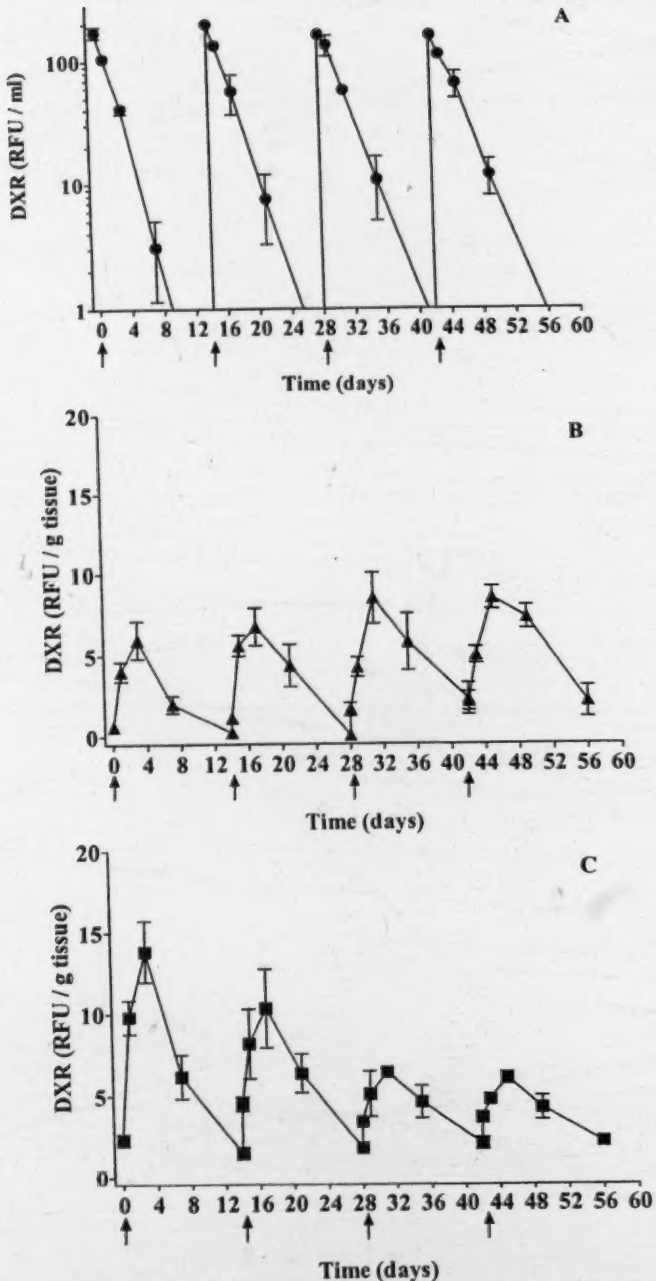


**Figure 5.2.** Tissue concentrations of DXR in mice given Caelyx® at a dose schedule of 9 mg/kg q2wk. Mice were injected i.v. via the lateral tail vein q2wk (arrows). Data represent the mean ± S.D. of triplicate aliquots from 4 to 5 mice and are reported as DXR RFU. A) plasma, B) skin, C) paws.

Caelyx® was given. As with the q1wk dosing schedule, plasma AUC values plateaued after the second dose (**Table 5.1**).

Skin and paws reached $C_{max}$ for total DXR for the q2wk dose schedule at approximately 72 hours post-injection. Prolonging the dose interval allowed more DXR to be cleared from the skin and paws compared to the q1wk dose schedule. Also, the nadir drug levels were significantly lower than those reached for the q1wk dose schedule ($p<0.001$ for skin and $p<0.01$-$0.001$ for paws). Again, paw concentrations of DXR were initially higher than those in skin. However, with subsequent doses, the skin $C_{max}$ increased ($p<0.05$ for Dose 1 vs. Doses 3 and 4) while, unexpectedly, the paw $C_{max}$ decreased significantly between the first and second doses ($p<0.05$) and between the second and third doses ($p<0.01$) (**Figure 5.2 and Table 5.1**). These changes are also reflected in their respective AUC values (**Table 5.1**).

**Figure 5.3** presents results for an i.v. dose schedule of 9 mg/kg Caelyx® q4wk x 4. Peak plasma levels were the same as for the previous two dosing schedules and, as was seen in mice receiving the q2wk x 4 dosing schedule, the longer dose interval resulted in plasma DXR concentrations that were below detectable limits between doses (**Figure 5.3A**). The $t_{1/2}$ and AUC values were also similar to those for previous dosing schedules (**Table 5.1**).

Skin and paw DXR concentrations for this dose schedule are presented in **Figures 5.3B** and **5.3C,** respectively. Again, the $C_{max}$ for total DXR was achieved at approximately 72 hours post-injection. For this dose schedule, the drug

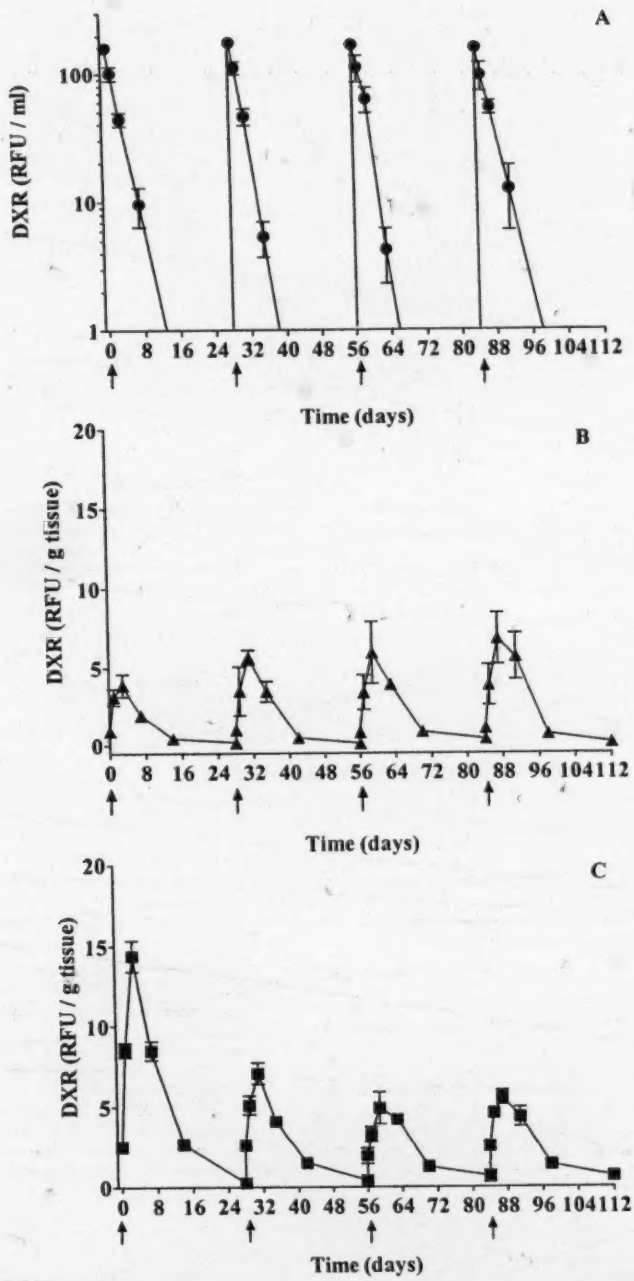


**Figure 5.3**. Tissue concentrations of DXR in mice given Caelyx® at a dose schedule of 9 mg/kg q4wk. Mice were injected i.v. via the lateral tail vein q4wk (arrows). Data represent the mean ± S.D. of triplicate aliquots from 4 to 5 mice and are reported as DXR RFU. A) plasma, B) skin, C) paws.

concentrations in both skin and paws fell to low levels before each successive injection. Skin $C_{max}$ and AUC values increased with each dose ($C_{max}$, dose 1 vs. dose 4, $p<0.05$), while those for paws decreased, particularly between the first and subsequent doses ($C_{max}$, $p<0.001$ for dose 1 vs. dose 2) (**Figure 5.3**).

PK parameters for all three dose schedules are presented in **Table 5.1.** Skin and paw elimination $t_{1/2}$ values could not be calculated for the q1wk dosing schedule because there were not sufficient points on the tissue concentration versus time curve. Modest increases in plasma $t_{1/2}$ were observed for all dosing schedules from the first to fourth dose. Mice receiving Caelyx® with a q4wk schedule had an increase in clearance $t_{1/2}$ for paws, while skin $t_{1/2}$ did not change appreciably. The average steady state drug concentration ($C_{ss}$) for each dose schedule was calculated by dividing the $AUC_{ss}$ ($4^{th}$ dose) by the dose interval in hours (**Table 5.1**). As expected the CL and $V_d$ were similar for all doses, and doubling the dose interval resulted in a halving of the $C_{ss}$ values for all tissues.

The dose schedules used in these experiments exposed mice to DXR over long periods of time. Similar to the clinical use of Caelyx®, mice developed PPE-like lesions. The lesions included hair loss on the mouse's muzzle (area exposed to pressure while the mouse feeds) and red inflamed paws with mild swelling. The presence of lesions did not, however, have an effect on the weight of the paws. As seen in **Table 5.2**, PPE-like lesions were more frequent in mice receiving the 9 mg/kg q1wk x 4 dose schedule. This is consistent with current clinical and laboratory data

**Table 5.2.** Numbers (percent) of mice developing PPE-like lesions as a function of dose schedule. Values represent the number of mice with PPE-like lesions at the time of receiving the stated dose. Lesions included hair loss on the mouse's muzzle and erythematous paws. For each dose schedule mice were injected i.v. with Caelyx® at a DXR dose of 9 mg/kg.

| Dose Schedule | Dose 2 | Dose 3 | Dose 4 |
|---|---|---|---|
| q1wk | 0/75 (0 %) | 8/50 (16 %) | 17/24 (70 %) |
| q2wk | 5/75 (7 %) | 5/50 (10 %) | 8/25 (32 %) |
| q4wk | 3/90 (3 %) | 3/60 (5 %) | 0/30 (0 %) |

demonstrating that PPE is more likely to occur with higher Caelyx® dose intensities (1, 48, 120, 169).

During these experiments some additional drug toxicity was observed, particularly for the q1wk dose schedule. Four mice from the 9 mg/kg q1wk schedule were euthanized due to severe weight loss (3 mice, no cause determined; 1 mouse, heart failure). Three mice from the 9 mg/kg q2wk schedule were euthanized (2 mice, no cause determined; 1 mouse, mild subacute cardiac and hepatic degeneration). In the 9 mg/kg q4wk group, 1 mouse was euthanized due to severe weight loss (no cause determined). The staff veterinary pathologist at the University of Alberta's Health Sciences Laboratory Animal Services performed all postmortem exams. The total cumulative Caelyx® dose for these animals was high (36 mg/kg, 108 mg/m$^2$). Since toxicity was encountered, mice in the subsequent experiments received only 2 doses of Caelyx® (18 mg/kg, 54 mg/m$^2$ total drug).

### 5.1.2 Therapeutic Experiments

From the previous PK and BD experiments it was determined that lengthening the dose interval for Caelyx® therapy, i.e., decreasing the dose intensity, from q1wk to q2wk or q4wk resulted in substantial decreases in the cutaneous concentration of DXR between doses, and a decrease in the incidence of PPE-like lesions. Therapeutic experiments were performed to determine if lengthening the dose interval altered the therapeutic activity of Caelyx®. Similar to therapeutic experiments performed in Chapters 3 and 4, female BALB/c mice (6-8 weeks) were orthotopically implanted with the 4T1 murine mammary carcinoma in the right #4 mammary fat

pad. Four days later treatment was started; mice (n=5) received 9 mg/kg (27 mg/m$^2$) Caelyx® (i.v.) q1wk, q2wk or q4wk (2 doses for a total drug dose of 18 mg/kg, 54 mg/m$^2$). Control mice received an equal number of injections of 200 μL D5W as this was the vehicle used to dilute Caelyx®. Similar to the other experiments in this thesis (Chapters 3 and 4), tumor growth was monitored by measuring perpendicular diameters (a and b) and tumor volume was calculated using the formula $v=0.4ab^2$ where a>b. The experiment was repeated once and the results from the pooled experiments are presented in **Figure 5.4**.

Tumor growth in control mice receiving sterile D5W was similar for all dose schedules. The therapeutic activities of Caelyx® were equivalent for mice receiving the drug for either a q1wk x 2 or a q2wk x 2 dose schedule. Caelyx® administered using a q4wk x 2 dose schedule appeared to have reduced therapeutic activity compared to the other two dose regimes. In other words, if the dose interval was too long, antitumor activity appeared to be adversely affected. Since lengthening the dose interval is one way that PPE is handled in the clinic, these results may have important clinical implications. It must be pointed out that for mice receiving Caelyx® q4wk, there may have not been enough time for the second dose to produce its antitumor effect before the large tumor volume necessitated euthanizing the mice.

Overall, these experiments focusing on the influence of dose delay on the PK and BD of Caelyx® suggest that this species is a reasonable animal model for studying factors influencing the development of Caelyx®-associated PPE. It was demonstrated that the repeated administration of Caelyx® at short dose intervals

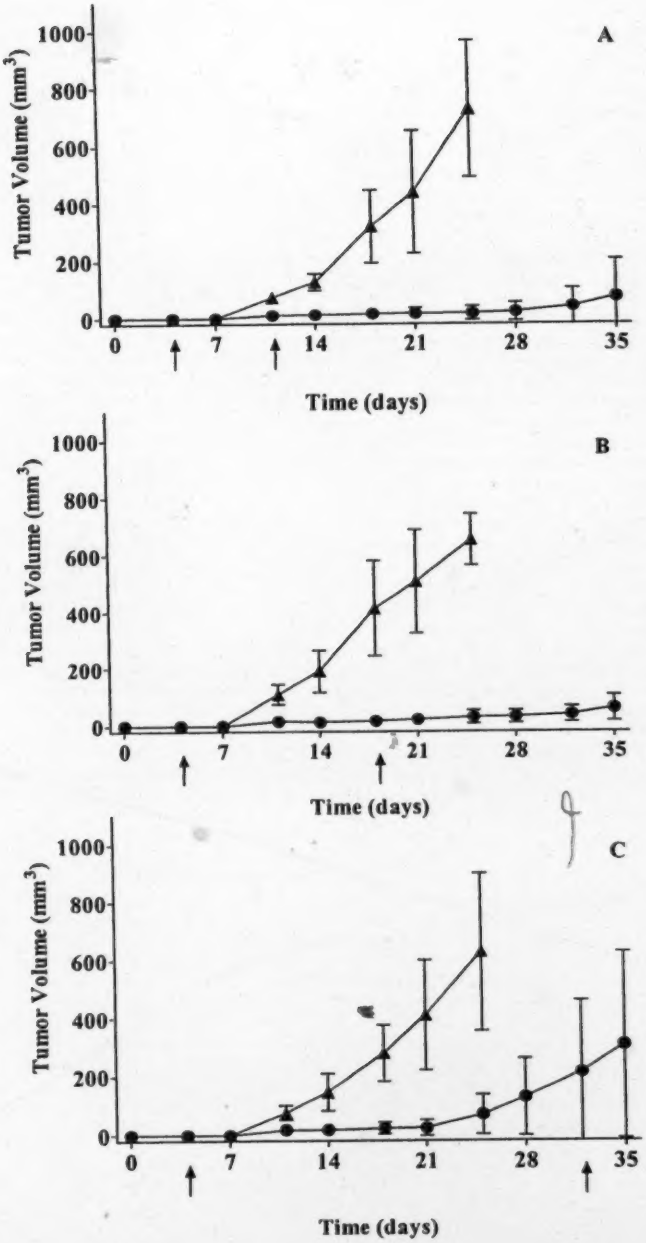


**Figure 5.4.** Therapeutic activity of Caelyx® against the 4T1 murine mammary carcinoma using different dose schedules. BALB/c mice were implanted in the #4 mammary fat pad with the 4T1 murine mammary carcinoma. Four days later mice began i.v. treatment with Caelyx® at a DXR dose of 9 mg/kg with one of three dose schedules: **(A)** q1wk, **(B)** q2wk, or **(C)** q4wk. Control mice received sterile D5W: (▲) control, (●) Caelyx®. Arrows indicate treatment days. Data represent the mean ± S.D. from 5 to 10 mice.

(q1wk) results in an accumulation of DXR in the cutaneous tissues of mice, and that these mice have a higher incidence of PPE-like lesions than mice receiving dose regimes with a lower dose intensity. Lengthening the dose interval allows for more accumulated drug to be cleared from cutaneous tissues, resulting in fewer PPE-like lesions in mice. These experimental results confirm clinical observations that longer dose intervals in humans reduced the incidence and severity of PPE lesions (1, 120). If these murine results can be extrapolated to humans, then dose delay appears to be useful in controlling PPE because it allows time for drug to be cleared from the skin and for existing lesions to heal. However, as demonstrated here, the advantages of dose delay may be offset by reduced therapeutic activity.

A recent review of toxicities associated with Caelyx® in patients with metastatic breast cancer provides support for this model (106). The recommended dose intensity for these patients is ~12 mg/m$^2$/wk and the average plasma $t_{1/2}$ was 79.4 hours; when Caelyx® is administered every 4 weeks this dose interval corresponds to 8.5 plasma $t_{1/2}$s. The murine data presented in this thesis mimic these clinical data. Naïve mice receiving Caelyx® q2wk (13.5 mg/m$^2$/wk) had an average plasma $t_{1/2}$ of 39.4 hours, which corresponds to 8.5 plasma $t_{1/2}$s. Interestingly, this dose schedule also gives good therapeutic efficacy in this model with a tolerable incidence of PPE-like lesions.

In this murine model, it is also important to note that the plasma $t_{1/2}$ did not change substantially for multiple doses of Caelyx®, although there was a modest increase in $t_{1/2}$ after the first dose for each schedule. This is significant because the

development of PPE has been correlated to the plasma half-life of Caelyx® (106). If Caelyx® was cytotoxic to the cells of the MPS, which is responsible for clearing liposomes, then multiple dose regimes could have resulted in extended $t_{1/2}$ as a result of impaired clearance mechanisms (77). At the dose schedules employed in this study, MPS function was not impaired to a degree that affected the PK of Caelyx®. This lack of substantial MPS toxicity with Caelyx® is consistent with studies from other laboratories (78).

The observation that the skin and paw PK values were different from those for plasma PK is interesting. The plasma drug levels fell to low values between doses for even a q1wk dose schedule, while the skin and paws drug levels remained elevated for several days. Plasma levels in mice have been important for determining the dosing schedule for liposomal drugs in efficacy studies, and a q1wk schedule is often chosen (109, 150, 170). This schedule is based on clearance of inert liposomal markers such as $^{125}$I-TI in naïve mice ($t_{1/2}$ of 18 –24 h in liposomes of similar composition to those used in these studies) (72). Hence, within 1 week (>8 plasma half-lives) this marker would be cleared almost completely from the plasma of mice. However, the clearance rate of DXR in these experiments is approximately 2-fold longer than the clearance rate of $^{125}$I-TI (an average 39 h in naïve mice) and 8 half-lives, in this case, corresponds to one dose every 2 weeks. The difference between the $t_{1/2}$ of DXR and $^{125}$I-TI reflects differences in the rate of release and volumes of distribution of the two compounds. Further, loading DXR into liposomes has been shown to increase their circulation times in other models (171). As in Chapter 4,

regardless of the model, PK studies that do not follow the pharmacologically active agent should be interpreted with caution (75, 76, 172).

Skin concentrations of DXR, and their respective AUCs, continued to increase with each successive dose (**Table 5.1**). This may be a consequence of skin cytotoxicity accompanied by inflammation. Similar to tumor tissue, inflamed tissue has increased capillary permeability and can accumulate liposomes via the enhanced permeability and retention (EPR) effect (88, 173). This will increase localization of liposomes into skin with subsequent injections in a vicious cycle. Alternatively, since our dorsal skin samples were not subject to pressure or irritation, the increased localization of liposomes into these samples may reflect an increase to steady-state levels, which normally occurs within 3 to 5 doses. For drug clearance, an interval of 5 half-lives results in approximately 3% of the total dose remaining in tissues. For skin, 5 half-lives would be approximately 23 days, which corresponds roughly to the q4wk dosing interval that produced the lowest incidence of PPE-like lesions.

One unexpected observation was the decrease in the $C_{max}$ and AUC for paws using the q2wk and q4wk dose schedules. This decrease was not due to the alterations in the plasma PK (i.e., $t_{1/2}$ values did not decrease). Therefore, fewer liposomes must have localized in the tissue. This may be a result of the longer dose interval allowing DXR-associated tissue damage to heal, causing tissue remodeling or scarring, which would in turn reduce the ability of subsequent doses to accumulate. Alternatively, it could be due to a reduction in the pressure-dependent extravasation

of liposomes if mice developed "sore paws" (PPE-like lesions) and moved around their cages less, although this was not specifically measured.

Based on these results, further experiments were undertaken to examine how different dose schedules with the same dose intensity influence the PK, BD and therapeutic activity of Caelyx®.

## 5.2 Dose Schedules With the Same Dose Intensity

The dose and dose interval were adjusted to deliver the same dose intensity of Caelyx® therapy. PK/BD and therapeutic experiments were compared for three dose schedules: 4.5 mg/kg q3d (x4), 9 mg/kg q1wk (x2) and 18 mg/kg (x1).

### 5.2.1 Pharmacokinetic and Biodistribution Experiments for the Same Dose Intensity

In humans the maximum tolerated dose intensity of Caelyx® is determined by cutaneous toxicities (10-12 mg/m$^2$/wk). Therefore, optimal dose schedules for this dose intensity must be determined. Recent evidence suggests that for a given dose intensity of Caelyx® it is therapeutically beneficial to administer larger infrequent doses than smaller frequent doses (152). To explore this hypothesis, PK and BD experiments were performed in mice bearing the orthotopically implanted 4T1 murine mammary carcinoma. Similar to experiments in Chapters 3 and 4, female BALB/c mice (6-8 weeks) were implanted with the 4T1 murine mammary carcinoma and 10 days later were injected i.v. with Caelyx® at a dose intensity of 9 mg/kg/wk (27 mg/m$^2$/wk). This dose intensity was chosen as it is close to the maximally tolerated

dose in mice, and patients with solid tumors receive maximally tolerated doses of Caelyx®.

The dose schedules used were 18 mg/kg x1, 9 mg/kg q2wk x 2 or 4.5 mg/kg every three days (q3d) x 4. Due to the toxicity seen in the previous PK and BD experiments, the total drug dose administered was 18 mg/kg (54 mg/m$^2$). At various time points after injection mice were euthanized and DXR concentrations were measured in plasma, tumor, skin and paws (see Section 2.8 Quantification of Doxorubicin). Tissue concentrations and PK parameters are given in **Figure 5.5** and **Table 5.3**, respectively.

The results for plasma DXR concentrations are presented in **Figure 5.5A**. For mice receiving 4.5 mg/kg q3d there was a significant increase in plasma $C_{max}$ from the first dose to the second and subsequent doses ($p<0.001$), and plasma levels appeared to reach steady state after the second dose, as evidence by the AUCs (**Table 5.3**). As with naïve mice, there was detectable drug in the plasma at 7 days after injection in tumor-bearing mice receiving 9 mg/kg q1wk (**Figure 5.1** vs. **Figure 5.5**). Interestingly, the plasma $t_{1/2}$ and AUC values were lower in tumor-bearing mice than for naïve mice receiving 9 mg/kg q1wk (**Table 5.3** vs. **Table 5.1A**). Distribution of liposomes to the tumor may account for the lower $t_{1/2}$ and tissue AUC values, which is consistent with results from studies using the C26 colon carcinoma tumor model in BALB/c mice (174).

A single dose of 18 mg/kg resulted in a plasma $C_{max}$ approximately twice that of the first dose of 9 mg/kg dose schedule and approximately 4 times that of the first.

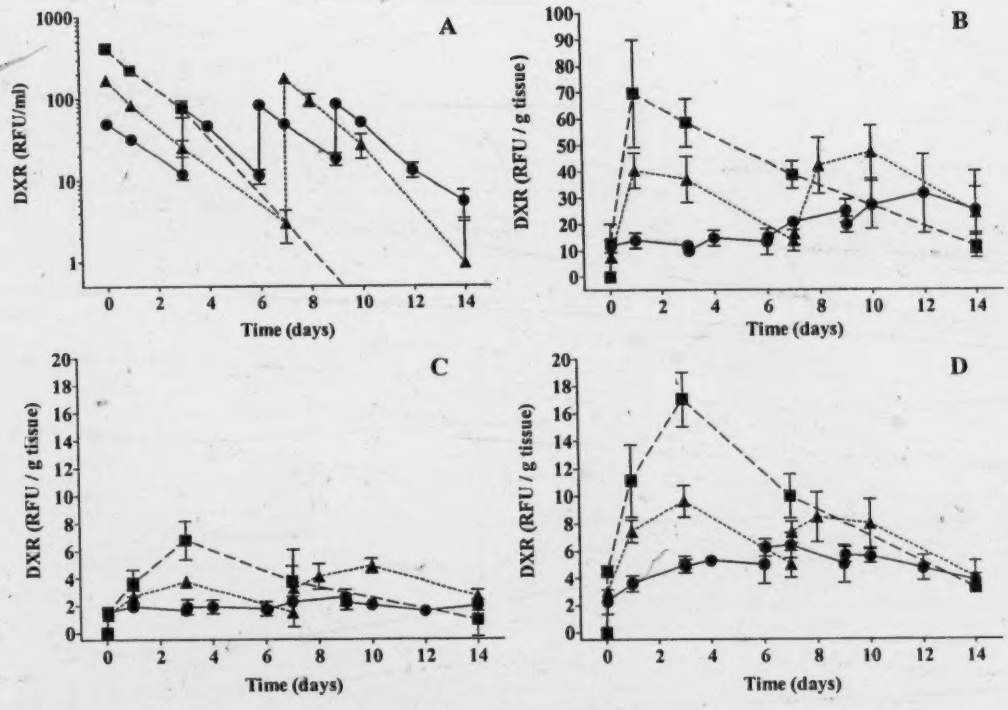


**Figure 5.5**. Tissue concentrations of DXR in mice given Caelyx® at the same dose intensity. BALB/c mice were implanted in the #4 mammary fat pad with the 4T1 tumor and injected i.v. with Caelyx® beginning 10 days later. Data represent the mean ± S.D. (n=5) and are expressed as DXR RFU. (A) plasma, (B) tumor, (C) skin, (D) paws. Symbols are as follows: (■) 18 mg/kg (1 dose); (▲) 9 mg/kg q1wk (2 doses), (●) 4.5 mg/kg q3d (4 doses).

**Table 5.3.** Pharmacokinetic parameters for mice receiving Caelyx® at a dose intensity of 9 mg/kg/wk to a total drug dose of 18 mg/kg. Mice received i.v. either four doses at 4.5 mg/kg q3d, two doses at 9 mg/kg q1wk or one dose at 18 mg/kg. AUC values were calculated using the trapezoidal rule. Plasma $t_{1/2}$ values were calculated using the formula $t_{1/2}=0.693/k_{elm}$, where $k_{elm}$ is the elimination constant derived from the plasma concentration versus time curve; $r^2$ was > 0.991 for each curve. For the purpose of AUC calculation, 1RFU is assumed to equal 1 μg of DXR and/or metabolites.

| | Plasma | | | | | Skin | | Paws | | Tumor | |
|---|---|---|---|---|---|---|---|---|---|---|---|
| Dose schedule | $t_{1/2}$ | $k_{elm}$ | AUC[a] | CL | $V_d$ | AUC[b] | $C_{max}$ | AUC[b] | $C_{max}$ | AUC[b] | $C_{max}$ |
| 4.5 mg/kg q3d | | | | | | | | | | | |
| Dose 1[c] | 34.6 | 0.020 | 2070 | 0.0017 | 0.0085 | 125 | 1.9 | 276 | 5.0 | 916 | 13.9 |
| Dose 2[c] | 25.4 | 0.027 | 4210 | 0.0013 | 0.059 | 132 | 1.9 | 368 | 5.3 | 965 | 14.7 |
| Dose 3[c] | 33.0 | 0.021 | 4510 | 0.0011 | 0.054 | 162 | 2.6 | 424 | 6.4 | 1520 | 25.0 |
| Dose 4[c] | 29.5 | 0.024 | 4500 | 0.0012 | 0.052 | 136 | 2.2 | 382 | 5.7 | 1970 | 31.4 |
| 9 mg/kg q1wk | | | | | | | | | | | |
| Dose 1[d] | 26.3 | 0.026 | 6990 | 0.0013 | 0.048 | 451 | 3.76 | 1240 | 9.63 | 4840 | 40.4 |
| Dose 2[d] | 22.2 | 0.031 | 7520 | 0.0012 | 0.039 | 661 | 4.86 | 1160 | 8.45 | 6250 | 47.0 |
| 18 mg/kg[e] | 29.5 | 0.024 | 17900 | 0.0010 | 0.041 | 1320 | 6.77 | 3780 | 17.0 | 14800 | 69.5 |

| | $AUC_{(0-\infty)}$ | | | |
|---|---|---|---|---|
| | Plasma[a] | Skin[b] | Paws[b] | Tumor[b] |
| 4.5 mg/kg q3d | 15900 | 963 | 2740 | 12200 |
| 9 mg/kg q1wk | 14500 | 1510 | 3140 | 14600 |
| 18 mg/kg | 17900 | 1320 | 3780 | 14800 |

[a] Units for plasma AUC are DXR μequivalents x h / mL

[b] Units for tumor, skin, and paw AUCs are DXR μequivalents x h / g

[c] $AUC_{(0\text{-}72hours)}$

[d] $AUC_{(0\text{-}168\ hours)}$

[e] $AUC_{(0-\infty)}$

dose of the 4.5 mg/kg dose schedule (**Table 5.3 and Figure 5.5**). The $AUC_{0-\infty}$ for the first dose of the 4.5, 9, and 18 mg/kg dose schedules were 2700 μg·h/ml, 7000 μg·h/ml, and 17000 μg·h/ml, repectively, and there is a linear relationship between these values and the dose ($r^2$=0.988). These observations are in line with the dose independence of the plasma PK for single doses of SL-DXR in this dose range (62, 138)

Tumor levels of DXR are given in **Figure 5.5B**. For mice receiving 18 mg/kg, and for the first dose at the 4.5 or 9 mg/kg dose schedules, tumor DXR reached $C_{max}$ at 24 hours, which is earlier than skin and paw levels reached $C_{max}$ for the two highest doses (72 hours). The $C_{max}$ for the 18 mg/kg dose schedule was approximately double that of the first dose of the 9 mg/kg q1wk dose schedule and approximately 4-fold higher than the $C_{max}$ for the first dose of the 4.5 mg/kg q3d dose schedule (**Figure 5.5B**), i.e., the $C_{max}$ increased proportionally with dose. The tumor $AUC_{(0-\infty)}$ values were similar for all dose schedules (**Table 5.3**).

Skin drug levels from each of the dose schedules are seen in **Figure 5.5C**. Results for mice receiving 9 mg/kg were similar to those for non-tumor bearing mice in that the $C_{max}$ for skin DXR in tumor-bearing mice peaked at 72 hours post-injection and the $C_{max}$ and AUCs for the second dose were higher than the first ($p<0.0008$, t-test) (**Table 5.1A** vs. **Table 5.3B**, **Figure 5.1B** vs. **Figure 5.5C**). As with tumor, the DXR $C_{max}$ in skin increased proportionally with dose for the first dose of each shedule (**Figure 5.5C**). The total $AUC_{(0-\infty)}$ values for the 18 mg/kg (1320 μg·h/ml) and and 9 mg/kg (1510 μg·h/ml) dose schedules were similar, and higher than that

seen for the 4.5 mg/kg (963 μg·h/ml ) dose schedule (**Table 5.3**). These results demonstrate that skin, like tumor, was exposed to sustained levels of DXR for all dose schedules, although the 9 and 18 mg/kg schedules resulted in exposure to higher drug concentrations.

The paw concentrations of DXR were higher than skin concentrations in tumor-bearing mice, as in naïve mice (**Figure 5.5D** versus **Figure 5.1C**), and the $C_{max}$ in paws continued to increase for seven days after initiation of therapy for mice receiving 4.5 mg/kg (**Figure 5.5D and Table 5.3**). The $C_{max}$, for the first dose, in paws also increased proportionally with dose. The $AUC_{(0-\infty)}$ for the 18 mg/kg dose was higher than the $AUC_{(0-\infty)}$ for the 9 mg/kg x 2 dose schedule which in turn was higher than the AUC for the 4.5 mg/kg x 4 dose schedule (**Table 5.3**). The increased paw AUC at higher doses may indicate a greater likelihood of developing skin toxicities such as PPE at these doses. For mice receiving 18 mg/kg, the tumor, skin, and paw clearance $t_{1/2}$ values were 117, 90, and 110 hours, respectively. It is notable that the tissue $t_{1/2}$ values were considerably longer than those for plasma $t_{1/2}$ (**Table 5.3**). The values for skin and paws are consistent with results from naïve mice receiving Caelyx® with different dose schedules.

Caelyx® has a shorter half-life in tumor-bearing mice than in naïve mice. These results are consistent with work by Hong et al., who found that $t_{1/2}$ values for Caelyx® were lower in mice bearing subcutaneous implants of the C26 colon carcinoma (19.1 hours) than in naïve mice (25.1 hours) (174). This can be explained partially by the significant distribution of drug-loaded liposomes to tumors.

These results, as well as data presented in Section 5.1.1, demonstrate that the half-lives for elimination of DXR from skin, paws, and tumors were longer than that for plasma. A longer $t_{1/2}$ will lead to retention of drug in tumors and, arguably, improved antitumor effects, but longer $t_{1/2}$ values in cutaneous tissues will lead to unwanted side effects such as PPE and mucositis. The challenge is to find the proper balance between minimizing PPE and maintaining therapeutic activity. As previously mentioned, increasing the dose interval to q2wk did not significantly affect the therapeutic outcome in our tumor model; however, extending the dose interval to q4wk did compromise the activity of the formulation.

In this study total DXR was measured, which includes both liposome-encapsulated and released drug. As stated in Chapter 4, an important consideration in PK, BD, and therapeutic studies with liposomes is the bioavailability of the drug. As long as the drug, e.g., DXR, remains encapsulated within the liposomes, it is not bioavailable and will have no biological activity. Therefore, to improve the therapeutic activity of SL drug delivery systems, it will be important to develop methods to quantify, and increase, concentrations of bioavailable drug.

### 5.2.2 Therapeutic Experiments

The results of therapeutic experiments for mice receiving the same dose intensity (9 mg/kg/wk, 27 mg/m$^2$/wk) at different dosing schedules are presented in **Figure 5.6**. All three schedules delayed tumor growth considerably. However, the two dosing schedules with larger doses given less frequently (9 mg/kg q1wk x 2 or18 mg/kg) appeared to delay tumor growth to a greater extent than smaller doses given

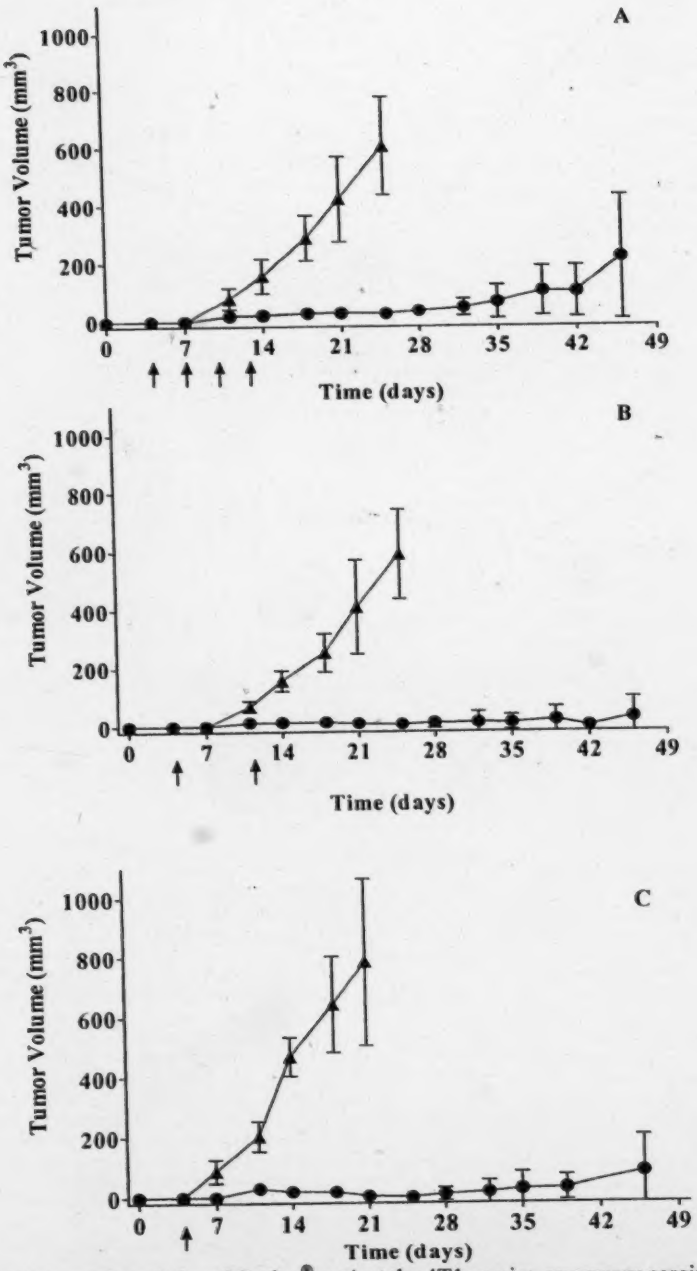


**Figure 5.6.** Therapeutic activity of Caelyx® against the 4T1 murine mammary carcinoma using dose schedules with the same dose intensity. BALB/c mice were implanted in the #4 mammary fat pad with the 4T1 murine mammary carcinoma. Four days later mice were treated i.v. with Caelyx® at a total drug dose of 18 mg/kg with one of three dose schedules: **(A)** 4.5 mg/kg q3days x4, **(B)** 9 mg/kg q1wk x2, or **(C)** 18 mg/kg x1. Control mice received sterile D5W: (▲) control, (●) Caelyx®. Arrows indicate treatment days. Data represent the mean ± S.D. from 5 to 10 mice, except for (C) where n=4-5.

more frequently. The cytotoxicity of DXR is not cell-cycle phase dependent; therefore, one can speculate that the antitumor activity of DXR might be dependent upon tumor $C_{max}$. For the dose schedules using larger doses, higher peak tumor drug concentrations are reached; this may lead to higher concentrations of bioavailable drug, which would explain the higher therapeutic activity of these dose schedules.

When this experiment was repeated, five mice were euthanized due to toxicity after receiving 18 mg/kg. Gross post mortem examination (performed by the University of Alberta's Health Sciences Laboratory staff veterinary pathologist) found evidence of cardiac toxicity. This dose is well below the reported $LD_{50}$ of 38 mg/kg reported for a bolus injection of SL-DXR in CD-1 mice (111). Whether this difference is because of strain-specific differences in sensitivity to DXR or is tumor-related was not examined further. No further experiments were carried out with this dose.

As previously observed in Chapters 3 and 4, and as verified in these experiments, solid tumor tissue accumulates liposomes at a faster rate than either skin or paws. Therefore it may be possible improve the therapeutic activity of Caelyx® by triggering drug release after tumor drug concentrations have peaked. The significant improvement in therapeutic outcome in experiments in tumor-bearing mice by Needham et al., in which DXR release was triggered by hyperthermia in single tumors (as opposed to metastatic disease) supports this hypothesis (175). Further, since larger doses appeared to have superior therapeutic activity compared to smaller doses, it may be clinically useful to administer Caelyx® at the maximum tolerated

dose for a single injection (60-70 mg/m$^2$) and then leave enough time for cutaneous drug to be cleared, i.e., q6wk, to achieve a dose intensity of 10 mg/m$^2$/wk (140).

**5.3 Conclusion**

In summary, these studies using a murine model reinforce the importance of dose schedule and dose intensity on the therapeutic activity and cutaneous toxicity of Caelyx®, and provide the first experimental data on the PK and BD of liposomal DXR in tumor and cutaneous tissue for multiple dosing schedules. They also provide experimental evidence supporting the utility of a mouse model for predicting side effects and therapeutic activity of SL products in the clinic.

# Chapter 6

## Summarizing Discussion and Future Directions

# Chapter 6 Discussion

## 6.1 Summary

The aim of the research described in this thesis was to explore the relationships between the PK and BD of SL-DXR into the tumor (4T1), the cutaneous tissues of mice and the side-effect profile and therapeutic activity of SL-DXR. The specific aim was to find liposomal formulations or drug dosing regimens that reduced the cutaneous accumulation of SL-DXR without altering the tumor accumulation and therapeutic activity. The underlying assumption of this goal was that reducing the amount of SL-DXR that localized in the cutaneous tissues of mice would decrease their likelihood of developing cutaneous toxicities related to SL-DXR therapy, and that this would have relevance for the clinical use of SL-DXR (Caelyx®) in humans.

The data presented in Chapters 3 and 4 explored how altering liposome diameter and drug release characteristics, respectively, influenced the accumulation of SL and their encapsulated DXR into the skin, paws and tumors (4T1 murine mammary carcinoma) of mice. Chapter 5 focused on how repeat administration of Caelyx®, using different dose regimes, influenced the tumor, skin and paw accumulation of DXR from the clinical product, Caelyx®.

It was determined in Chapter 3, and confirmed in both Chapters 4 and 5, that the PK of SL-DXR accumulation for tumor were not the same as for cutaneous tissues. The former accumulated SL-DXR more rapidly, and to higher concentrations, than the latter. These data also demonstrated, using the orthotopically implanted 4T1 murine mammary carcinoma, that small (approximately 100 nm

diameter), stable, DXR-loaded SL (i.e., Caelyx®) produced the highest tumor total DXR concentrations, but these data did not provide a measurement of what portion of the total DXR was bioavailable. Moreover, it was determined that the higher overall tumor concentrations of total DXR resulted in increased therapeutic activity. This suggests that concentrations of bioavailable drug were sufficient to impair tumor growth. Further, when multiple dose regimes were used, dose schedules with high dose intensities resulted in improved therapeutic activity over dose schedules with lower dose intensities. Unfortunately, these formulations and dose schedules also produced the highest concentrations of SL-DXR in cutaneous tissues, i.e., skin and paws. With respect to repeat administration, the data in Chapter 5 demonstrated that frequent administration of Caelyx® resulted in accumulation of DXR in cutaneous tissues when the dose interval was shorter that the wash out period of the drug. It was also demonstrated that the likelihood of developing PPE-like lesions in mice was reduced when the dose interval was lengthened to allow for complete elimination of drug from cutaneous tissues. This parallels clinical findings. Finally, for a given dose intensity of Caelyx®, it appeared more therapeutically beneficial to administer larger doses less frequently than smaller more frequent doses. Overall, Caelyx® is an efficacious formulation of DXR, and, in order to improve its therapeutic index, optimal dose schedules will need to be determined, along with new strategies to reduce or alleviate its cutaneous toxicities.

## 6.2 Reducing Cutaneous Toxicities of STEALTH® Liposomal Doxorubicin

In order to improve the therapeutic index of Caelyx® it will be important to reduce its cutaneous toxicities. This can be achieved in two ways. First, the dose schedule can be altered to reduce the likelihood of patients developing cutaneous toxicities. Second, once PPE or mucositis develops, newer, more effective methods are needed to treat lesions.

### 6.2.1 Altering the Dose Schedule to Reduce Cutaneous Toxicities

Although Caelyx® is currently approved for clinical use in humans for two indications, further refinement of its dose schedule could take place in clinical trials for additional indications. If the data presented in this thesis were used as a starting point to plan these additional clinical trials, then the following strategy should be considered: administering the maximum tolerated single dose of Caelyx®, i.e., 60-70 $mg/m^2$ (1), and then allowing time for the drug to be cleared from cutaneous tissues before subsequent doses are given. A recently published Phase I trial dealt with this topic and determined that Caelyx® administered at 60 $mg/m^2$ q6wk had an acceptable toxicity profile (140). There was no grade 3 or 4 skin toxicity for 9 patients receiving a total of 33 cycles of therapy. The purpose of the study was to determine if Caelyx® could be administered using a six-week protocol in order to better coincide with the q3wk dose schedule used for other agents (e.g., carboplatin and paclitaxel) (176). The authors stated that a q6wk dose schedule would increase patients' quality of life due to fewer hospital visits to receive treatments. This study also presented a starting point to optimize Caelyx® therapy; based on these data, 60 $mg/m^2$ of Caelyx® q6wk is

a reasonable dose schedule for Phase II and Phase III studies, in both monotherapy and in combination therapy.

### 6.2.2 Treating Cutaneous Lesions (Palmar-Plantar Erythrodysesthesia)

Another approach to improving the therapeutic index of Caelyx® would be to develop more efficacious treatments for cutaneous lesions once they develop. Patients are currently counseled to avoid activities that increase pressure on, and blood flow to the skin, for example leaning on one's elbows or taking hot baths. These activities increase the cutaneous accumulation of SL-DXR. Patients are also counseled to recognize the early signs of toxicity, so that precautions can be taken early (i.e., cooling affected areas or dose delay or dose reduction) to avoid the development of high-grade toxicity.

Several pharmacological interventions have been suggested to reduce the severity of PPE lesions. Topical treatments containing corticosteroids have been used for PPE associated with conventional anticancer drugs (e.g., 5-FU), but they were not efficacious (135, 177). Oral pyridoxine (vitamin $B_6$), given prophylacticaly, helped some patients with 5-FU-associated PPE, and it has also been used to treat Caelyx®-associated PPE in humans (177, 178). It is hypothesized that pyridoxine acts as an antioxidant to reduce DXR-associated oxidative damage in the skin (177). In a veterinary clinical trial, pyridoxine delayed the occurrence of PPE lesions in dogs, but it did not reduce the severity of lesions once they developed (142). Pyridoxine is readily available and nontoxic at standard doses, so it presents an easy and

inexpensive treatment for PPE. However, its effectiveness should still be tested in prospective trials.

Other strategies to reduce the incidence and severity of PPE included treatments originally designed to treat DXR extravasation injuries, such as the use of topical 99% dimethylsulfoxide (DMSO) (179). Lopez et al. reported preliminary data that showed topical 99% DMSO was useful in the treatment of Caelyx®-associated PPE (143). The authors speculated that the activity of DMSO may be due to its ability to solubilize DXR and remove it from the skin, or due to its antioxidant activity (143). The latter explanation is consistent with the hypothesized mechanism of pyridoxine, and suggests that antioxidant therapy may play a key role in the treatment of these lesions. Regardless, prospective trials are needed to determine the true effectiveness of these interventions.

Another compound used to treat DXR extravasation injury is Bi(3,5-dimethy-5-hydroxymethyl-2-oxomorpholin-3-yl, DMH3), which converts DXR to the less toxic metabolite deoxydoxorubicin aglycone (180). DMH3 showed promise in early animal models for the treatment of DXR extravasation injury. However, for maximal therapeutic effect it needed to be injected cutaneously near the site of injury, soon after extravasation (180). This fact will probably not allow its use in PPE, as the lesions are relatively diffuse and develop over a period of several days.

Finally, vasoconstrictive agents, such as ergotamine or its derivatives, have been proposed as a possible treatment for Caelyx®-associated PPE (56). Given the complex pharmacological properties of ergot alkaloids, including their emetogenic

potential, oncologists may be hesitant to use these drugs in patients already receiving complex multi-drug regimes (181). On the other hand, the application of short acting, topically applied, vasoconstrictors may prove useful if they can be formulated to have reasonable skin penetration. Topical astringents may prove useful in this regard (Professor Hamid Mohgini, personal communication).

Regardless of what strategies are employed to reduce the cutaneous toxicities of Caelyx®, it may be advantageous to perform pre-clinical testing of these strategies on small animal models. In the literature, PPE has been described in rabbits and dogs treated with Caelyx® (103, 133, 142). These species can be difficult and expensive to use as models. The murine model presented in this thesis provides an alternative for the initial testing of some of these toxicity-reducing strategies. As stated in Chapter 5, mice treated with Caelyx® developed PPE-like lesions similar to those observed with the clinical use of Caelyx®. We observed similarities to the human syndrome in the anatomical distribution of lesions, the dose intensity required to induce lesions, and the number of plasma half-lives between doses that results in a decrease in lesions. Further refinement of this model should focus on functional studies to determine if the lesions cause limitations in activities in mice like they do in humans and on developing better, non-invasive measurements for quantitating the severity of the PPE lesions in mice. This will allow testing of potential treatments for PPE in a functional model, as opposed to measuring tissue drug concentrations, which is a terminal procedure. With these improvements, this murine model will be a useful tool to further investigate treatments for the cutaneous toxicities of Caelyx®.

PPE as a side effect of treatment with SL-DXR was described almost 10 years ago (46). The data presented in this thesis represent the first systematic examination of the cutaneous biodistribution of SL-DXR. Reasons for this most likely reflect the fact that the clinical usefulness of Caelyx® has been firmly established and that re-formulation is not desirable for a pharmaceutical company from an economic standpoint. Every antineoplastic drug has unique dose-limiting toxicities. With conventional DXR the major acute dose-limiting toxicity is myelosuppression and the cumulative dose-limiting toxicity is a life-threatening cardiomyopathy. Both of these toxicities are reduced by encapsulation of DXR in SL (105, 107). PPE is considered to be the dose-limiting toxicity of Caelyx®, but it is more of a chronic than an acute toxicity, which, although painful and inconvenient, is not life-threatening. It can be managed in large part by dose delay and dose reduction. If given a choice between a serious, life-threatening toxicity like irreversible cardiac damage and a reversible, more manageable, non life-threatening toxicity like PPE, the choice should be obvious.

### 6.3 Increasing the Therapeutic Activity of STEALTH® Liposomal Doxorubicin

The data presented in this thesis suggests that the clinical formulation of Caelyx®, with its small size and slow drug release rate, appears to be close to optimal in terms of therapeutic activity since all of the manipulations of formula and dose schedule that were tried in this thesis resulted in decreased therapeutic activity. Clinical studies resulted in the recommendation of a maximal dose intensity of 10-12 $mg/m^2/wk$ (106). In the absence of newer and more efficacious treatments for the

toxicities of Caelyx®, new strategies to improve its therapeutic activity will have to be developed in order to improve its therapeutic index. Three strategies that are being studied are 1) the use of targeting ligands to selectively deliver liposomal drug to tumor cells, which will further increase the amount of drug delivered into the tumor cells (150, 182-189) 2) the substitution of SL-DXR for conventional DXR in combination chemotherapeutic regimens to decrease the side-effects and allow larger cumulative doses (121-123, 176, 190, 191) and 3) combining treatment modalities (e.g., radiation therapy or hyperthermia) to yield additive or synergistic antitumor interactions (192-196). Each of these strategies is discussed below.

### 6.3.1 Ligand Targeted Liposomes

As recently reviewed by Allen, targeted therapeutics such as monoclonal antibodies and radioimmunotherapeutics and are finding their way into clinical use, and ligand targeted liposomes are approaching Phase I clinical trials (197). Until recently, liposomes targeted via whole monoclonal antibodies, often of murine origin, have been commonly used. Newer strategies using humanized or chimeric antibodies or antibody fragments (Fab' fragments or better still, single chain variable fragments, scFv) should overcome the major immunogenicity problem associated with the use of whole murine antibodies (197). These targeted liposomal formulations have demonstrated considerable activity in pre-clinical models, due to their greater selectivity for tumor cells. Two of the most advanced models are anti-CD19 targeted liposomal DXR for the treatment of B-cell malignancies (183, 184, 186, 187) and

anti-HER2 immunoliposomal DXR for the treatment of HER2 overexpressing breast cancer (182, 189).

With respect to the use of targeted liposomal formulations, it will be important to carefully select the cellular target as well as the targeting ligand. The target antigen or receptor should be expressed to a significantly greater degree on tumor cells than on normal cells. Further, a high percentage of the tumor cell population should express the target of interest. As well, the biological function of the target antigen or receptor will be an important consideration. For example, if binding of the liposome to its target effects a biological response, it may lead to synergistic interactions between signaling pathways and the liposomal drug. Further, recent data has demonstrated that targeting liposomal drugs to internalizing epitopes (antibody targeted SL-DXR) on tumor cells results in superior therapeutic results versus targeting via non-internalizing epitopes (198).

### 6.3.2 Combination Chemotherapy With STEALTH® Liposomal Doxorubicin

The principle underlying the use of combination chemotherapy is that, by exposing tumors to combinations of drugs with different mechanisms of action, it should be possible to achieve additive or synergistic effect and reduce the possibility of selecting drug-resistant clones. Further, by using drugs with non-overlapping toxicities, it is possible to administer maximal or near-maximal doses of each individual drug to achieve a maximal therapeutic response. Combination chemotherapy with conventional anticancer drugs has resulted in cures for childhood

leukemias as well as Hodgkin's lymphoma, and excellent survival rates for some solid tumor such as testicular cancer (42).

Caelyx® will be a useful agent in combination therapy due to its relatively unique toxicity profile (i.e., low incidence of myelosuppression and cardiac toxicity) and its high degree of therapeutic activity in a variety of tumors. Further, the decreased incidence and severity of cardiomyopathy and myelosuppression seen with Caelyx® should make it useful in treating frail or elderly cancer patients so that it may replace conventionally administered DXR in some protocols. A recent Phase II clinical trial explored these issues by substituting Caelyx® for conventional DXR in the treatment of aggressive non-Hodgkin's lymphoma in patients over 60 years of age (191). The investigators used Caelyx® instead of conventional DXR in combination with cyclophosphamide, vincristine and predinsone (CHOP regime) and demonstrated an overall response rate of 64%, which is similar to dose regimes containing conventional DXR in a similar patient population (199). Importantly, no patients (0/33) developed congestive heart failure while receiving the regime containing Caelyx® (191). This is compared to another study where 4/72 patients developed cardiac toxicity after receiving a similar regime containing conventional DXR (199). Caelyx® should not be substituted automatically for DXR in all treatment regimes without proper, prospective, randomized trials. However, these results are encouraging and if they are applicable to other treatment regimes, Caelyx® will offer an efficacious, low toxicity alternative for patients not able to tolerate conventional chemotherapy.

Caelyx® has also been tested in several Phase I trials in combination with other anticancer drugs for the treatment of metastatic breast cancer (vinorelbine, gemcitabine or docetaxel) as well as ovarian and other malignancies (platinum compounds and paclitaxel) (121-123, 176, 190). These reports demonstrate favorable toxicity profiles for these regimes when the dose intensity for Caelyx® therapy remains within the currently recommended range (i.e., between 8-12 $mg/m^2/wk$). Further, the doses of the other agents do not need to be reduced, thus providing the opportunity for maximal therapeutic effect. One interesting note is that Caelyx®, when given in combination with cisplatin, had a decreased incidence of PPE (190). The authors attributed this to cisplatin-activated macrophages increasing the clearance of liposomes (cisplatin lowered the $t_{1/2}$ of Caelyx® and 7 day post-injection DXR plasma concentrations).

Moreover, a clinical trial is currently underway using Caelyx® in combination with trastuzumab (Herceptin®) for the treatment of HER2-overexpressing metastatic breast cancer[2]. Trastuzumab is a humanized monoclonal antibody against the extracellular portion of the HER2 protein that has activity against HER2-overexpressing breast cancer (200-202). The combination of trastuzumab and conventional DXR is effective in the treatment of HER2-overexpressing breast cancer (202). Trastuzumab is capable of producing cardiac toxicity (202), therefore, in this

[2] Official trial title "Phase I/II study of doxorubicin HCl liposome and trastuzumab (Herceptin) in women with advanced HER-2/NEU-overexpressing breast cancer". Study ID NCI-G00-1878, more information can be found at www.clinical trials.gov

trial Caelyx® is being substituted for conventional DXR to reduce the likelihood of adverse cardiac events as well as to maximize therapeutic activity.

### 6.3.3 Combined Modality Therapy and Triggered Release Formulations

Another strategy to improve the therapeutic activity of Caelyx® is to combine it with other treatment modalities, such as radiotherapy or hyperthermia, to obtain additive or synergistic antitumor effects (192-196). Combining treatment modalities offers many of the same advantages as combination chemotherapy, including the potential for additive or synergistic effects between modalities and reducing the likelihood of selecting for resistant clones (203). In addition there is the potential for spatial cooperation between radiotherapy and chemotherapy. This occurs when radiation therapy is used to treat localized disease and chemotherapy is used to treat distant metastasis (as well as local disease) (203). External beam radiation therapy penetrates the skin and can produce toxicities that are enhanced by conventional DXR (204). Accordingly, there will be concern regarding DXR-associated skin and heart damage when radiation therapy is combined with Caelyx®; indeed, radiation recall injury has already been described in patients receiving Caelyx® (48, 193). In order to reduce the severity of these toxicities, radiation therapy should be administered after tumor liposome concentrations peak, but before skin concentrations reach maximum levels.

Clinically, Caelyx® has been tested in Phase I studies in combination with radiation therapy to treat non-small cell lung cancers as well as head and neck cancers (193). In both indications, the primary tumor received 44 Gray (Gy) given in 2 Gy

fractions. For patients with lung cancer the maximum tolerated dose of Caelyx® was 25 mg/m$^2$ q2wk; esophageal toxicity was the only cause of radiation treatment delays and no grade 3 skin toxicity was observed. For patients with head and neck cancers the maximum tolerated dose of Caelyx was 20 mg/m$^2$ q2wk; higher doses led to an increase in mucosal toxicity (in the field of radiation treatment). Results from this small study were encouraging, with overall responses of 54% for lung cancer (3/14 complete responses) and 100% for head and neck cancer (9/12 complete responses) (193). These results may lead to combining radiation therapy with other agents encapsulated within STEALTH® liposomes. For example, in pre-clinical experiments, Caelyx® and SL-cisplatin demonstrated activity as radiosensitizers in human xenograft models using concomitant chemotherapy and radiotherapy (205).

Other small clinical studies have examined the use of Caelyx® in conjunction with less established treatment modalities like hyperthermia and radiofrequency ablation therapy (195, 206, 207). These local modalities kill tumor cells using heat, and they offer three mechanisms to increase the therapeutic activity of Caelyx® or other DDS. First, heat increases the localization of liposomes into tumor tissue due to alterations in organ perfusion (208); secondly, heating liposomes may induce drug release and increase the tumor levels of bioavailable drug in the vicinity of liposomes (194). Lastly, heat is known to enhance the effect of certain anticancer drugs (192). Potential mechanisms include increased tumor perfusion leading to an increased drug delivery, inhibition of cellular repair mechanisms, and alterations in membrane permeability to increase the accumulation of drugs into tumor cells (192). For

example, radiofrequency ablation can generate intratumor temperatures in excess of 70°C, well above the 42-48°C needed to increase the activity of anticancer drugs (192, 195). This temperature should also be more than sufficient to increase DXR leakage from Caelyx®. Combining the two treatments improved response rates in patients with liver tumors (195). Further, Kong et al. recently demonstrated that newly developed long-circulating thermosensitive liposomes were able to release DXR in a narrow temperature range (39-40°C) (175, 194). Due to the low threshold of thermosensitivity of these liposomes, they were able to release a large portion of their drug as they passed through the tumor vasculature, thus providing higher concentrations of bioavailable drug and better therapeutic responses (194).

Combined modality therapy represents an exciting and expanding area of cancer research, but it must be kept in mind that potential clinical indications will need to be selected carefully as local modalities (e.g., hyperthermia and radiation therapy) may not be applicable to widespread disease. As technologies improve to deliver heat to diseased tissues, more indications will be likely be developed for these modalities (209).

Other attempts at modifying drug release rates to increase the amount of bioavailable drug from liposomal carriers include the generation of pH-sensitive liposomes that will release their contents in an acidic environment, and other triggered release strategies that will allow liposomal contents to be released in a controlled manner (40, 210). pH-sensitive liposomes are composed of lipids (e.g., dioleoylphosphatidylethanolamine) that form bilayers at relatively high pH or when

they are stabilized by the presence of mPEG-derivatized lipids. At lower pH, or after the loss of the stabilizing mPEG coating, the lipids will spontaneously revert from a bilayer configuration to a hexagonal II phase, releasing their contents in the process. pH-sensitive formulations are designed to release their contents in the acidic lysosomal compartment of cells when targeted via an internalizing receptor, but they may also have some increase in contents release in the acidic tumor interstitial fluid (40, 187, 210, 211). Unlike the strategy of triggering the release of liposomal contents using an externally applied modality (e.g., heat), this strategy has the advantage of being able to target minimal residual or metastatic disease, and thus will be more useful in the treatment of advanced or disseminated tumors.

The main goal of these approaches is to increase the amount of bioavailable drug in the tumor in order to increase tumor cell kill. It is becoming evident that, in order to test this and similar hypotheses, it is necessary to develop methodologies to differentiate between bioavailable and non-bioavailable drug in tumors and other tissues, as discussed below.

**6.4 Measuring Bioavailability of Drug From Liposomal Carriers**

As mentioned in Chapter 1, the concept of bioavailability is of fundamental importance to drug delivery systems. If the drug is not released from the carrier it will not be able to produce a therapeutic, or toxic, effect. To further the development of new technologies to control the rate of release of drug, e.g., triggered release systems, it is necessary to develop methods that can reliably quantify the levels of bioavailable drug released from liposomal carriers *in vivo*. One of the primary

locations for the cytotoxic actions of DXR is the cell nucleus, where it intercalates with DNA, forming a stable complex (97). Hence, measurement of nuclear DXR may be a reliable method for quantifying bioavailable DXR in tumor cells, since only released DXR and not liposomal DXR can reach the nucleus. Standard extraction techniques cannot extract DXR from DNA. Attempts have been made to measure DXR bound to DNA using a silver nitrate extraction technique, which releases DXR from DNA (212). This technique was recently applied to quantify total (DNA-bound and non-DNA-bound) DXR from tumors subjected to hyperthermia after injection of thermosensitive liposomes (194). The authors defined bioavailable DXR as the difference between the drug concentrations determined by the two extraction techniques and demonstrated better therapeutic activity for formulations that produced higher bioavailable drug concentrations (194).

An alternative approach (unpublished data from the Allen lab) has been to purify nuclei from DXR-treated tumor-bearing mice and then quantify the DXR associated with the nucleus, using a DNase I digestion (213). Early results have demonstrated that released liposomal DXR that associated with the tumor nuclei, i.e., bioavailable DXR, had AUCs that were lower and peaked later than tumor AUCs from total liposomal DXR. These data support the hypothesis that liposomes localize in tumors and then release their contents. Refinement of these techniques will allow improvements in the design of liposomal drug delivery systems by increasing our understanding of how to engineer liposomal formulations that produce optimal levels of bioavailable drugs in target tissues.

### 6.5 Chemotherapy With Liposomal Antineoplastic Agents

The goals of chemotherapy can be curative or palliative, depending on the stage of disease and the overall condition of the patient. Frail patients with advanced disease are less able to tolerate the toxicities of systemic chemotherapy, so low toxicity alternatives are continuingly being sought that will offer a reasonable quality of life, while modestly increasing survival (5, 214). As previously stated, encapsulating DXR within SL decreases the incidence of DXR-associated toxicities, and this offers a potential alternative for patients who cannot tolerate conventional cytotoxic chemotherapy. The recent trial substituting Caelyx® for conventional DXR in the treatment of non-Hodgkin's lymphoma in patients over 60 year old highlights this point (discussed in Section 6.3.2) (191).

The rational use of DDS will increase as more knowledge is generated regarding their mechanisms of action. For example, Ian Tannock has argued that the long dose interval (3-4 weeks) necessary for host tissue recovery between cycles of chemotherapy, allows tumor repopulation with potentially drug resistant cells (3). He has recently proposed employing cytostatic agents (e.g., hormones or growth factor inhibitors) between cycles of conventional chemotherapy to reduce tumor repopulation, while normal tissues recover. This inhibition would then be removed before the next cycle of conventional chemotherapy (215). The use of SL in combination with cytostatic agents could give superior tumor suppression due to the ability of SL to localize to tumors and act as a depot for sustained release. In the case

of Caelyx®, the drug delivered would be cytotoxic, further increasing the efficacy of such regimes.

**6.6 Conclusion**

The data presented in this thesis have clinical implications for the use of SL-DXR. They support the stated hypothesis for the development of PPE and demonstrate that the current formulation of Caelyx® is near optimal with respect to therapeutic activity. This is inferred from the fact that manipulating the formula decreased its therapeutic activity in the 4T1 murine mammary carcinoma model. Unfortunately, the characteristics of Caelyx® that make it therapeutically efficacious (i.e., its small size and stable drug retention) are also implicated in the development of its cutaneous toxicities. Therefore, in future clinical studies, attention must be paid to the dose schedule to maximize antitumor activity while minimizing the incidence of cutaneous toxicities. Further, newer treatments for the PPE will need to be developed to increase the therapeutic index of Caelyx®, and these data present a murine model with which to start these studies. SL have, and will continue to, improve the lives of cancer patients, and the results of further trials are eagerly awaited.

## References


1. Uziely, B., Jeffers, S., Isacson, R., Kutsch, K., Wei-Tsao, D., Yehoshua, Z., Libson, E., Muggia, F. M., and Gabizon, A. Liposomal doxorubicin: antitumor activity and unique toxicities during two complementary phase I studies, J. Clin. Oncol. *13:* 1777-1785, 1995.
2. Canadian Cancer Statistics. Toronto: National Cancer Institute of Canada, 2001.
3. Tannock, I. F. Conventional cancer therpay: promise broken of promise delayed?, Lancet. *351:* 9-16, 1998.
4. Naboltz, J.-M., Reese, D., Lindsay, M.-A., and Riva, A. Evidence for the use of chemotherapy in breast cancer, Int. J. Clin. Oncol. *7:* 254-264, 2002.
5. Crown, J., Dieras, V., Kaufmann, M., von Minckwitz, G., Kaye, S., Lenard, R., Marty, M., Misset, J.-L., Osterwalder, B., and Piccart, M. Chemotherapy for metastatic breast cancer-report of a European expert panel, Lancet Oncol. *3:* 719-26, 2002.
6. Capdeville, R., Buchdunger, E., Zimmermann, J., and Matter, A. Glivec (STI571, imatinib), a rationally developed, targeted anticancer drug, Nature Rev. Drug Discov. *1:* 493-502, 2002.
7. Druker, B. J., Sawyers, C., Kantarjian, H., Resta, D. J., S., R., Ford, J. M., Capdeville, R., and Talpaz, M. Activity of a specific inhibitor of the BCR-ABL tyrosine kinase in the blast crisis of chronic myeloid leukemia and acute lymphoblastic leukemia with the Philadelphia chromosome, N. Eng. J. Med. *344:* 1038-42, 2001.
8. Druker, B. J., Talpaz, M., Resta, D. J., Peng, B., Buchdunger, E., Ford, J. M., Lydon, N. B., Kantarjian, H., Capdeville, R., Ohno-Jones, S., and Sawyers, C. Efficacy and safety of a specific inhibitor of the BCR-ABL tyrosine kinase in chronic myeloid leukemia, N. Eng. J. Med. *344:* 1031-1037, 2001.
9. Demtri, G. D., von Mehren, M., Blanke, C., Van den Abbeele, A. D., Eisenberg, B., Roberts, P. J., Heinrich, M. C., Tuveson, D. A., Singer, S., Janicek, M., Fletcher, J. A., Silverman, S. G., Silberman, S. L., Capdeville, R., Kiese, D., Peng, B., Dimitrijevic, S., Druker, B. J., Corless, C., Fletcher, C. D. M., and Joensuu, H. Efficacy and safety of imatinib mesulate in advanced gastrointesitinal stomal tumors, N. Engl. J. Med. *347:* 472-480, 2002.
10. Gabizon, A., Dagan, A., Goren , D., Barenholz , Y., and Fuks , Z. Liposomes as in vivo carriers of adriamycin: reduced cardiac uptake and preserved antitumor activity in mice, Cancer Res. *42:* 4734-4739, 1982.
11. Gabizon, A. Pegylated liposomal doxorubicin: metamorphosis of an old drug into a new form of chemotherapy, Cancer Invest. *19:* 424-436, 2001.
12. Bangham, A. D., Standish, M. M., and Watkins, J. C. Diffusion of univalent ions across the lamellae of swollen phospholipids, J. Mol. Biol. *13:* 238-252, 1965.
13. Lasic, D. D. Liposomes: from physics to applications, p. 575. Amsterdam: Elsevier Science Publishers B.V., 1993.

14. Woodle, M. C. and Papahadjopoulos, D. Liposome preparation and size characterization, Meth. Enzymol. *171:* 193-217, 1989.
15. Hauser, H. Phospholipid vesicles. *In:* G. Cevc (ed.) Phospholipids Handbook, 1993.
16. Olson, F., Hunt, C. A., Szoka, F. C., Vail, W. J., and Papahadjopoulos, D. Preparation of liposomes of defined size distribution by extrusion through polycarbonate membranes, Biochim. Biophys. Acta. *557:* 9-23, 1979.
17. Mayer, L. D., Hope, M. J., and Cullis, P. R. Vesicles of variable sizes produced by a rapid extrusion procedure, Biochim. Biophys. Acta. *858:* 161-168, 1986.
18. Batzri, S. and Korn, E. D. Single bilayer liposomes prepared without sonication, Biochim. Biophys. Acta. *16:* 1015-1019, 1973.
19. Szoka, F. and Papahadjopoulos, D. Procedure for preparation of liposomes with large internal aqueous space and high capture by reverse-phase evaporation, Proc. Natl. Acad. Sci. USA. *75:* 4194-4198, 1978.
20. Gregoriadis, G. Drug entrapment in liposomes, FEBS Lett. *36:* 292, 1973.
21. Ginevra, F., Biffanti, S., Pagnan, A., Biolo, R., Reddi, E., and Jori, G. Delivery of the tumour photosensitizer zinc(II)-phthalocyanine to serum proteins by different liposomes: studies in vitro and in vivo, Cancer Lett. *49:* 59-65, 1990.
22. Mayer, L. D., Hope, M. J., Cullis, P. R., and Janoff, A. S. Solute distributions and trapping efficiencies observed in freeze-thawed multilamellar vesicles, Biochim. Biophys. Acta. *817:* 193-196, 1985.
23. Mayer, L. D., Bally, M. B., and Cullis, P. R. Uptake of adriamycin into large unilamellar vesicles in response to a pH gradient, Biochim. Biophys. Acta. *857:* 123-126, 1986.
24. Mayer, L. D., Bally, M. B., Loughrey, H., Masin, D., and Cullis, P. R. Liposomal vincristine preparations which exhibit decreased drug toxicity and increased activity against murine L1210 and P388 tumors, Cancer Res. *50:* 575-9, 1990.
25. Haran, G., Cohen, R., Bar, L. K., and Barenholz, Y. Transmembrane ammonium sulfate gradients in liposomes produce efficient and stable entrapment of amphipathic weak bases, Biochim. Biophys. Acta. *1151:* 201-215, 1993.
26. Bolotin, E. M., Cohen, R., Bar, L. K., Emanuel, S. N., Lasic, D. D., and Barenholz, Y. Ammonium sulphate gradients for efficient and stable remote loading of amphipathic weak bases into liposomes and ligandosomes, J. Liposome Res. *4:* 455-479, 1994.
27. Webb, M. S., Harasym, T. O., Masin, D., Bally, M. B., and Mayer, L. D. Sphingomyelin cholesterol liposomes significantly enhance the pharmacokinetic and therapeutic properties of vincristine in murine and human tumour models, Br. J. Cancer. *72:* 896-904, 1995.

28. Lim, H. J., Masin, D., Madden, T. D., and Bally, M. B. Influence of drug release characteristics on the therapeutic activity of liposomal mitoxantrone, J. Pharmacol. Exp. Therap. *281:* 566-573, 1997.
29. Xingong, L., Hirsh, D. J., Cabral-Lilly, D., Zirkel, A., Gruner, S. M., Janoff, A. S., and Perkins, W. R. Doxorubicin physical state in solution and inside liposomes loaded via a pH gradient, Biochim. Biophys. Acta. *1415:* 23-40, 1998.
30. Allen, T. M. A study of phospholipid interactions between high-density lipoproteins and small unilamellar vesicles, Biochim. Biophys. Acta. *640:* 385-397, 1981.
31. Senior, J., Crawley, J. C. W., and Gregoriadis, G. Tissue distribution of liposomes exhibiting long half-lives in the circulation after intravenous injection, Biochim. Biophys. Acta. *839:* 1-8, 1985.
32. Gabizon, A. A., Barenholz, Y., and Bialer, M. Prolongation of the circulation time of doxorubicin encapsulated in liposomes containing a polyethylene glycol-derivatized phospholipid: pharmacokinetic studies in rodents and dogs, Pharm. Res. *10:* 703-708, 1993.
33. Kim, E. S., Lu, C., Khuri, F. R., Tonda, M., Glisson, B. S., Liu, D., Jung, M., Hong, W. K., and Herbst, R. S. A phase II study of STEALTH cisplatin (SPI-77) in patients with advanced non-small cell lung cancer, Lung Cancer. *34:* 427-432, 2001.
34. Vail, D. M., Kurzman, I. D., Glawe, P. C., O'Brien, M. G., Chun, R., Garrett, L. D., Obradovich, J. E., Fred, R. M., Khanna, C., Colbern, G. T., and Working, P. K. STEALTH liposome-encapsulated cisplatin (SPI-77) versus carboplatin as adjuvant therapy for spontaneously arising osteosarcoma (OSA) in the dog: a randomized multicenter clinical trial, Cancer Chemother. Pharmacol. *50:* 131-136, 2002.
35. Bandak, S., Goren, D., Horowitz, A., Tzemach, D., and Gabizon, A. Pharmacological studies of cisplatin encapsulated in long-circulating liposomes in mouse tumor models, Anticancer Drugs. *10:* 911-920, 1999.
36. Cuomo, V., Jori, G., Rihter, B., Kenney, M. E., and Rodgers, M. A. J. Liposome-delivered Si(IV)-naphthalocyanine as a photodynamic sensitiser for experimental tumours: pharmacokinetic and phototherapeutic studies, Br. J. Cancer. *62:* 966-970, 1990.
37. Mayer, L. D., Nayar, R., Thies, R. L., Boman, N. L., Cullis, P. R., and Bally, M. B. Identification of vesicle properties that enhance the antitumour activity of liposomal vincristine against murine L1210 leukemia, Cancer Chemother. Pharmacol. *33:* 17-24, 1993.
38. Allen, T. M., Mehra, T., Hansen, C. B., and Chin, Y. C. Stealth liposomes: an improved sustained release system for 1-β-D-arabinofuranosylcytosine, Cancer Res. *52:* 2431-2439, 1992.
39. Lim, H. J., Masin, D., Mcintosh, N. L., Madden, T. D., and Balley, M. B. Role of drug release and liposome-mediated drug delivery in governing the

therapeutic activity of liposomal mitoxatrone used to treat human A431 and LS180 solid tumors, J. Pharm. Exp. Ther. *292:* 337-345, 2000.

40. Adlakha-Hutcheon, G., Bally, M. B., Shew, C. R., and Madden, T. D. Controlled destabilization of a liposomal drug delivery system enhances mitoxantrone antitumor activity, Nat. Biotechnol. *17:* 775-779, 1999.
41. Weiss, R. B., Donehower, R. C., Wiernik, P. H., Ohnuma, T., Gralla, R. J., Trump, D. L., Bake, J. R., Van Echo, D. A., Van Hoff, D. D., and Leyland-Jones, B. Hypersensitivity reactions with taxol, J. Clin. Oncol. *8:* 1263-1268, 1990.
42. Chabner, B. A., Allegra, C. J., Curt, G. A., and Calabresi, P. Antineoplatic agents. *In:* J. G. Hardman, E. Limbird, P. B. Molinoff, R. W. Ruddon, and A. G. Gilman (eds.), Goodman and Gilman's the pharmacological basis of therapeutics, 9 edition, pp. 1233-1288: McGraw Hill, 1996.
43. Sharma, A., Straubinger, R. M., Ojima, I., and Bernacki, R. J. Antitumor efficacy of taxane liposomes on a human ovarian tumor xenograft in nude athymic mice, J. Pharm. Sci. *84:* 1400-1404, 1995.
44. Treat, J., Damjanov, N., Huang, C., Zrada, S., and Rahman, A. Liposomal-encapsulated chemotherpay:preliminary results of a Phase I study of a novel liposomal paciltaxel, Oncology. *15:* 44-48, 2001.
45. Kuntsfeld, R., Wickenhauser, G., Michaelis, U., Teifel, M., Umek, W., Naujoks, K., Wolff, K., and Petzelbauer, P. Paclitaxel encapsulated in cationic liposomes diminishes tumor angiogenesis and melanoma growth in a "humanized" SCID mouse model, J. Invest. Dermatol. *120:* 476-482, 2003.
46. Gabizon, A., Catane, R., Uziely, B., Kaufman, B., Safra, T., Cohen, R., Martin, F., Huang, A., and Barenholz, Y. Prolonged circulation time and enhanced accumulation in malignant exudates of doxorubicin encapsulated in polyethylene-glycol coated liposomes, Cancer Res. *54:* 987-992, 1994.
47. Cowens, J. W., Creaven, P. J., Greco, W. R., Brenner, D. E., Tung, Y., Osto, M., Pilkiewicz, F., Ginsberg, R., and Petrelli, N. Initial clinical (phase I) trial of TLC D-99 (doxorubicin encapsulated in liposomes), Cancer Res. *53:* 2796-2802, 1993.
48. Lotem, M., Hubert, A., Lyass, O., Goldenhersh, M. A., Ingber, A., Peretz, T., and Gabizon, A. Skin toxic effects of polyethylene glycol-coated liposomal doxorubicin, Arch. Dermatol. *136:* 1474-1480, 2000.
49. Charrois, G. J. R. and Allen, T. M. Rate of biodistribution of STEALTH® liposomes to tumor and skin: influence of liposome diameter and implications for toxicity and therapeutic activity, Biochim. Biophys. Acta. *1609:* 102-108, 2003.
50. Juliano, R. L. and Stamp, D. Effects of particle size and charge on the clearance of liposomes and liposome-encapsulated drugs, Biochim. Biophys. Acta. *1113:* 651-658, 1975.
51. Juliano, R. L. and Stamp, D. Pharmacokinetics of liposome-entrapped anti-tumor drugs, Biochem. Pharmacol. *27:* 21-27, 1978.

52. Gregoriadis, G. The carrier potential of liposomes in biology and medicine. Part 1, New Engl. J. Med. *295:* 704-710, 1976.
53. Gregoriadis, G. The carrier potential of liposomes in biology and medicine. Part 2, New Engl. J. Med. *295:* 765-770, 1976.
54. Hwang, K. J. Liposome pharmacokinetics, p. 109-156. New York, NY: Marcel Dekker, 1987.
55. Allen, T. M., Hansen, C. B., and Lopes de Menezes, D. E. Pharmacokinetics of long circulating liposomes, Adv. Drug Del. Rev. *16:* 267-284, 1995.
56. Drummond, D. C., Meyer, O., Hong, K. L., Kirpotin, D. B., and Papahadjopoulos, D. Optimizing liposomes for delivery of chemotherapeutic agents to solid tumors, Pharmacological Reviews. *51:* 691-743, 1999.
57. Abra, R. M. and Hunt, C. A. Liposome disposition in vivo. III. Dose and vesicle-size effects, Biochim. Biophys. Acta. *666:* 493-503, 1981.
58. Gregoriadis, G. and Senior, J. The phospholipid component of small unilamellar liposomes controls the rate of clearance of entrapped solutes from the circulation, FEBS Lett. *119:* 43-46, 1980.
59. Chonn, A., Semple, S. C., and Cullis, P. R. Association of blood proteins with large unilamellar liposomes in vivo. Relation to circulation lifetimes, J. Biol. Chem. *267:* 18759-18765, 1992.
60. Abra, R. M., Bosworth, M. E., and Hunt, C. A. Liposome disposition in vivo: effects of pre-dosing with liposomes, Res. Commun. Chem. Pathol. Pharmacol. *29:* 349-360, 1980.
61. Proffitt, R. T., Williams, L. E., Presant, C. A., Tin, G. W., Uliana, J. A., Gamble, R. C., and Baldeschwieler, J. D. Liposomal blockade of the reticuloendothelial system: improved tumor imaging with small unilamellar vesicles, Science. *220:* 502-505, 1983.
62. Allen, T. M. and Hansen, C. B. Pharmacokinetics of Stealth versus conventional liposomes: effect of dose, Biochim. Biophys. Acta. *1068:* 133-141, 1991.
63. Allen, T. M. and Chonn, A. Large unilamellar liposomes with low uptake into the reticuloendothelial system, FEBS Lett. *223:* 42-46, 1987.
64. Gabizon, A. and Papahadjopoulos, D. Liposome formulations with prolonged circulation time in blood and enhanced uptake by tumors, Proc. Natl. Acad. Sci. U S A. *85:* 6949, 1988.
65. Woodle, M. C., Newman, M., Collins, L., Redemann, C., and Martin, F. Improved long circulating (Stealth$^{R}$) liposomes using synthetic lipids, Proceed. Intern. Symp. Control. Rel. Bioact. Mater. *17:* 77, 1990.
66. Klibanov, A. L., Maruyama, K., Torchilin, V. P., and Huang, L. Amphipathic polyethyleneglycols effectively prolong the circulation time of liposomes, FEBS Lett. *268:* 235-237, 1990.
67. Senior, J., Delgado, C., Fisher, D., Tilcock, C., and Gregoriadis, G. Influence of surface hydrophilicity of liposomes on their interaction with plasma protein and clearance from the circulation: studies with the poly(ethylene glycol)-coated vesicles, Biochim. Biophys. Acta. *1062:* 77-82, 1991.

68. Allen, T. M., Hansen, C. B., Martin, F., Redemann, C., and Yau-Young, A. Liposomes containing synthetic lipid derivatives of poly(ethylene glycol) show prolonged circulation half-lives in vivo, Biochim. Biophys. Acta. *1066:* 29-36, 1991.

69. Allen, T. M. The use of glycolipids and hydrophilic polymers in avoiding rapid uptake of liposomes by the mononuclear phagocyte system, Adv. Drug Del. Rev. *13:* 285-309, 1994.

70. Chonn, A., Semple, S. C., and Cullis, P. R. Beta 2 glycoprotein I is a major protein associated with very rapidly cleared liposomes in vivo, suggesting a significant role in the immune clearance of "non-self" particles, J. Biol. Chem. *270:* 25845-25849, 1995.

71. Woodle, M. C., Matthay, K. K., Newman, M. S., Hidayat, J. E., Collins, L. R., Redemann, C., Martin, F. J., and Papahadjopoulos, D. Versatility in lipid compositions showing prolonged circulation with sterically stabilized liposomes, Biochim. Biophys. Acta. *1105:* 193-200, 1992.

72. Allen, T. M., Hansen, C. B., and Guo, L. S. S. Subcutaneous administration of liposomes: a comparison with the intravenous and intraperitoneal routes of injection, Biochim. Biophys. Acta. *1150:* 9-16, 1993.

73. Dams, E. T. M., Laverman, P., Oyen, W. J., Storm, G., Scherphof, G. L., Van Der Meer, J. W. M., Corstens, F. H., and Boerman, O. C. Accerlerated blood clearance and altered biodistribution of repeated injections of sterically stabilized liposomes, J. Pharmacol. Exp. Ther. *292:* 1071-1079, 2000.

74. Laverman, P., Brouwers, A. H., Dams, E. T. M., Oyen, W. J., Storm, G., Rooijen, N. V., Corstens, F. H., and Boerman, O. C. Preclinical and clinical evidence for dissappearance of long-circulating characteristics of polyethylene glycol liposomes at low lipid dose, J. Pharmacol. Exp. Ther. *293:* 996-1001, 2000.

75. Ishida, T., Maeda, R., Ichihara, M., Irimura, K., and Kiwada, H. Accelerated clearance of PEGylated liposomes in rats after repeated injections, J. Control. Release. *88:* 35-42, 2003.

76. Laverman, P., Carstens, M. G., Boerman, O. C., Dams, E. T. M., Oyen, W. J., Rooijen, N. V., Corstens, F. H., and Storm, G. Factors affecting the accelerated blood clearance of polyethylene glycol-liposomes upon repeat injection, J. Pharmacol. Exp. Ther. *298:* 607-612, 2001.

77. Daemen, T., Hofstede, G., Ten Kate, M. T., Bakker-Woudenberg, I. A., and Scherphof, G. L. Liposomal doxorubicin-induced toxicity: depletion and impairment of phagocytic activity of liver macrophages, Int. J. Cancer. *61:*, 1995.

78. Storm, G., ten Kate, M. T., Working, P. K., and Bakker-Woudenberg, I. A. J. M. Doxorubicin entrapped in sterically stabilzed liposomes: effects on bacterial blood clearance of the mononucear phagocyte system, Clin. Cancer Res. *3:*, 1998.

79. Gabizon, A., Shiota, R., and Papahadjopoulos, D. Pharmacokinetics and tissue distribution of doxorubicin encapsulated in stable liposomes with long circulation times, J. Natl. Cancer Inst. *81:* 1484-1488, 1989.

80. Papahadjopoulos, D., Allen, T. M., Gabizon, A., Mayhew, E., Matthay, K., Huang, S. K., Lee, K. D., Woodle, M. C., Lasic, D. D., Redemann, C., and Martin, F. J. Sterically stabilized liposomes: improvements in pharmacokinetics and antitumor therapeutic efficacy, Proc. Natl. Acad. Sci. U S A. *88:* 11460-11464, 1991.

81. Gabizon, A. A. Selective tumor localization and improved therapeutic index of anthracyclines encapsulated in long-circulating liposomes, Cancer Res. *52:* 891-896, 1992.

82. Huang, S. K., Lee, K. D., Hong, K., Friend, D. S., and D., P. Pharmacokinetics and therapeutics of sterically stabilized liposomes in mice bearing C-26 colon carcinoma, Cancer Res. *52:* 677-681, 1992.

83. Hobbs, S., Monsky, W. L., Yuan, F., Roberts, W. G., Griffith, L., Torchillin, V. P., and Jain, R. K. Regulation of transport pathways in tumor vessels: role of tumur type and microenvironment, Proc. Natl. Acad. Sci. U.S.A. *95:* 4607-4612, 1998.

84. Ning, Z. W., Daphne, D., Rudoll, T. L., Needham, D., Whorton, A. R., and Dewhirst, M. W. Increased microvascular permeability contributes to preferential accumulation of Stealth liposomes in tumor tissue, Cancer Res. *53:*, 1993.

85. Wu, N. Z., Da, D., Rudoll, T. L., Needham, D., Whorton, A. R., and Dewhirst, M. W. Increased microvascular permeability contributes to preferential accumulation of Stealth liposomes in tumour tissue, Cancer Res. *53:* 3765-3770, 1993.

86. Yuan, F., Dellian, M., Fukumura, D., Leunig, M., Berk, D. A., Torchilin, V. P., and Jain, R. K. Vascular permeability in a human tumor xenograft: molecular size dependence and cutoff size, Cancer Res. *55:* 3752-3756, 1995.

87. Hashizume, H., Baluk, P., Morikawa, S., McLean, J. W., Thurston, G., Roberge, S., Jain, R. K., and McDonald, D. M. Openings between defective endothelial cells explain tumor vessel leakiness, Am. J. Pathol. *156:* 1363-1380, 2000.

88. Matsumura, Y. and Maeda, H. A new concept for macromolecular therapeutics in cancer chemotherapy; mechanism of tumoritropic accumulation of proteins and the antitumor agent SMANCS, Cancer Res. *6:* 6387-6392, 1987.

89. Maeda, H., Sawa, T., and Konno, T. Mechanism of tumor-targeted delivery of macromolecular drugs, including the EPR effect in solid tumor and clinical overview of the prototype polymeric drug SMANCS, J. Control. Release. *74:* 47-61, 2001.

90. Huang, S. K., Lee, K. D., Hong, K., Friend, D. S., and Papahadjopoulos, D. Microscopic localization of sterically stabilized liposomes in colon carcinoma-bearing mice, Cancer Res. *52:* 5135-5143, 1992.

91. Ishida, O., Maruyama, K., Sasaki, K., and Iwatsuru, M. Size-dependent extravastion and interstial localization of polyethyleneglycol liposomes in solid tumor-bearing mice, Int. J. Pharm. *190:* 49-56, 1999.
92. Yuan, F., Leunig, M., Huang, S. K., Berk, D. A., Papahadjopoulos, D., and Jain, R. K. Microvascular permeability and interstitial penetration of sterically stabilized (Stealth) liposomes in a human tumor xenograft, Cancer Res. *54:* 3352-3356, 1994.
93. Pluen, A., Boucher, Y., Ramanujan, S., McKee, T. D., Gohongi, T., di Tomaso, E., Brown, E. B., Izumi, Y., Campbell, R. B., Berk, D. A., and Jain, R. K. Role of tumor-host interactions in interstitial diffusion of macromolecules: cranial vs. subcutaneous tumors, Proc. Natl. Acad. Sci. U.S.A. *98:* 4628-4633, 2001.
94. Allen, T. M., Hansen, C., and Rutledge, J. Liposomes with prolonged circulation times: factors affecting uptake by reticuloendothelial and other tissues, Biochim. Biophys. Acta. *981:* 27-35, 1989.
95. Gabizon, A. and Papahadjopoulos, D. The role of surface charge and hydrophilic groups on liposome clearance in vivo, Biochim. Biophys. Acta. *1103:* 94-100, 1992.
96. Gabizon, A., Goren, D., Horowitz, A. T., Tzemach, D., Lossos, A., and Siegal, T. Long-circulating liposomes for drug delivery in cancer therapy: a review of biodistribution studies in tumor-bearing animals, Adv. Drug Del. Rev. *24:* 337-344, 1997.
97. Doroshow, J. H. Anthracyclines and Antracenediones. *In:* B. A. Chabner and D. L. Longo (eds.), Cancer chemotherapy & biotherapy: priniciples and practice, 3 edition, pp. 500-537. Philidelphia: Lippincott Williams & Wilkins, 2001.
98. Gewirtz, D. A. A critical evaluation of the mechanisms of action proposed for the antitumor effects of the anthracycline antibiotics adriamycin and daunorubicin, Biochemical pharmacology, Biochem. Pharmacol. *57:* 727-741, 1999.
99. Ferraro, C., Quemeneur, L., Prigent, A.-F., Taverne, C., Revillard, J.-P., and Bonnefoy-Berard, N. Anthracyclines trigger apoptosis of both $G_o$-$G_1$ and cycling peripheral blood lymphocytes and induce massive deletion of mature T and B cells, Cancer Res. *60:* 1901-1907, 2001.
100. Speth, P. A. J., van Hoesel, Q. G. C. M., and Haanen, C. Clinical pharmacokinetics of Doxorubicin, Clinical Pharmacokinetics. *15:* 15-31, 1988.
101. Legha, S. S., Benjamin, R. S., Mackay, B., Ewer, M., Wallace, S., Valdivieso, M., Rasmussen, S. L., Blumenschein, G. R., and Freireich, E. J. Reduction of doxorubicin cardiotoxicity by prolonged continuous intravenous infusion, Ann. Intern. Med. *96:* 133-139, 1982.
102. Samuels, B. L., Vogelzang, N. J., Ruane, M., and Simon, M. A. Continuous venous infusion of doxorubicin in advanced sarcomas, Cancer. Treat. Rep. *71:* 971-972, 1987.

103. Working, P. K., Newman, M. S., Sullivan, T. M., and Yarrington, J. Reduction of the cardiotoxicity of doxorubicin in rabbits and dogs by encapusulation in long-circulating pegylated liposomes, J. Pharmacol. Exp. Ther. *289:* 1128-1133, 1999.

104. Batist, G., Ramakrishnan, G., Rao, C. S., Chandrasekharan, A., Gutheil, J., Guthrie, T., Shah, P., Khojasteh, A., Nair, M. K., Hoelzer, K., Tkaczuk, K., Park, Y. C., and Lee, L. W. Reduced cardiotoxicity and preserved antitumor efficacy of liposome-encapsulated doxorubicin and cyclophosphamide compared with convententional doxorubicin and cyclophosphamide in a randomized, multicenter trial of metastatic breast cancer, J. Clin. Oncol. *19:* 1444-1454, 2001.

105. Berry, G., Billingham, M., Alderman, E., Richardson, P., Torti, F., Lum, B., Patek, A., and Martin, F. J. The use of cardiac biopsy to demonstrate reduced cardiotoxicity in AIDS Kaposi's sarcoma patients treated with pegylated liposomal doxorubicin, Ann. Oncol. *9:* 711-716, 1998.

106. Lyass, O., Uziely, B., Ben-Yosef, R., Tzemach, D., Heshing, N. I., Lotem, M., Brufman, G., and Gabizon, A. Correlation of toxicity with pharmacokinetics of pegylated liposomal doxorubicin (Doxil) in metastatic breast carcinoma, Cancer. *89:* 1037-47, 2000.

107. Safra, T., Muggia, F., Jeffers, S., Tsao-Wei, D. D., Groshen, S., Lyass, O., Henderson, R., Berry, G., and Gabizon, A. Pegylated liposomal doxorubicin (Doxil): reduced clinical cardiotoxicity in patients reaching or exceeding cumulative doses of 500 mg/m$^2$, Ann. Oncol. *11:* 1029-1033, 2000.

108. Vaage, J., Working, P., and Uster, P. S. Inhibition of mouse mammary carcinoma development with doxorubicin in liposomes, Int. J. Cancer. *75:* 158-159, 1998.

109. Vaage, J., Mayhew, E., and Martin, F. Therapy of primary and metastatic mouse mammary carcinomas with doxorubicin encapsulated in long circulating liposomes, Intl. J. Cancer. *51:* 942-948, 1992.

110. Williams, S. S., Alosco, T. R., Mayhew, E., Lasic, D. D., Martin, F. J., and Bankert, R. B. Arrest of human lung tumor xenograft growth in severe combined immunodeficient mice using doxorubicin encapsulated in sterically stabilized liposomes, Cancer Res. *53:* 3964-3967, 1993.

111. Working, P. and Dayan, A. D. Pharmacological-toxocological expert report: Caelyx® (Stealth® liposomal doxorubicin HCl), Hum. Exp. Toxicol. *15:* 751-785, 1996.

112. Siegal, T., Horowitz, A., and Gabizon, A. Doxorubicin encapsulated in sterically stabilized liposomes for the treatment of a brain tumor model: biodistribution and therapeutic efficacy, J. Neurosurg. *83:* 1029-1037, 1995.

113. Zhou, R., Mazurchuk, R., and Straubinger, R. M. Antivascular effects of doxorubicin-containing liposomes in an intracranial rat brain tumor model, Cancer Res. *62:* 2561-2566, 2002.

114. Northfelt, D. W., Martin, F. J., Working, P., Volberding, P. A., Russell, J., Newman, M., Amantea, M. A., and Kaplan, L. D. Doxorubicin encapsulated

in liposomes containing surface-bound polyethylene glycol: pharmacokinetics, tumour localization, and safety in patients with AIDS-related Kaposi's sarcoma, J. Clin. Pharmacol. *36:* 55-63, 1996.

115. Northfelt, D. W., Dezube, B. J., Thommes, J. A., Miller, B. J., Fischl, M. A., Friedman-Kien, A., Kaplan, L. D., Du Mond, C., Mamelak, R. D., and Henry, D. H. Pegylated-liposomal doxorubicin versus doxorubicin, bleomycin, and vincristine in the treatment of AIDS-related Kaposi's sarcoma: results of a ramdomized phase III clinical trial, J. Clin. Oncol. *17:* 2445-2451, 1998.
116. Stewart, S., Jablonowski, H., Goebel, F. D., Arasteh, K., Spittle, M., Rios, A., Aboulafia, D., Galleshaw, J., and Dezube, B. J. Randomized comparative trial of pegylated liposomal doxorubicin versus bleomycin and vincristine in the treatment of AIDS-related Kaposi's sarcoma, J. Clin. Oncol. *16:* 683-691, 1998.
117. Muggia, F., Hainsworth, J. D., Jeffers, S., Miller, P., Groshen, S., Tan, M., Roman, L., Uziely, B., Muderspach, L., Garcia, A., Burnett, A., Greco, F. A., Morrow, C. P., Paradiso, L. J., and Liang, L.-J. Phase II study of liposomal doxorubicin in refractory ovarian cancer: antitumor activity and toxicity modification by liposomal encapsulation, J. Clin. Oncol. *15:* 987-993, 1997.
118. Gordon, A. N., Granai, C. O., Rose, P. G., Hainsworth, J., Lopez, A., Weissman, C., Rosales, R., and Sharpington, T. Phase II study of liposomal doxorubicin in platinum- and paclitaxel-refractory epithelial ovarian cancer, J. Clin. Oncol. *18:* 3093-3100, 2000.
119. Gordon, A. N., Fleagle, J. T., Guthrie, D., Parkin, D. E., Gore, M. E., and Lacave, A. J. Recurent epithelial ovarian carcinoma: a randomized phase III study of pegylated liposomal doxourbicin versus topotecan, J. Clin. Oncol. *19:* 3312-3322, 2001.
120. Ranson, M. R., Carmichael, J., O'Byrne, K., Stewart, S., Smith, D., and Howell, A. Treatment of advanced breast cancer with sterically stabilized liposomal doxorubicin: results of a multicenter phase II trial, J. Clin. Oncol. *15:* 3185-3191, 1997.
121. Burstein, H. J., Ramirez, M. J., Pertos, W. P., Clarke, K. D., Warmuth, M. A., Marcom, P. K., Martulonis, U. A., Parker, L. M., Harris, L. N., and Winer, E. P. Phase I study of Doxil and vinorelbine in metastatic breast cancer, Ann Oncol. *10:* 1113-1116, 1999.
122. Rivera, E., Valero, V., Syrewicz, L., Rahman, Z., Esteva, F. L., Theriault, R. L., Rosales, M. M., Booser, D., Murray, J. L., Bast, R. C. J., and Hortobagyi, G. N. Phase I study of Stealth liposomal doxorubicin in combination with gemcitabine in the treatment of patients with metastatic breast cancer, J.Clin. Oncol. *19:* 1716-1722, 2001.
123. Sparano, J. A., Malik, U., Rajdev, L., Sarta, C., Hopkins, U., and Wolff, A. Phase I trial of pegylated liposomal doxorubicin an docetaxel in advanced breast cancer, J. Clin. Oncol. *19:* 3117-3125, 2001.
124. Samantas, E., Kalofonos, H., Linardou, H., Nicolaides, C., Mylonakis, N., Fountzilas, G., Kosmidis, P., and Skarlos, D. Phase II study of pegylated

liposomal doxorubicin: inactive in recurrent small-cell lung cancer, Ann. Oncol. *11:* 1395-1397, 2000.

125. Fabel, K., Dietrich, J., Hau, P., Wismeth, C., Winner, B., Przywara, S., Steinbrecher, A., Ullrich, W., and Bogdahn, U. Long-term stabilizaion in patients with malignant glioma after treatment with liposomal doxorubcin, Cancer. *92:* 1936-42, 2001.
126. Harrington, K. J., Lewanski, C., Northcote, A. D., Whittaker, J., Peters, A. M., Vile, R. G., and Stewart, J. S. W. Phase II study of pegylated liposomal doxorubicin (Caelyx) as induction chemotherapy for patients with squamous cell cancer of the head and neck, Eur. J. Cancer. *37:* 2015-2022, 2001.
127. Judson, I., Radford, J. A., Harris, M., Blay, J.-Y., van Hoesel, Q., le Cesne, A., van Oosterom, A. T., Clemons, M. J., Kamby, C., Hermans, C., Whittaker, J., Donato di Paola, E., Verweij, J., and Nielsen, S. Randomized phase II trial of pegylated liposomal doxorubicin (Doxil®/Caelyx®) versus doxorubicin in the treament of advanced or metastatic soft tissue sarcoma: a study by the EORTC soft tissue and bone sarcoma group, Eur. J. Cancer. *37:* 870-877, 2001.
128. Shields, A. F., Lange, L. M., and Zalupski, M. M. Phase II study of liposomal doxorubicin in patients with advanced colorectal cancer, Am. J. Clin. Oncol. *24:* 96-98, 2001.
129. Thomas, A. L., O'Byrne, K., Furber, L., Jeffery, K., and Steward, W. P. A phase II study of Caelyx, liposomal doxorubicin: lack of activity in patients with advanced gastric cancer, Cancer Chemother. Pharmacol. *48:* 266-268, 2001.
130. Wollina, U., Graefe, T., and Kaatz, M. Pegylated doxorubicin for primary cutaneousT-cell lymphoma: a report on ten patients with follow up, J. Cancer Res. Clin. Oncol. *127:* 128-134, 2001.
131. Skubitz, K. M. Phase II trial of pegylated-liposomal doxorubicin (Doxil) in mesothelioma, Cancer Investig. *20:* 692-699, 2002.
132. Rivera, E., Valero, V., Esteva, F. L., Syrewicz, L., Cristofanilli, M., Rahman, Z., Booser, D. J., and Hortobagyi, G. N. Lack of activity of stealth liposomal doxorubicin in the treatment of patients with anthracycline-resistant breast cancer, Cancer Chemother. Pharmacol. *49:* 299-302, 2002.
133. Amantea, M., Newman, M. S., Sullivan, T. M., Forrest, A., and Working, P. K. Relationship of dose intensity to the induction of palmar-plantar erythrodysesthia by pegylated liposomal doxorubicin in dogs, Hum. Exp. Tox. *18:* 17-26, 1999.
134. Lokich, J. J. and Moore, C. Chemotherapy-associated palmar-plantar erythrodysesthesia syndrome, Ann. Internal Med.. *101:* 798-800, 1984.
135. Feldman, L. D. and Ajani, J. A. Fluoruracil-associated dermatitis of the hands and feet, JAMA. *254:* 3479, 1985.
136. Comandone, A., Bretti, S., La Grotta, G., Manzoni, S., Bonardi, G., Berardo, R., and Bumma, C. Palmar-plantar erythrodysestasia syndome associated with 5-fluoruracil treatment, Anticancer Res. *13:* 1781-1784, 1993.

137. Gordon, K. B., Tajuddin, A., Guitart, J., Kuzel, T. M., Eramo, L. R., and VonRoenn, J. Hand-foot syndrome associated with liposome-encapsulated doxorubicin therapy, Cancer. *75:* 2169-2173, 1995.

138. Gabizon, A., Isacson, R., Libson, E., Kaufman, B., Uziely, B., Catane, R., Ben-Dor, C. G., Rabello, E., Cass, Y., Peretz, T., Sulkes, A., Chisin, R., and Barenholz, Y. Clinical studies of liposome-encapsulated doxorubicin, Acta Oncol. *33:* 779-786, 1994.

139. Ranson, M., O'Bryne, K., Carmichael, J., Smith, D., Stewart, S., and Howell, A. Phase II dose-finding trial of DOX-SL (Stealth® liposomal doxorubicin HCl) in the treatment of advanced breast cancer, Proc. Am. Soc. Clin. Oncol. *15:* 124, 1996.

140. Hamilton, A., Biganzoli, L., Coleman, R., Mauriac, L., Hennebert, P., Awada, A., Nooij, M., Beex, L., Piccart, M., Van Hoorebeeck, I., Bruning, P., and de Valeriola, D. EORTC 10968: a phase I clinical and pharmacokinetic study of polyethylene glycol liposomal doxorubicin (Caelyx®, Doxil®) at a 6-week interval in patients with metastatic breast cancer, Ann Oncol. *13:* 910-918, 2002.

141. Vukelja, S. J., Baker, W. J., and Burris, H. A. Pyridoxine therapy for palmar-plantar erythrodysesthesia associated with taxotere, J. Natl. Cancer Inst. *85:* 1432-1433, 1993.

142. Vail, D. M., Chun, R., Thamm, D. H., Garrett, L. D., Cooley, A. J., and Obradovich, J. E. Efficacy of pyridoxine to ameliorate the cutaneous toxicity associated with doxorubicin containing pegylated (Stealth) liposomes: a randomized, double-blind clinical trial using a canine model, Clin. Cancer. Res. *4:* 1567-71, 1998.

143. Lopez, A. M., Wallace, L., Dorr, R. T., Koff, M., Hersh, E. M., and Alberts, D. S. Topical DMSO treatment for pegylated liposomal doxorubicin-induced palmar-plantar erythrodysesthesia, Cancer Chemother. Pharmacol. *44:* 303-306, 1999.

144. Markman, M., Kennedy, A., Webster, K., Peterson, G., Kulp, B., and Belinson, J. Phase 2 trial of liposomal doxorubicin (40 mg/m$^2$) in platinum/paclitaxel-refractory ovarian and fallopian tube cancers and primary carcinoma of the peritoneum, Gynecol Oncol. *78:* 369-372, 2000.

145. Papahadjopoulos, D., Allen, T. M., Gabizon, A., Mayhew, E., Matthay, K., Huang, S. K., Lee, K. D., Woodle, M. C., Lasic, D. D., Redemann, C., and Martin, F. J. Sterically stabilized liposomes: pronounced improvements in blood clearance, tissue disposition, and therapeutic index of encapsulated drugs against implanted tumors, Proc. Natl. Acad. Sci. USA. *88:* 11460, 1991.

146. Aslakson, C. J. and Miller, F. R. Selective events in the metastatic process defined by analysis of the sequential dissemination of subpopulations of a mouse mammary tumor, Cancer Res. *52:* 1399-1405, 1992.

147. Miller, F. R., McInerney, D. J., Rogers, C., Aitken, D. R., and Wei, W.-Z. Use of drug resistance markers to recover clonogenic cells from occult metastases in host tissues, Invasion Metastasis. *6:* 197-208, 1986.

148. Miller, B. E., Miller, F. R., Wilburn, D. J., and Heppner, G. H. Analysis of tumor cell composition in tumors composed of paired mixtures of mammary tumor cell lines, Br. J. Cancer. *56:* 561-569, 1987.
149. Miller, F. R., Medina, D., and Heppner, G. H. Preferential growth of mammary tumours in intact mammary fatpads, Cancer Res. *41:* 3863-3867, 1981.
150. Moase, E., Qi, W., Ishida, T., Gabos, Z., Longenecker, B. M., Zimmermann, G. L., Ding, L., Krantz, M., and Allen, T. M. Anti-MUC-1 immunoliposomal doxorubicin in the treatment of murine models of metastatic breast cancer, Biochim. Biophys. Acta. *1510:* 43-55, 2001.
151. Hobbs, S., Monsky, W. L., Yuan, F., Roberts, W. G., Griffith, L., Torchillin, V. P., and Jain, R. K. Regulation of transport pathways in tumor vessels: role of tumor type and microenvironment, Proc. Natl. Acad. Sci. USA. *95:* 4607-4612, 1998.
152. Gabizon, A. Stealth liposomal doxorubicin: An analysis of the effect of dose on tumor targeting and therapy. *In:* Fifth International Conference: Liposome Advances: progress in drug and vaccine delivery 2001.
153. Sommerman, E. F., Pritchard, P. H., and Cullis, P. R. $^{125}$I labelled inulin: a convenient marker for deposition of liposomal contents *in vivo*, Biochem. Biophys. Res. Commun. *122:* 319-324, 1984.
154. Bartlett, G. R. Phosphorus assay in column chromatography, J. Biol. Chem. *234:* 466-468, 1959.
155. Derksen, J. T., Morselt, H. W., and Scherphof, G. L. Processing of different liposomal markers after *in vitro* uptake of immunoglobulin-coated liposomes by rat liver macrophages, Biochim. Biophys. Acta. *931:* 33-40, 1987.
156. Mayer, L. D., Dougherty, G., Harasym, T. O., and Bally, M. B. The role of tumor-associated macorphages in the delivery of liposomal doxourbicin to solid muirne fibrosarcoma tumors, J. Pharmacol. Exp. Ther. *280:* 1406-1414, 1997.
157. Harasym, T. O., P.R., C., and Balley, M. B. Intratumor distribution of doxorubicin following i.v. administration of drug encapsulated in egg phosphaticdylcholine/cholesterol liposomes, Cancer Chemother Pharmacol. *40:* 309-317, 1997.
158. Parr, M. J., Masin, D., Cullis, P. R., and Bally, M. B. Accumulation of liposomal lipid and encapsulated doxorubicin in murine Lewis lung carcinoma: the lack of beneficial effects by coating liposomes with poly(ethylene glycol), J. Pharmacol. Exp. Ther. *280:* 1319-1327, 1997.
159. Freireich, E. J., Gehan, E. A., Rall, D. P., Schmidt, L. H., and Skipper, H. E. Quantitative comparison of toxicity of anticancer agents in mouse, rat, hamster, dog, monkey and man, Cancer Chemother. Reports. *50:* 219-244, 1966.
160. Shargel, L. and Yu, A. B. C. Applied biopharmaceutics and pharmacokinetics, 4 edition, p. 768. Toronto, 1999.

161. Moase, E., Qi, W., Ding, L., Ishida, T., Gabos, Z., Longenecker, B. M., Zimmermann, G. L., Krantz, M., and Allen, T. M. Anti-MUC-1 immunoliposomal doxorubicin in the treatment of murine models of metastatic breast cancer, Biochim. Biophys. Acta. *1510:* 43-55, 2001.

162. Awasthi, V. D., D., G., Goins, B. A., and Phillips, W. T. Circulation and biodistribution profiles of long-circulating PEG-liposomes of various sizes in rabbits, Int. J. Pharm. *253:* 121-132, 2003.

163. Maruyama, K., Ishida, O., Takizawa, T., and Moribe, K. Possibility of active targeting to tumour tissues with liposomes, Adv. Drug Del. Rev. *40:* 89-102, 1999.

164. Mayer, L. D., Tai , L. C., Ko, D. S., Masin, D., Ginsberg, R. S., Cullis, P. R., and Bally , M. B. Influence of vesicle size, lipid composition, and drug-to-lipid ratio on the biological activity of liposomal doxorubicin in mice, Cancer Res. *49:* 5922-5930, 1989.

165. Zou, Y. Y., Ling, Y. H., Reddy, S., Priebe, W., and Perezsoler, R. Effect of vesicle sze and lipid composition on the in vivo tumor selectivity and toxicity of the non cross resistant anthracycline annamycin incorporated in liposomes, Intl. J. Cancer. *61:* 666-671, 1995.

166. Gabizon, A., Huberty, J., Straubinger, R. M., Price, D. C., and Papahadjopoulos, D. An improved method for in vivo tracing and imaging of liposomes using a gallium 67-desferoximine complex, J. Liposome Res. *1:* 123-135, 1989.

167. Woodle, M. C. $^{67}$Ga-labelled lipsomes with prolonged circulation, Preparation and potential as nuclear imaging agents, Nucl. Med. Bio./Int. J. Rad. App. B. *20:* 149-155, 1993.

168. Sarris, A. H., Hagemeister, F., Romaguera, J., Rodriguez, M. A., McLaughlin, P., Tsimberidou, A. M., Medeiros, L. J., Samuels, B., Pate, O., Oholendt, M., Kantarjian, H., Burge, C., and Cabanillas, F. Liposomal vincristine in relapsed non-Hodgkin's lymphomas: early results of an ongoing phase II trial, Ann. Oncol. *11:* 69-72, 2000.

169. Vail, D. M., Kravis, L. D., Cooley, A. J., Chun, R., and MacEwan, E. G. Preclinical trial of doxorubicin entrapped in sterically stabilized liposomes in dogs with spontaneously arising malignant tumors, Cancer Chemother. Pharmacol. *39:* 410-416, 1997.

170. Vaage, J. and Barbera, E. Tissue uptake and therapeutic effects of stealth doxorubicin. Boca Raton: CRC Press, Inc., 1995.

171. Bally, M. B., Nayar, R., Masin, D., Hope, M. J., Cullis, P. R., and Mayer, L. D. Liposomes with entrapped doxorubicin exhibit extended blood residence times, Biochim. Biophys. Acta. *1023:* 133-139, 1989.

172. Oussoren, C. and Storm, G. Effect of repeated intravenous administration on the circulation kinetics of poly(ethyleneglycol)-liposomes in rats, J. Liposome Res. *9:* 349-355, 1999.

173. Maeda, H., Wu, J., Sawa, T., Matsumura, Y., and Hori, K. Tumor vascular permeability and the ERP effect in macromolecular therapeutics: a review, J Control Release. *65:* 271-284, 2000.

174. Hong, R.-L., Huang, C.-J., Tseng, Y.-L., Pang, V. F., Chen, S.-T., Liu, J.-J., and Chang, F.-H. Direct comparison of liposomal doxorubicn with or without polyethylene glycol coating in C-26 tumor-bearing mice: Is surface coating with polyethylene glycol beneficial?, Clin. Cancer Res. *5:* 3645-3652, 1999.

175. Needham, D., Anyarambhatla, G., Kong, G., and Dewhirst, M. W. A new tempertature-sensitive liposome for use with mild hyperthermia: characterization and testing in a human tumour xenograft model, Cancer Res. *60:* 1197-1201, 2000.

176. Gibbs, D. D., Pyle, L., Allen, M., Vaughan, M., Webb, A., Jonhnston, S. R. D., and Gore, M. E. A phase I dose-finding study of a combination of pegylated liposomal doxorubicin (Doxil), carboplatin and paclitaxel in ovarian cancer, Br. J. Cancer. *86:* 1379-1384, 2002.

177. Remlinger, K. A. Cutaneous Reactions to Chemotherapeutic Drugs, Arch. Dermatol. *139:* 77-81, 2003.

178. Fabian, C. J., Molina, R., Slavik, M., Dahlberg, S., Giri, S., and Stephens, R. Pyridoxine therapy for palmar-plantar erythrodysesthesia associated with continuous 5-fluorouracil infusion, Invest. New Drugs. *8:* 57-63, 1990.

179. Bertelli, G., Gozza, A., Forno, G. B., Vidili, M. G., Silvestro, S., Venturini, M., Del Mastro, L., Garrone, O., Rosso, R., and Dini, D. Topical dimethylsulfoxide for prevention of soft tissue injury after extravasation of vesicant cytotoxic drugs: a propestive clinical study, J. Clin. Oncol. *13:* 2581-2855, 1995.

180. Averbuch, S. D., Gaudiano, G., Koch, T. H., and Bachur, N. R. Doxorubicin-induced skin necrosis in the swine model: protection with a novel radical dimer, J. Clin. Oncol. *4:* 88-94, 1986.

181. Peroutka, S. J. Drugs effective in the treatment of migraine. *In:* J. G. Hardman, L. E. Limbird, P. B. Molinoff, R. W. Ruddon, and A. G. Gilman (eds.), Goodmand and Gilman's: The pharmacological basis of therapeutics, 9 edition, pp. 487-502, 1996.

182. Park, J. W., Hong, K., Carter, P., Asgari, H., Guo, L. Y., Keller, G. A., Wirth, C., Shalaby, R., Kotts, C., Wood, W. I., Papahadjopoulos, D., and Benz, C. C. Development of anti-p185$^{HER2}$ immunoliposomes for cancer therapy, Proc. Natl. Acad. Sci. U.S.A. *92:* 1327-1331, 1995.

183. Lopes de Menezes, D. E., Pilarski, L. M., and Allen, T. M. In vitro and in vivo targeting of immunoliposomal doxorubicin to human B-cell lymphoma, Cancer Res. *58:* 3320-3330, 1998.

184. Lopes de Menezes, D. E., Pilarski, L. M., Belch, A. R., and Allen, T. M. Selective targeting of immunoliposomal doxorubicin against human multiple myeloma *in vitro* and *ex vivo*, Biochim. Biophys. Acta. *1466:* 205-220, 2000.

185. Eliaz, R. E. and Szoka, F. C. J. Liposome-encapsulated doxorubicin targeted to CD44: a strategy to kill CD44-overexpressing tumor cells, Cancer Res. *61:* 2592-2601, 2001.

186. Iden, D. L. and Allen, T. M. In vitro and in vivo comparison of immunoliposomes made by conventional coupling techniques with those made by a new post-insertion technique, Biochim. Biophys. Acta. *1513:* 207-216, 2001.

187. Ishida, T., Kirchmeier, M. J., Moase, E. H., Zalipsky, S., and Allen, T. M. Targeted delivery and triggered release of liposomal doxorubicin enhances cytotoxicity against human B lymphoma cells, Biochim. Biophys. Acta. *1515:* 144-158, 2001.

188. Moreira, J. N., Gaspar, R., and Allen, T. M. Targeting Stealth liposomes in a murine model of human small cell lung cancer, Biochim. Biophys. Acta. *1515:* 167-176, 2001.

189. Park, J. W., Hong, K., Kirpotin, D. B., Colbern, G., Shalaby, R., Baselga, J., Shao, Y., Nielsen, U. B., Marks, J. D., Moore, D., Papahadjopoulos, D., and Benz, C. C. Anti-HER2 immunoliposomes: Enhanced efficacy attributable to targeted delivery, Clin. Cancer Res. *8:* 1172-1181, 2002.

190. Lyass, O., Hubert, A., and Gabizon, A. Phase I study of Doxil-cisplatin combination chemotherapy in patients with advanced malignancies, Clin Cancer Res. *7:* 3040-3046, 2001.

191. Martino, R., Perea, G., Caballero, M. D., Maeteos, M. V., Ribera, J. M., Perez-de-Oteyza, J., Arranz, R., Terol, M. J., Sierra, J., and San Miguel, J. F. Cyclophosphamide, pegylated liposomal doxorubicin (Caelyx®), vincristine and prednisone (CCOP) in elderly patietns with diffuse large B-cell lymphoma: results from a propective phase II study, Haematologica. *87:* 822-827, 2002.

192. Lui, F.-F. and Wilson, B. C. Hyperthermia and Photodynamic Therapy. *In:* I. F. Tannock and R. P. Hill (eds.), The Basic Science of Oncology. Toronto: McGraw-Hill, 1998.

193. Koukourakis, M. I., Koukouraki, S., Giatromanolaki, A., Archimandritis, S. C., Skarlatos, J., Beroukas, K., Bizakis, J. G., Retalis, G., Karkavitsas, N., and Helidonis, E. S. Liposomal doxorubicin and conventionally fractionated radiotherapy in the treatment of locally advanced non-small-cell lung cancer and head and neck cancer, J. Clin. Oncol. *17:* 3512-3521, 1999.

194. Kong, G., Anyarambhatla, G., Petros, W. P., Braun, R. D., Colvin, O. M., Needham, D., and Dewhirst, M. W. Efficacy of liposomes and hyperthermia in a human tumor xenograft model: importance of triggered drug release, Cancer Res. *60:* 6950-6957, 2000.

195. Goldberg, S. N., Kamel, I. R., Kruskal, J. B., Reynolds, K., Monsky, W. L., Stuart, K. E., Ahmed, M., and Raptopoulos, V. Radiofrequency ablation of hepatic tumor:increased tumor destruction with adjuvant liposomal doxorubicin therapy, AJP. *179:* 93-101, 2002.

196. Monsky, W. L., Kruskal, J. B., Lukyanov, A. N., Girnun, G. D., Ahmed, M., Gazelle, G. S., Huertas, J. C., Stuart, K. E., Torchilin, V. P., and Goldberg, S. N. Radio-frequency ablation increases intratumoral liposomal doxorubicin accumulation in a rat breast tumor model, Radiology. *224:* 823-829, 2002.
197. Allen, T. M. Ligand-targeted therapeutics in anticancer therapy, Nature Reviews Cancer. *2:* in press, 2002.
198. Sapra, P. and Allen, T. M. Internalizing antibodies are necessary for improved therapeutic efficacy of antibody-targeted liposomal drugs, Cancer Res. *62:* 7190-7194, 2002.
199. Sonneveld, P., de Ridder, M., van der Lelie, H., Nieuwenhuis, K., Schouten, H., Mulder, A., van Reijswoud, I., Hop, W., and Lowenberg, B. Comparison of doxorubicin and mitoxantrone in the treatment of elderly patients with advanced diffuse non-Hodgkin's lymphoma using CHOP versus CNOP chemotherapy, J. Clin. Oncol. *13:* 2530-2539, 1995.
200. Baselga, J., Tripathy, D., Mendelsohn, J., Baughman, S., Benz, C. C., Dantis, L., Sklarin, N. T., Seidman, A. D., Hudis, C. A., Moore, J., Rosen, P. P., Twaddell, T., Henderson, I. C., and Norton, L. Phase II study of weekly intravenous recombinant humanized anti-p185HER2 monoclonal antibody in patients with HER2/neu-overexpressing metastatic breast cancer, J. Clin. Oncol. *14:* 737-744, 1996.
201. Cobleigh, M. A., Vogel, C. L., Tripathy, D., Robert, N. J., Scholl, S., Fehrenbacher, L., Wolter, J. M., Paton, V., Shak, S., Lieberman, G., and Slamon, D. J. Multinational study of the efficacy and safety of humanized anti-HER2 monoclonal antibody in women who have HER2-overexpressing metastatic breast cancer that has progressed after chemotherapy for metastatic disease, J. Clin. Oncol. *17:* 2639-2648, 1999.
202. Slamon, D. J., Leyland-Jones, B., Shak, S., Fuchs, H., Paton, V., Bajamonde, A., Fleming, T., Eiermann, W., Wolter, J., Pegram, M., Baselga, J., and Norton, L. Use of chemotherapy plus a monoclonal antibody against HER2 for metastatic breast cancer that overexpresses HER2, N. Engl. J. Med. *344:* 783-792, 2001.
203. Philips, T. L. Biochemical modifiers: drug-radiation interactions. *In:* P. M. Mauch and J. S. Loeffler (eds.), Radiation Oncology: Tecchnology and Bioloogy, pp. 113-151. Toronto: W.B. Saunders Company, 1994.
204. Cirrone, J., Aziz, H., and Rotman, M. Clinical princples and applications of chemoirradiation. *In:* S. H. Levitt, F. M. Kahn, R. A. Potish, and C. A. Perez (eds.), Technological basis of radiation therapy, pp. 14-29. New York, 1999.
205. Harrington, K. J., Rowlinson-Busza, G., Syrigos, K. N., Vile, R. G., Uster, P. S., Peters, A. M., and Stewart, J. S. W. Pegylated liposome-encapsulated doxorubicin and cisplatin enhance the effect of radiotherapy in a tumor xenograft model, Clin. Cancer Res. *6:* 4939-4949, 2000.
206. Kouloulias, V. E., Dardoufas, C. E., Kouvaris, J. R., Gennatas, C. S., Polyzos, A. K., Gogas, H. J., Sandilos, P. H., Uzunoglu, N. K., Malas, E. G., and Vlahos, L. J. Liposomal doxorubicin in conjunction with reirradiation and

local hyperthermia treatment in recurrent breast cancer: a phase I/II trial, Clin Cancer Res. *8:* 374-382, 2002.

207. Dvorak, J., Zoul, Z., Melichar, B., Jandik, P., Mergancova, J., Motyckova, I., Kalousova, D., and Petera, J. Pegylated liposomal doxorubicin in combination with hyperthermia in the treatment of a case of advanced hepatocelluar carcinoma, J. Clin. Gastroenterol. *34:* 96-98, 2002.
208. Matteucci, M. L., Anyarambhatla, G., Rosner, G., Azuma, C., Fisher, P. E., Dewhirst, M. W., Needham, D., and Thrall, D. E. Hyperthermia increases accumulation of technetium-99m-labeled liposomes in feline sarcomas, Clin. Cancer Res. *6:* 3748-3755, 2000.
209. Wust, P., Hildebrant, B., Sreenivasa, G., Rau, B., Gellermann, J., Riess, H., Felix, R., and Schlag, P. M. Hyperthermia in combined treatment of cancer, Lancet Oncol. *3:* 487-97, 2002.
210. Slepushkin, V. A., Simoes, S., Dazin, P., Newman, M. S., Guo, L. S., Pedroso de Lima, M. C., and Duzgunes, N. Sterically stabilized pH-sensitive liposomes: Intracellular delivery of aqueous contents and prolonged circulation in vivo, J. Biol. Chem. *272:* 2382-2388, 1997.
211. Simoes, S., Slepushkin, V., Duzgunes, N., and Pedroso de Lima, M. C. On the mechanisms of internalization and intracellular delivery mediated by pH-sensitive liposomes, Biochim. Biophys. Acta. *1515:* 23-37, 2001.
212. Cummings, J. and McArdle, C. S. Studies on the *in vivo* disposition of adriamycin in human tumour which exhibit different responses to the drug, Br. J. Cancer. *53:* 835-838, 1986.
213. Kirchmeier, M. J., Ishida, T., Chevrette, J., and Allen, T. M. Correlations between the rate of intracellular release of endocytosed liposomal doxorubicin and cytotoxicity as determined by a new assay, J. Liposome Res. *11:* 15-29, 2001.
214. Martin, F. J. Future prospects for Stealth liposomes in cancer therapy, Oncololgy. *11 (S11):* 63-68, 1997.
215. Davis, A. J. and Tannock, I. F. Repopulation of tumour cells between cycles of chemotherapy: a neglected factor, Lancet Oncol. *1:* 86-93, 2000.